# Physiological Investigation of Periosteum Structure and Its Application in Periosteum Tissue Engineering

Wei Fan BSc, MSc

Institute of Health and Biomedical Innovation

Faculty of Built Environment & Engineering

**Queensland University of Technology**

**June, 2010**

**Thesis submitted for the award of Doctor of Philosophy**

# ABSTRACT

Although many different materials, techniques and methods, including artificial or engineered bone substitutes, have been used to repair various bone defects, the restoration of critical-sized bone defects caused by trauma, surgery or congenital malformation is still a great challenge to orthopedic surgeons. One important fact that has been neglected in the pursuit of resolutions for large bone defect healing is that most physiological bone defect healing needs the periosteum and stripping off the periosteum may result in non-union or non-healed bone defects. Periosteum plays very important roles not only in bone development but also in bone defect healing. The purpose of this project was to construct a functional periosteum *in vitro* using a single stem cell source and then test its ability to aid the repair of critical-sized bone defect in animal models. This project was designed with three separate but closely-linked parts which in the end led to four independent papers.

The first part of this study investigated the structural and cellular features in periostea from diaphyseal and metaphyseal bone surfaces in rats of different ages or with osteoporosis. Histological and immunohistological methods were used in this part of the study. Results revealed that the structure and cell populations in periosteum are both age-related and site-specific. The diaphyseal periosteum showed age-related degeneration, whereas the metaphyseal periosteum is more destructive in older aged rats. The periosteum from osteoporotic bones differs from normal bones both in terms of structure and cell populations. This is especially evident in the cambial layer of the metaphyseal area. Bone resorption appears to be more active in the periosteum from osteoporotic bones, whereas bone formation activity is comparable between the osteoporotic and normal bone. The dysregulation of bone resorption and formation in the periosteum may also be the effect of the interaction between various neural pathways and the cell populations residing within it.

One of the most important aspects in periosteum engineering is how to introduce new blood vessels into the engineered periosteum to help form vascularized bone tissues in

bone defect areas. The second part of this study was designed to investigate the possibility of differentiating bone marrow stromal cells (BMSCs) into the endothelial cells and using them to construct vascularized periosteum. The endothelial cell differentiation of BMSCs was induced in pro-angiogenic media under both normoxia and $CoCl_2$ (hypoxia-mimicking agent)-induced hypoxia conditions. The VEGF/PEDF expression pattern, endothelial cell specific marker expression, in vitro and in vivo vascularization ability of BMSCs cultured in different situations were assessed. Results revealed that BMSCs most likely cannot be differentiated into endothelial cells through the application of pro-angiogenic growth factors or by culturing under $CoCl_2$-induced hypoxic conditions. However, they may be involved in angiogenesis as regulators under both normoxia and hypoxia conditions. Two major angiogenesis-related growth factors, VEGF (pro-angiogenic) and PEDF (anti-angiogenic) were found to have altered their expressions in accordance with the extracellular environment. BMSCs treated with the hypoxia-mimicking agent $CoCl_2$ expressed more VEGF and less PEDF and enhanced the vascularization of subcutaneous implants *in vivo.*

Based on the findings of the second part, the $CoCl_2$ pre-treated BMSCs were used to construct periosteum, and the in vivo vascularization and osteogenesis of the constructed periosteum were assessed in the third part of this project. The findings of the third part revealed that BMSCs pre-treated with $CoCl_2$ could enhance both ectopic and orthotopic osteogenesis of BMSCs-derived osteoblasts and vascularization at the early osteogenic stage, and the endothelial cells (HUVECs), which were used as positive control, were only capable of promoting osteogenesis after four-weeks. The subcutaneous area of the mouse is most likely inappropriate for assessing new bone formation on collagen scaffolds. This study demonstrated the potential application of $CoCl_2$ pre-treated BMSCs in the tissue engineering not only for periosteum but also bone or other vascularized tissues.

In summary, the structure and cell populations in periosteum are age-related,

site-specific and closely linked with bone health status. BMSCs as a stem cell source for periosteum engineering are not endothelial cell progenitors but regulators, and $CoCl_2$-treated BMSCs expressed more VEGF and less PEDF. These $CoCl_2$-treated BMSCs enhanced both vascularization and osteogenesis in constructed periosteum transplanted in vivo.

**Key words:** periosteum, osteoporosis, bone marrow, vascularization, osteogenesis, angiogenesis, differentiation, endothelial cell, tissue engineering, bone defect healing

# LIST OF PUBLICATIONS

**The following is a list of published, accepted or submitted manuscripts that are relevant to the work performed in this PhD project:**

1. **Wei Fan,** Ross Crawford, Yin Xiao. Enhancing in vivo vascularized bone formation by cobalt chloride-treated bone marrow stromal cells in a tissue engineered periosteum model. **Biomaterials (2010) 31: 3580–3589.**

2. **Wei Fan,** Ross Crawford, Yin Xiao. The ratio of VEGF/PEDF expression in bone marrow mesenchymal stromal cells regulates neovascularization. **Differentiation (2010) submitted.**

3. **Wei Fan,** Stefan AW Bouwense, Ross Crawford, Yin Xiao. Structural and Cellular Features in Metaphyseal and Diaphyseal Periosteum of Osteoporotic Rats. **Journal of Molecular Histology (2010) 41:51–60**.

4. DongChoon Sin, Xigeng Miao, Gang Liu, **Wei Fan,** Gary Chadwick, Cheng Yan, Thor Friis. Polyurethane (PU) Scaffolds Prepared by Solvent Casting/Particulate Leaching (SCPL) Combined with Centrifugation. **Materials Science and Engineering C 2009 (2010) 30: 78–85**.

5. **Fan W,** Crawford R, Xiao Y. Structural and cellular differences between metaphyseal and diaphyseal periosteum in different aged rats. **Bone (2008) 42: 81-89**.

6. Yufeng Zhang, **Wei Fan**, Zhaocheng Ma, Chengtie Wu, Wei Fang, Gang Liu, Yin Xiao. The effects of pore architecture in silk fibroin scaffolds on the growth and differentiation of mesenchymal stem cells expressing BMP7. **Acta Biomaterialia (2010) [Epub ahead of print].**

7. Yin Xiao, **Wei Fan**, Stefan AW Bouwense, Ross Crawford. The role of periosteum: a neglected aspect of osteoporosis. **Book chapter in Osteoporosis: Etiology, Diagnosis and Treatment**. **(2009)** 235-250. Nova Science Publishers, Inc.

**The following is a list of publications that are not relevant to the work performed in this PhD project but published during the PhD candidature:**

1. **Fan W**, Fan B, Gutmann JL, Fan MW. Identification of a C-shaped canal system in

mandibular second molars - Part III: Anatomic features revealed by digital subtraction radiography. **Journal of Endodontics (2008) 34: 1187-1190.**

2. Fan B, Gao Y, **Fan W,** Gutmann JL. Identification of a C-shaped canal system in mandibular second molars - Part II: The effect of bone image superimposition and intraradicular contrast medium on radiograph interpretation. **Journal of Endodontics (2008) 34: 160-165.**

3. **Fan W**, Fan B, Gutmann JL, Cheung GSP. Identification of C-shaped canal in mandibular second molars. Part I: Radiographic and anatomical features revealed by intraradicular contrast medium. **Journal of Endodontics (2007) 33: 806-810.**

4. **Fan W**, Fan B, Gutmann JL, Bian Z, Fan MW. Evaluation of the accuracy of three electronic apex locators using glass tubules. **International Endodontic Journal (2006) 39: 127-135.**

## PRESENTATIONS AND PAPERS IN REFERRED CONFERENCE PROCEEDINGS

1. **Wei Fan,** Ross Crawford, Yin Xiao. Angiogenic differentiation potential of bone marrow mesenchymal stem cells (BMSCs) in VEGF and hypoxia treatments**. Mater Medical Research Institute Annual Stem Cell Symposium.** 21st -22nd May 2009, Brisbane.

2. Wei Fang, **Wei Fan,** Yin Xiao. Assessing angiogenesis associated factors in tissue engineering fibrocartilage. **Mater Medical Research Institute Annual Stem Cell Symposium.** 21st -22nd May 2009, Brisbane.

3. **Wei Fan,** Ross Crawford, Yin Xiao. Subcutaneous assessment of tissue engineered periosteum in osteogenesis and vascularization at early osteogenic stage. **19th Annual Conference of the Australasian Society for Biomaterials and Tissue Engineering (ASBTE).** 21st -23rd January 2009, Sydney.

4. **Wei Fan,** Ross Crawford, Yin Xiao. Structural and cellular differences of periosteum are site-specific and age-dependent. **13rd Annual Scientific Meeting of Australian & New Zealand Research Orthopaedic Society (ANZORS)**. 17th -18th October, 2007, Auckland.

# DECLARATION

The work contained within this thesis has not been previously submitted for a degree or diploma at any other higher education institute. To the best of my knowledge and belief, this thesis contains no materials previously published or written by another person except where due references were made.

Signed_____(Wei Fan)

Date _____

# ACKNOWLEDGEMENTS

At the end of my PhD candidature, I would like to extend my appreciation and gratitude to the following teachers and friends. Without them, I would not have finished my PhD project.

First of all, I would like to thank my supervisor team: A/Prof. Yin Xiao, Prof. Ross Crawford and A/Prof. Clayton Adam. They guide, support and encourage me with great patience during my whole PhD study. They support me not only in my study but also in my life. They work with me as my teachers as well as friends. I really cherish and appreciate that.

I thank the Faculty of Built Environment & Engineering for granting me the tuition fee waiver and living allowance scholarship, without which my PhD study would not have been possible.

I would also like to show my gratitude to Prof. Dietmar W. Hutmacher, A/Prof. Ben Goss, Ms. Wei Shi, Dr. Lance Wilson, Dr. Cameron Lutton, Dr. Siamak Saifzadeh, Dr. Travis Klein, Dr. Sadahiro Sugiyama, and other staff in our domain. Thanks for their great help and precious suggestions to my study.

My appreciation also goes to other PhD students in our group and domain. They are Dr. Yufeng Zhang, Dr. Chentie Wu, Dr. Shobha Mareddy, Dr. Sanjleena Singh, Dr. DongChoon Sin, Ms. Navdeep Kaur, Ms. Indira Prasadam, Ms. Lu Liu, Ms. Xueli Mao, Dr. Jian Li, Mr. Wei Fang, and other students. The friendship we established during the PhD study will become my spiritual property accompanying me for the rest of my life.

Mr. Thor Friis showed great patience in helping me with my experiments and proofreading my thesis. He is always very nice and willing to help, and his contributions will be deeply appreciated.

A special thank-you to IHBI supporting staff, especially Mr. David Smith and Scott Tucker. It is them who keep our lab running smoothly and well-organized. Without them, our experiments would not have been possible.

At last, I wish to dedicate my thesis to my wife Juan and our parents for their forever and unconditional love and support. Their love is the origin of strength that makes me

keep going in my study.

# TABLE OF CONTENTS

# ABRRIVIATIONS APPEARING IN THIS THESIS

**ALP** alkaline phosphatase

**ACP** amorphous calcium phosphate

**BMSCs** bone marrow derived mesenchymal stem cells

**BMP** bone morphogenic protein

**Bost** Osteogenic differentiated BMSCs

**CFU** colony forming unit

**$CoCl_2$** cobalt chloride

**D-LA** D- lactide

**DMEM** Dubbucal's Modified Eagle's Medium

**EC** endothelial cell

**ECM** extracellular matrix

**EDTA** ethylenediaminetetraacetic acid

**EGM** endothelial cell growth media

**eNOSIII** endothelial nitrite oxidate synthase III

**EPC** endothelial progenitor cell

**FACS** fluorescence activated cell sorting

**FBS** fetal bovine serum

**FGF** fibroblast growth factor

**HA** hydroxyapatite

**HUCV** human umbilical cord vein

**HUVEC** human umbilical vein endothelial cell

**IGF** insulin-like growth factor

**L-LA** L- lactide

**MCSF** macrophage colony stimulating factor

**MEC** mature endothelial cell

**MSC** mesenchymal stem cell

**OCN** osteocalcin

**PDLA** poly(D- lactide)

**PEDF** pigment epithelium derived factor

**PGA** poly(glycolide)

**PLA** poly(lactide)

**PLGA** poly(lactide-co-glycolide)

**PLLA** poly(L- lactide)

**Real time q-PCR** real time quantitative reverse transcription polymerase chain reaction

**RGD** Arg-Gly-Asp

**SCID mice** severely combined immunodeficiency mice

**TCP** tricalcium Phosphate

**TGF** transforming growth factor

**TRAP** tartrate-resistant acid phosphatase

**VEGF** vascular endothelium growth factor

**VEGFR2** vascular endothelium growth factor receptor 2

**vWF** von Willebrand factor

# CHAPTER 1 *INTRODUCTION*

## *1.1 PREFACE*

Orthopedic surgeons have long held the aspiration to properly heal bone defects - caused by trauma, inflammation or tumors - and regain its normal function, despite the size of the defect. To realize this ambition, innumerable studies have been conducted into autogeneic, allogeneic and even xenogeneic bone transplantation therapies [1]. However, insufficient donor tissue, coupled with concerns about donor site morbidity, has hindered autologous transplantation for large-scale applications. On the other hand, immunological repulsive reactions in the recipient against allo or xenogeneic bone grafts impose severe limitations on the clinical application of these approaches. Added to these considerations, additional operations to harvest bone substitute in allograft may further compromise the health of the patient.

Advances in cell and molecular biology, especially in the knowledge of the underlying mechanisms of bone defect healing and tissue engineering techniques, have thrown a new light on the repair of various sized bone defects. The main purpose of bone tissue engineering is to construct a substitute for bone defects, *in vitro* and *in vivo,* in order to restore defects and normal function. Natural biomaterials (e.g. collagen, chitosan, hyaluronic acid, decalcified bone matrix, etc), synthetic polymers (e.g. PLA, PGA, PLLA, PDLA, PLGA) and bioceramics (e.g. HA, TCP, bioglass etc.) are most frequently used in bone tissue engineering [2]. These materials serve both as templates to restore the shape of bone defects and also as scaffolds to deliver therapeutic cells and/or various related growth factors[3-5]. The expectation is that the engineered bone substitutes can integrate with host bone tissues and thus restore the physiological structure and function of the defects. However, there remain obvious problems as to the practical application of bone tissue engineering technology. The *in vitro* engineered bone substitute is usually an "ossified block" rather than "physiologically and anatomically restored bone defect substitute". How these "engineered ossified blocks" integrate with host bone tissues,

at the implant/host junction, is obviously different from natural bone fracture healing. The final mechanical strength at the implant/host junction needs to be carefully investigated and compared to that in natural bone fracture healing. Another concern is the cell viability of large cell containing substitutes, since these are 3-dimensional and the diffusion distance of nutrients and oxygen for cell survival is in the order of 150-200μm[6]. Even if the scaffold used to deliver cells could be designed with larger pore size and greater porosity to maximize the permeability of the materials, decreased mechanical strength of the scaffold would then become another problem in the *in vivo* application, especially at the load-bearing site. Consequently, critical-sized bone defects, requiring large 3D engineered substitutes in order to restore function, pose a great challenge in orthopedic surgery [7]. Many methods have been developed to increase the vascularization of bone implants such as combining angiogenic growth factors (e.g. VEGF and FGF) with the scaffold as well as gene transfection[8]. However, the results to date have been disappointing due to difficulties associated with the controlled release of growth factors, causing an unpredictable degree of vascularization and even oncogenesis.

In terms of bone physiology the periosteum plays a determining role in bone formation and defect healing in addition to the involvement of other important factors. The periosteum is a highly vascularized tissue that contains osteogenic and chondrogenic progenitor cells as well as other related bioactive factors. Transplantation of autogenous or allogenous periosteum has been applied successfully in the repair of various sized bone defects, especially in large bone defects. Bone healing induced by periosteum has natural advantages over the other methods mentioned above such as: healing with natural bone structure, optimal implant/host integrity, appropriate vascularization and minimal ectopic ossification through encasing of the defect site. This therapeutic concept for bone defect restoration is “membrane-cell-based” rather than “bone-structure-based”. However, some major concerns in relation to this concept exist in the harvesting of periosteum, namely insufficient donor material, donor site morbidity and immunological concerns.

## 1.2 MAIN PURPOSES OF THIS STUDY

The main purpose of this study is to construct a dual-layered periosteum *in vitro*, based on the natural structure and cell populations of the periosteum during active osteogenesis. This engineered periosteum will contain osteogenic progenitors in the inner layer and blood vessel forming or recruiting cells in the outer layer. The induction of new bone formation by engineered periosteum will be tested *in vivo*.

## 1.3 QUESTIONS TO BE ADDRESSED

1. What are the structural and cellular features of periosteum? Are these features same or different at different sites on the bone surface? Does the age affect these features? Will these features change in osteoporosis?

2. Could we use bone marrow mesenchymal stem cells (BMSCs) to construct a dual-layered periosteum in vitro? Could the BMSCs be differentiated into endothelial cells or could the BMSCs be used to help vascularization of the engineered periosteum and how?

3. Could the engineered perioteum induce new bone formation and help restore large-sized bone defect in vivo?

## 1.4 POSSIBLE OUTCOMES AND SIGNIFICANCE

Based on earlier attempts to artificially engineer periosteum *in vitro*, the concept of "membrane-cell-based" engineering for bone defect restoration will be emphasized in this project. More knowledge about the periosteum and cell-cell interactions within may be revealed through this project. This project is believed the first to construct a dual-layered periosteum tissue using a single stem cell source and test its osteogenic function in vivo. Interactions between different cell populations in the periosteum can be investigated using the engineered periosteum as a model. A possible

commercial outcome may arise should the artificially engineered periosteum be of a quality that it could to be manufactured and marketed as a medical product.

# CHAPTER 2 *OVERVIEW OF PROJECT DESIGN*

## *2.1 UNDERSTANDING THE STRUCTURE OF PERIOSTEUM*

### 2.1.1 PERIOSTEUM CHANGES DURING BONE DEVELOPMENT

The femoral periostea of twelve female Lewis rats of various age groups were fixed and stained with hematoxylin and eosin. The thickness of cambial and fibrous layers of periostea at different periosteal sites (diaphyseal and metaphyseal) were measured and the number of cells in each layer counted. Changes in the structure and cell number from different age groups and periosteal sites were analyzed. Subsequent immunohistochemical staining was performed using several specific antibodies to identify the cell populations in the periosteum in different age groups and periosteal sites.

### 2.1.2 PERIOSTEUM CHANGES IN NORMAL AND OSTEOPOROTIC RATS

The femoral periostea of three normal and four osteoporotic Lewis rats were fixed and stained with hematoxylin and eosin. The thickness of cambial and fibrous layers of periostea at different periosteal sites (diaphyseal and metaphyseal) were measured and the number of cells in each layer counted. Changes in the structure and cell number between the two groups were analyzed. Subsequent immunohistochemical staining was performed using several specific antibodies to identify the cell populations in the periosteum from the two groups.

## *2.2 ANGIOGENIC DIFFERENTIATION OF BMSCs*

### 2.2.1 Angiogenic differentiation of BMSCs in normoxia

BMSCs were cultured in complete DMEM (10% FBS, 1% Pen/Strep) until passage 2. The cells were then seeded into 6-well culture plates and cultured in media supplemented with 5% FBS and 20, 40 or 80ng/ml VEGF. After 6-day culturing, the expression of relevant endothelial cell markers (vWF, VEGFR2, eNOS and CD31), pro- and anti-angiogenic growth factors (VEGF and PEDF) was determined by RT-qPCR, western blot, flow cytometry or immunohistochemistry staining and compared with undifferentiated BMSCs and human umbilical vein endothelial cells (HUVECs) as controls. The ability to form vessel network structures on the matrigel of BMSCs cultured in different situations was assessed.

### 2.2.2 Angiogenic differentiation of BMSCs in $CoCl_2$-induced hypoxia

BMSCs were cultured in complete DMEM (10% FBS, 1% Pen/Strep) until passage 2. The cells were then seeded into 6-well culture plates and cultured in media supplemented with 5% FBS, 100μM $CoCl_2$ and/or 20ng/ml VEGF. After 6-day culturing, the expression of relevant endothelial cell markers (vWF, VEGFR2, eNOS and CD31), pro- and anti-angiogenic growth factors (VEGF and PEDF) was determined by RT-qPCR, western blot, flow cytometry or immunohistochemistry staining and compared with untreated BMSCs and human umbilical vein endothelial cells (HUVECs) as controls. The ability to form vessel network structures on the matrigel of BMSCs cultured in different situations was assessed.

### 2.2.3 In vivo angiogenesis of BMSCs cultured under different conditions

The HUVECs, untreated BMSCs and the BMSCs treated with VEGF and/or 100μM $CoCl_2$ were mixed with matrigel and injected into the subcutaneous area of three SCID mice. After 10 days, the implants were harvested, fixed and sliced. The density of blood vessels on each slice was analyzed and compared among groups.

## *2.3 PERIOSTEUM ENGINEERING AND ITS IN VIVO ASSESSMENT*

### 2.3.1 Periosteum engineering using BMSCs-derived osteoblasts (Bost) together with HUVECs or $CoCl_2$-treated BMSCs

BMSCs were seeded on to one side of a collagen membrane and cultured in osteogenic media for 2 weeks, and then undifferentiated BMSCs, HUVECs or $CoCl_2$-treated BMSCs were seeded onto the other side of the membrane. The membrane without cells or seeded with only undifferentiated BMSCs or carrying Bost only was used as controls. The osteogenesis and vascularization of all these scaffolds were tested in vivo.

### 2.3.2 In vivo test for subcutaneous osteogenesis and vascularisation

4 SCID mice were used for this experiment. On the dorsal area of each mouse, 6 scaffolds from each group mentioned above were implanted under the skin. After 2 weeks, the implants were harvested. Then the Micro-CT scanning analysis, histological and immunohistochemical were performed to analyze the ectopic osteogenesis and vascularization in the engineered periosteum.

### 2.3.3 In vivo test for osteogenesis and vascularization in a skull defect model

28 SCID mice were used for this experiment. On the skull of each mouse, a hole defect was created using a dental drill. Scaffolds from each group mentioned above were implanted into the defect. Defects without implants were included as negative control. After 4 weeks, the defect-implant complex was harvested. Then the Micro-CT scanning analysis, histological and immunohistochemical were performed to analyze

the orthotopic osteogenesis and vascularization in the engineered periosteum.

# CHAPTER 3 *LITERATURE REVIEW*

## *3.1 THE HISTOLOGICAL STRUCTURE OF PERIOSTEUM*

Periosteum is a dense connective tissue membrane covering the outer surface of all bones except the joint of long bones. It attaches tightly to various bone surfaces through Sharpy's fibers, forming a thin but tough membrane. The Sharpy's fibers represent a direct continuation of the periosteal collagen fibers around which the cortical lamellae have grown [9]. Histologically the periosteum is thought to consist of two or three distinct layers [10-11]. In the "two layer" theory (Fig. 1), the periosteum consists of an outer fibrous layer which contains fibroblast, blood vessels, sensory and sympathetic nerve fibres, collagen fibers and extracellular matrix [12]; The inner layer, referred to as the cambium layer, serves as a reservoir of undifferentiated progenitor cells able to differentiate into chondrogenic and osteoblastic cell lineages [13-15]. Osteogenic progenitor cells from the periosteal cambium layer may work with osteoblasts in initiating and driving the cell differentiation process of bone repair characterized by the development of the initial fracture callus and subsequent remodeling [16]. Periosteum can be described as an *osteoprogenitor cell-containing bone envelope*, capable of being activated to proliferate by trauma, retroviruses, tumors, and lymphocyte mitogens [17].

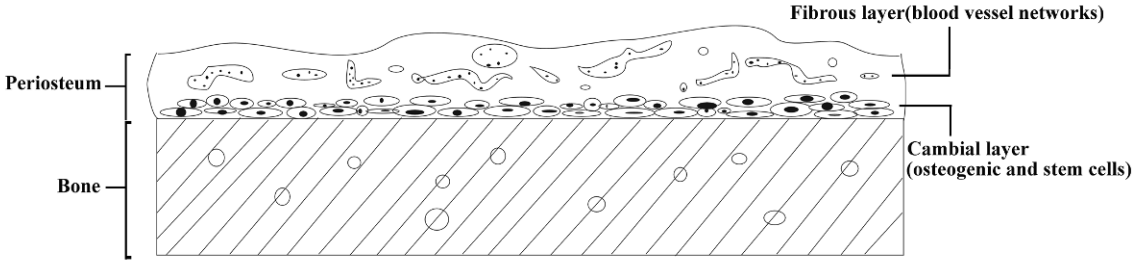


Figure 1. An illustration of the structure of two-layered periosteum

Studies of the periosteum ultrastructure suggest it is made up of three discrete zones [11]. Zone I has an average thickness of 10 to 20 μm consisting predominantly of osteoblasts representing about 90% of the cell population, while collagen fibrils occupy 15% of the volume[11]. Transmission electron microscopy (TEM) pictures have revealed a supraosteoblast layer consisting of smaller, more compact cells containing large quantities of endoplasmic reticulum [11]. In zone II, fibroblasts and collagen make up half the volume in roughly equal proportions of 25% each, while capillary networks are around 15% of the volume [11]. The predominant cell type in zone II are fibroblasts, with endothelial cells being most of the remainder. Zone III has the highest volume of collagen fibrils and fibroblasts compared to zones I and II [11]. Fibroblasts take up more than 90% of all cells in zone III. Interestingly, fibroblast cells display morphological difference across the three zones. In zone I the fibroblast-like cells adjacent to the osteoblasts are less numerous and have a lower surface density combined with a smaller cell volume and lower cell-to-volume ratio. Hence, they can be defined as more compact and isodiametric than normal fibroblasts [18]. Although slight differences exist between the “two layer” and “three layer” periosteum theories, one common characteristic feature of periosteum is that periosteum consists of an inner cambium layer and an outer vascularised and innervated fibrous layer.

The structure of periosteum varies with age [19] . In infants and children it is thicker, more vascular, active and loosely attached, while in adults or older people, it is relatively thinner, inactive and more firmly attached [9, 19-20]. The structure of periosteum is also found to be different at different periosteal sites in a rat model, e.g. diaphyseal or metaphyseal site [19]. The metaphyseal periosteum seems thicker and more cellular than the diaphyseal periosteum, and this difference is more obvious in older rats [19]. The differences in periosteum at different periosteal sites are also reported in osteoposis [10, 21].

Periosteum is described as a well vascularised ‘‘osteogenic and/or chondrogenic

organ'' [9]. It provides blood circulation to bone, especially the cortical bone [18] and is regarded as the "umbilical cord" of bone [22]. Stripping periosteum from the diaphysis typically destroys the arterial nutrient supply to bone [20]. The vasculature system of periosteum was first studied in detail by Zucman and later by Brookes [20]. Brookes's studies showed that the capillaries supplying blood to bone reside within the cortex linking the medullary and periosteal vessels. Some authors have argued that the blood supply of periosteum has a number of features analogous to the blood supply of skin [23]. In skin, blood vessels in the dermal area provide nutritions and oxygen, and remove metabolic wastes from dermis and epidermis.

Some reports have been published about the neurological aspects of bone and periosteum [24-26]. It has been reported that sympathetic and sensory nerves are prominent in the periosteum of mammalian bones and exist among blood vessels and osteogenic cells in these areas [24-26]. Sympathetic innervation of periosteum and bone contributes to the regulation of bone cell activity and, therefore, the equilibrium between bone modeling and remodeling [27]. It is known that surgical and chemical sympathectomy can both modulate bone cell function. However, the sympathetic nervous system (SNS) can give rise to both anabolic and catabolic effects [28-31] and its role in regulating bone remodeling is, therefore, controversial. For example, some researches reported that if bone is deprived of its sympathetic innervation, bone deposition and mineralization is reduced and bone resorption increases [31], while in some other reports a sympathectomy impairs bone resorption [28]. Sensory nerves also appear to be important in normal bone metabolism and in bone fracture repair [32]. Increased sensory and sympathetic innervation of fracture calluses has been reported in animal experiments [26]. These findings suggest that innervation of bone is involved in both normal bone metabolism as well as fracture repair.

## *3.2 THE ROLE OF PERIOSTEUM IN BONE FORMATION*

By publishing the article "Sur le Development et la Cruedes Os des Animaux" in 1742, Duhame can claim credit as the first investigator to study the osteogenic potential of

periosteum [18]. In a number of animal experiments he placed silver wires under the periosteum of long bones and revealed that after several weeks of implantation the wires were embedded in a bonelike matrix. A century later another French surgeon, Ollier, discovered, while working with bone grafts in animals and human, that transplanted periosteum could induce *de novo* bone formation [18]. More recently the osteogenic/chondrogenic capacity of periosteum, and related mechanisms, have been confirmed and the underlying biology is better understood through a number of studies [33-35].

During embryogenesis there are two distinct patterns of *in vivo* bone formation, in both of which the periosteum play an indispensable role namely *intramembranous* and *endochondral* ossification. Irregularly shaped bones, such as those in the craniofacial area, are formed through intramembranous patterning whereas regularly shaped long bones, such as the extremities, are formed by endochondral ossification. During intramembranous ossification, the mesenchymal cells first differentiate into osteoprogenitor cells forming a primitive periosteum together with surrounding fibroblasts. After osteoprogenitor cells in periosteum differentiate into osteoblasts, bone formation process takes place. Together with the secretion and bio-mineralization of osteoids, osteoblasts are embedded and become osteocytes, and the new bone tissue wrapped in periosteum appears. During endochondral ossification chondrocytes and perichondreum also develop from mesenchymal cells and results in the formation of chondra which has a primitive configuration of bone. The perichondreum of the diaphysis transforms into periosteum and forms cortical bone layers over chondra, after which ossification of chondra takes place until all chondral tissues have been replaced by mineralized bone tissues with the exception of those chondra covering the joint or in the epiphyseal plate. In adults the bone-forming potential of periosteum is reactivated by trauma, infection and also in some tumors. A number of studies have shown that periosteum regenerates both cartilage and bone from its progenitor cells within the cambium layer [36-38].

## 3.3 THE ROLE OF PERIOSTEUM IN BONE HEALING

In classical histological terms fracture healing has been divided into direct (primary) and indirect (secondary) fracture healing[39]. Direct fracture healing occurs when there is an anatomical reduction of fracture fragments by rigid internal fixation and decreased intra fragmentary strain[39]. This process involves a direct attempt by the cortex to reestablish new haversian systems by the formation of discrete remodeling units known as "cutting cones" in order to restore mechanical continuity [39]. During this process little or no periosteal response is noted (i.e. no callus formation). The major parts of fractures heal through indirect fracture healing. The indirect process basically reiterates the intramembranous and endochondral ossification processes as described above. During intramembranous fracture healing the process involves no cartilage formation but rather direct bone callus (hard callus) development via osteoprogenitor cells from periosteum differentiating into osteoblasts. In the case of more severe fractures with associated haemorrhaging, both intramembranous and endochondral ossification is involved in the fracture healing process. Haematomas in the fracture site will activate an acute inflammatory response that is followed by angiogenesis and cartilage formation that will finally be replaced by bone callus. During the bone healing process, mesenchymal cells are supplied from periosteum, endosteum, and bone marrow. Several studies indicate that central to the healing response is the supply of mesenchymal cells from periosteum [10, 15, 40-44]. Uddstromer and colleagues have shown that periosteum play the most important role in fracture healing [45-46]. Oni and colleagues demonstrated fracture healing was delayed when periosteum was removed [47-48]. Other factors appear to play only minor roles in fracture healing [49-50].

## 3.4 PERIOSTEUM ENGINEERING STRATEGIES

Currently, periosteal grafting (auto- or allo-) is accepted as the standard for periosteum replacement therapy to aid the repair of bone and/or cartilage tissue. Similar to other tissue transplantation process, a periosteal graft serves as a cell source,

scaffold for delivering and retaining cells and a source of local growth factors critical for regeneration [51-53]. Although they have been fairly promising, the use of periosteal grafts is not without limitations. Auto-grafting poses limitations of donor site morbidity, supply shortage and unpredictable resorption of graft, while allo-grafting poses immunogenic rejection and possible disease transmission [54].

As recently pointed out in a review by Zhang et el, periosteum engineering could assist in structural de novo bone formation and is therefore a promising method for bone defect restoration [55]. To engineer a periosteum, three basic strategies could be used: acellular bioactive membrane; membrane seeded with osteogenic cells; membrane seeded with both osteogenic and angiogenic cells. Most studies at the present use acellular bioactive membranes or membranes carrying osteogenic cells. Encouraging results were achieved by Neel [56] when a periosteal replacement membrane was used for bone graft containment at the allograft-host junction. The membrane, however, was acellular. Koji Hattori [57] was able to demonstrate healing of a severe open fracture by applying bio-artificial periosteum composed of osteogenic cells and a collagen sponge. In another study, submucosa from the small intestine was used to mimic periosteum onto which bone marrow stromal cells (BMSCs) were seeded [58]. The obvious drawback of this approach is that scaffold materials have to be sourced from the small intestine necessitating the need for an operation to harvest donor materials. As these engineered periosteum are either acellular or single cell carrying, they differ considerably from the structure of natural periosteum; the cell viability, stability, long-term function and clinical applicability of these artificial periostea are therefore in doubt [56-58]. Although much work has been done under the subject of periosteum [18-19, 35, 59], few, if any, references were found addressing bi-layered engineered periosteum which contains both osteogenic and angiogenic cells in particular, not to mention an in vivo assessment of any such constructs.

## *3.5 SCAFFOLD MATERIALS CURRENTLY USED IN TISSUE*

### 3.5.1 Bioceramics: Hydroxyapatite (HA) and Beta-Tricalcium Phosphate (β-TCP)

Mineral-based scaffolds, or bioceramics, have long been recognized as potent osteoconductive materials for hard tissue engineering such as bone [60]. This application is based on the fact that bioceramics are chemically similar to the calcium phosphate found in natural bone, typically in the form of hydroxyapatite (HA) [4, 60]. In natural bone the three main components are calcium phosphate, water and collagen (predominantly type I collagen), together with other organic materials in smaller quantities, such as non-collagenous proteins, polysaccharides, and lipids [61]. Calcium phosphate in bone is in the form of crystallized HA and amorphous calcium phosphate (ACP). The HA crystals are needle or plate shaped and are deposited along and parallel to the collagen filaments [61].

A key feature of bioceramics, their bioactivity, makes these materials attractive candidates as scaffolds in hard tissue engineering. Most researches agree, however, that HA is primarily osteoconductive rather than osteoinductive although this is a topic of some debate [1, 4, 62]. HA do not appear capable of inducing new bone formation in the absence of osteogenic cells or growth factors such as BMPs [62]. Also, HA does not readily biodegrade, retarding the bone replacement by host tissues, something which limits the material's application in some circumstances [63]. In clinical cases, an HA scaffold can still persist for 5 years after implantation[64].

β-TCP is another type of calcium phosphate found in the human body, which is highly biocompatible, as well as bioactive. Although β-TCP also appears to be primarily osteoconductive, the material biodegrades more readily than HA. Once it degrades it is resorbed by the body and is gradually replaced by host tissue [65]. The mechanical strength of β-TCP is relatively weaker than that of HA [66]. In order to optimize the application of both HA and β-TCP, some researchers have mixed them to form a HA-TCP composite so that resorption time and mechanical properties of the

composite material can be adjusted by varying the ratios of HA to β-TCP [66-67].

HA and β-TCP are both porous materials. The pore size, porosity and inter-connections between pores directly influence their osteoconductivity, osteogenic cells ingrowth, vascularisation, osseointegration and scaffold material resorption [68]. The optimal pore size for bone ingrowth is thought to be 200-400μm [68]. A higher total porosity coupled with a greater degree of interconnections among pores will make the material better suited for bone reconstruction [62]. However, greater porosity poses a problem in that the inherent porosity of the bioceramic scaffolds also renders the constructs brittle and thus prone to stress fracture when placed in load bearing situations. In an effort to increase the strength of these bioceramics and, more importantly, mimic the chemical composition and structure of natural bone tissue, collagen and other biodegradable synthetic polymers are bound to bioceramics. These composite materials have been found to have osteoconductive properties [2, 69-70].

### 3.5.2 Natural polymer biomaterials: Collagen

Collagen is the most abundant protein in mammalian tissues, accounting for up to one-third of all proteins [71]. Collagen fibers are the main component of the extracellular matrix in various tissues, especially the connective tissue such as dermis, tendon, bone, cartilage, mucosa and periosteum. The main function of collagen is as a mechanical reinforcement of the connective tissue.

The individual polypeptide chains of collagen contain 20 different amino acids and the precise composition varies among different tissues [72]. Variations in the amino acid sequence generate the different types of collagen: type I, II, III X and XIX and the most common types are types I, II and III. Type I collagen is dominantly found in skin, tendon, periosteum and bone; type II is the main collagen type in cartilage, whereas type III is found in blood vessels.

Collagen is increasingly being used as a scaffold material in both soft and hard tissue engineering. It is used to repair tissues such as skin, blood vessel, bone and cartilage given it is a natural polymer already existing in the body and has excellent biocompatible properties and bioactivity [73-76]. Collagen is also easily biodegraded and resorbed by the body and allows for optimal cell attachment. The main disadvantage of collagen is its low mechanic strength, especially compared with bone. To increase its mechanical property, collagen is therefore highly crosslinked or combined with other materials, such as collagen-glycosaminoglycans for skin regeneration [77], and collagen-HA for bone repairing [69]. When collagen is bound with growth factors (e.g. BMPs, VEGF, FGF, TGF-β) and/or seeded with various pluripotent cells, its bioactivity inducing tissue growth and regeneration is enhanced [5, 78-79]. One major concern about the application of allogeneic or xenogeneic collagen is its potential immunogenicity. However, studies have shown that adverse immunological responses only occur in rare cases and generally settle within a few months never lasting longer than 1 year, especially in the case of type I collagen [1, 80]. Premature resorption or other adverse effects of collagen implantation have rarely been reported and the combined use with immunosuppressants has been shown to be effective [80-81].

### 3.5.3 Synthetic biodegradable polymer biomaterials: poly(glycolide), poly(lactide) and poly(lactide-co-glycolide)

Poly(glycolide) (PGA), poly(lactide)(PLA) and poly(lactide-co-glycolide)(PLGA) are aliphatic polyesters and the most commonly used synthesised biodegradable polymer scaffold materials. The US Federal Drugs Administration has already approved their use in certain human applications [68]. Poly(glycolide) (PGA) is synthesized from dimerization of glycolic acid, and is the simplest linear aliphatic polyester. PGA fibers show high strength and modulus because of their high degree of crystallinity [82]. PGA was developed as the first totally synthetic absorbable suture and has been marketed as Dexon$^{TM}$ since 1960s by David and Geck [82]. Sutures of PGA lose about 50% of their strength after two weeks and 100% after four weeks and are

completely absorbed within 4-6 months [82-83]. PGA has successfully been used as scaffold material in skin, tendon, cartilage and bone reparation [84-86]. Since the glycolide can be copolymerized with other monomers, such as lactide and trimethylene carbonate, PGA is often involved in yielding copolymer with various mechanical and biodegradation properties for different applications [82, 87-88].

Poly(lactide) (PLA) is synthesized in a similar way to PGA by the dimerization of lactic acid. Lactic acid is a chiral molecule with two stereo-isometric forms: D-LA and L-LA referred to as PDLA and PLLA respectively. Both form crystalline polymers. PLLA is more commonly used than PDLA because the biodegradation product of PLLA, namely L-LA, is the naturally occurring isomer of lactic acid in the human body[82]. What is more, as a biodegradable material, PLLA has a satisfactory biocompatibility profile *in vitro*[82]. It is non-toxic and stimulates only a mild inflammatory response[82]. The hydrolysis product L-LA is the normal intermediate of carbohydrate metabolism and will not accumulate in vital organs [82]. It has been successfully used in the reconstruction of bone, articular defects, for suture materials, drug carriers and fixation devices [1, 60, 72, 82, 89]. The degradation time of PLLA is longer. PLLA has been reported to take up to 3 years to be completely absorbed [90]. In order to overcome this problem, D-LA has been added as a co-monomer to obtain the copolymer PDLA which has a lower crystallinity than PLLA and consequently a higher rate of degradation [82].

Poly(lactide-co-glycolide) (PLGA) is synthesized through copolymerizing lactide and glycolide, the mechanical and biogradation properties of which are based on the ratio of individual monomers in the composite. A copolymer of 50% glycolide and 50% D-LA degrades faster than both homopolymers [91]. The degradation rate strongly depends on the structure of the copolymers[91]. Copolymers of 25%-70% L-LA with glycolide are amorphous due to the disruption of the regularity of the polymer chain by the other monomer[91]. Therefore, these copolymers show much greater degradation rates than either individual homopolymers [91]. PLGA has been used

with different cell types and/or growth factors to enhance the tissue regeneration and reparation, especially in blood vessel, bone, cartilage engineering [8, 92-93]. A modified PLGA could provide attachment sites for specific peptides, such as Arg-Gly-Asp (RGD) sequences thus modulating cell adhesion and growth [94]. A major concern about the application of these synthetic polymers is the chemicals (additives, traces of catalysts, inhibitors etc.) and monomers (glycolic acid, lactic acid) released from polymer degradation, which may induce local and systemic host reactions that cause clinical complications [69]. Lactic acid, the by-product of PLA degradation, is reported to potentially create an adverse cellular response at the implant site by reducing the local pH triggering the release of prostaglandin $E_2$ ($PEG_2$), a bone resorbing and inflammatory mediator, by human synovial fibroblasts and murine macrophages [95]. However, the addition of carbonate to the implant seems to be a potential way of stabilizing the local pH [96]. Some potential toxic residues during chemical crosslinking treatments (e.g. glutaraldehyde) may also make this crosslinking technique less desirable for implantable devices[97-98].

## *3.6 CELL DELIVERY METHODS*

### 3.6.1 Cell delivery through porous scaffold materials

One of the most commonly used cell delivery methods is to seed cells into solid porous scaffolds. Following implantation these scaffold–cell constructs stimulate the formation of reparative tissue while maintaining adequate integrity [99]. In skeletal tissues cells are distributed within a dense ECM made up of collagens, proteoglycans, a complex mixture of phosphoproteins and other inorganic materials[99]. For regeneration of these types of tissues a homogeneous spatial distribution of cells within all areas of the reparative implant is preferable [99]. Despite seeding cells on flat surfaces is easy to perform, on three-dimensional porous constructs it will be more difficult [99].

Seeding cells onto porous membranes or solid scaffolds rarely results in an even cell

distribution [99]. Pore size, porosity and inter-pore connection are the main factors influencing cell distribution in three dimensional porous scaffolds. Sufficient pore size allows cells to migrate or adhere to the surface layer of a material, whereas interconnecting pores permit cells to grow into the interior region of the scaffold [99]. Interconnecting porosity will also facilitate nutrient supply into the central region of engineered transplants [99]. With currently available engineered bone implants, cells receive their nutrition through diffusion before new blood vessels are formed to support tissue formation [99]. Consequently, the optimal geometries and dimensions of tissue-engineered bone for orthopedic applications are still under investigation.

Adhesion of cells to the material surface is the first step in construction of a cell and scaffold complex. Attachment to surfaces activated with biomimetic peptides or growth factors can induce cell proliferation, differentiation and tissue maturation[99] [100]. Mesenchymal cells, when expanded in a monolayer culture, will undergo a process of phenotypic and functional dedifferentiation [99]. On the other hand, three dimensional cell cultures provide the advantage of independent cell growth and maintaining the differentiated phenotype [99, 101]. Evidences have suggested that anchorage independent growth in a semisolid medium is superior for chondrogenic differentiation of mesenchymal stem cells (MSCs) [99]. Osteogenic differentiation of cells can be positively influenced by strong adhesion to surfaces[99]. However, recent studies have shown osteogenic differentiation of MSCs in hydrogel cultures without the conventional methods of cell attachment on biomimetic surfaces [99, 102].

### 3.6.2 Cell delivery through homogeneous scaffolds

Homogeneous scaffolds refer to polymer solutions that subsequently form gels. Collagen, hyaluronate, fibrin, agarose, alginate and chitosan are commonly used embedding gels in tissue engineering applications[99]. Cells can distribute evenly and 3-dimensionally in these type of scaffolds, which is why this is a preferred pattern for tissue regeneration [99]. The main disadvantage of these scaffolds is the

immobility of the cells and coupled with weak mechanical properties, limiting their application in load-bearing tissue reparation, such as bone. However, when combined with other materials, such as HA, TCP, or synthetic polymers, homogenous scaffolds can be used successfully in hard tissue engineering [69-70].

### 3.6.3 Cell delivery through injectable scaffolds

Bioresorbable and injectable polymers can more easily fill defects of all shapes and sizes compared to prefabricated scaffolds and require only minimal surgical intervention for implantation. In order to provide the mechanical strength required for orthopedic applications, injectable polymers must be polymerized or crosslinked *in situ*, something which places a major constraints on these material's usefulness. All reagents involved in the polymerization, as well as the reaction products, must be non-toxic. Furthermore, the heat release and local pH variation must be within the tolerance of cells in implants and surrounding tissues in order to protect cells from damage [68].

Injectable cell delivery systems will provide early mechanical stabilization by *in situ* polymerization and could be used to treat irregularly shaped joint defects [99, 103-104]. Thermoreversible, biocompatible *in situ* gelling, formulations have been tested for chondrocyte delivery [99, 105]. Recent studies have evaluated the suitability of injectable carriers to support MSC function [99, 106]. However, it is still uncertain if injections of MSCs into the joint cavity can be directed into regenerative healing and produce significant clinical improvement for the patient [99, 107]. Chondrocyte transplantation into sites other than articular defects has so far been unsuccessful in immunocompetent animals[99]. In irregular bone defects, injectable bone forming cell-matrix composites might be a more appropriate method than conventional scaffolds[99]. Early stabilization could be achieved using injectable gels (fibrin or collagen) in combination with tricalcium phosphate or hydroxyapatite particles[99, 108]. Similarly, if cell anchorage is achieved before *in vivo* delivery, injectable carrier beads with attached cells can be used [99, 109].

## *3.7 BONE MARROW MESENCHYMAL CELLS*

### 3.7.1 The nature and biology of bone marrow mesenchymal cells

Bone marrow cells comprise a dual system of stem or progenitor cells: the hematopoietic cell system and non-hematopoietic bone marrow mesenchymal stem cell system (BMSCs) [110-111]. Hematopoietic stem cells (HSCs) in bone marrow are the reservoir of various blood cells, such as erythrocytes, leukocytes, macrophages or platelets, and they also contain endothelial progenitor cells (EPCs) which can become mature endothelial cells when needed [112-113]. BMSCs, when cultured in vitro, are negative for CD45, CD14, CD31 and CD34 but positive for CD105, CD 44, CD73 and CD90. They are a mixture of multipotent progenitor cells which can differentiate into various other mesodermal cells, such as osteoblasts, chondrocytes, fibroblasts or adipocytes [114]. Because there is very little extracellular matrix (ECM) present in bone marrow, gentle mechanical disruption can easily dissociate stromal and hematopoietic cells into a single-cell suspension. When these cells are cultured in vitro, BMSCs rapidly adhere and can be easily separated from the nonadherent hematopoietic cells by repeated washing. BMSCs form colonies and are therefore defined as Colony Forming Units—Fibroblasts (CFU-Fs), indicating that each colony derives from a single proliferating progenitor [115]. The BMSCs consist of heterogeneous cell populations, typically exemplified by a broad range of colony sizes, representing varying growth rates, and different cell morphologies ranging from fibroblast-like spindle-shaped cells to large flat cells [115]. Furthermore, if such cultures are allowed to develop for up to 20 days, phenotypic heterogeneity is also observed [110]. A method to distinguish the subsets of BMSCs with the most active replication and individual differentiation potential would certainly be very important for both theoretical and applicative reasons. Several laboratories have developed monoclonal antibodies using BMSCs as immunogens in order to identify one or more markers suitable for identification and sorting [116-118]. However, to date the isolation of a “pure” population of multipotent marrow mesenchymal stem cells

remains elusive.

### 3.7.2 The application of BMSCs in angiogenesis and osteogenesis

As mentioned above, bone marrow cells are a mixture of multipotent cells with the latent ability to differentiate into different cell lineages depending on the cell culture environment, a fact that makes applying bone marrow cells as a cell source for various tissue engineering and cell-delivery therapy possible. For *in vitro* vasculargenesis and angiogenesis there are several potential cell sources, e.g. mature endothelial cells (MEC, or EC) from vessels, such as adult tissue veins or arteries; MEC from human umbilical cord veins (HUCV); endothelial progenitor cells (EPC) from adult bone marrow cells , adult peripheral blood, fetal umbilical cord blood or some tissues such as fat, muscle or neural. MECs, especially those from the HUCV, are often used as a cell source for *in vitro* angiogenesis [119-120]. A limiting factor with these cells is that allogeneic MECs may induce immunological responses through resting T-cells [121]. EPCs are actually a fraction of leukoctyes found in peripheral blood and bone marrow. Bone marrow cells are a valuable source of autologous and immunologically neutral cells for vasculogenesis and angiogenesis [122]. Although the phenotype of EPC has not been completely clarified, they are now thought to be $CD133^+$ / $CD34^+$ / $VEGFR2^+$ (Flk-1/KDR) / $MUC18^+$ / VE-$Cadherin^+$ and $CD45^-$ / $CD14^-$ cells. MECs on the other hand lose the CD133 / MUC18 markers, but express CD31 / CD34 / VEGFR2 (Flk-1/KDR) / VE-Cadherin markers [122-124]. MECs also contain vWF (von Willebrand factor) in the cytoplasmic granules named Weibel-Palade bodies. Thus, $CD133^+$/ $MUC18^+$/$CD34^+$/$VEGFR2^+$(Flk-1/KDR) cells are more likely to represent the EPCs, while $CD31^+$/$CD34^+$/$VEGFR2^+$(Flk-1/KDR)/ $vWF^+$ (Weibel-Palade body) may identify the MECs. Based on these markers EPCs and MECs could be selected out and distinguished from each other in peripheral blood or bone marrow. It is still almost impossible to completely purify EPCs from the mononuclear cells, even if EPCs markers are identified, since EPCs and haematopoietic progenitor cells descend from the same precursor cells and have many cell markers in common. A recent

study suggests that there may be another way to characterize ECs, especially those derived from the bone marrow [112]. Despite the broad overlap in both antigenic and functional assays, there appears to be three characteristics unique to ECs: i) eNOS (NO synthase III) is confined to ECs; ii) only ECs can integrate into tube-like structures formed by HUVEC; iii) only ECs can significantly stimulate tube formation by HUVEC [113]. Although the number of EPCs in bone marrow or peripheral blood is very low, when isolated and expanded in culture, EPCs proliferate rapidly and can be expanded for at least 20 population doublings compared with ECs [125]. Cultured with certain cytokines in gelatin-coated dishes, such as VEGF and bFGF, the EPCs can differentiate into ECs and exhibit a cobblestone morphology characteristic of ECs [126].

As multipotent adult progenitor cells (MAPCs) and a pool of cells committed to various lineages and stages of differentiation, the BMSCs contain potentially osteogenic colonies [110-111]. These colonies can be referred to as "skeletal stem cells" meaning they are ancestors to mesodermal supportive tissues such as bone, cartilage, fibrous tissues, adipocytes, smooth muscle cells and so on [111]. These "skeletal stem cells", however, stay in different commitment stages of differentiation. Some are tripotential and are able to differentiate into osteoblasts, chondrocytes, and adipocytes *in vitro*; others are bipotential differentiating only into a chondrogenic-osteogenic phenotype, whereas a third group comprises only osteogenic clones [127]. Interestingly, it appears that, over a prolonged time in culture, the differentiation potential is reduced and that tripotential clones progressively lose adipogenic, then chondrogenic, and finally osteogenic potential, suggesting a preferential commitment of the progenitors towards the osteogenic phenotype [127]. Many researches have shown the osteogenic abilities of BMSCs, both *in vitro* and *in vivo*, and applied it to bone defect restoration [128-129]. There is little doubt that following ex vivo expansion under certain conditions, BMSCs are able to differentiate into osteogenic progenitor cells and finally osteoblasts. These osteoblasts are able to regenerate segments of bone lost through trauma or disease by direct orthotopic

placement in conjunction with appropriate scaffolds, most commonly those containing hydroxyapatite/tricalcium phosphate (HA/TCP).

## 3.8 SUMMARY

Developing bone substitute materials for bone defect repair has inspired orthopedic surgeons, bioengineering scientists and bone biologist to work collaboratively in order to design and develop the promising products for clinical applications. Tissue engineered periosteum is aimed to mimic the natural structure of periosteum to guide bone formation in a physiological manner. This review summarizes anatomical structure and physiological functions of periosteum in bone development and defect healing. The potential technology for periosteum scaffold fabrication, potential applicable scaffold materials and cells for cell-scaffold complex construction and strategies to engineer functional periosteum are reviewed and discussed based on current publications and the laboratory work conducted in our research projects.

# CHAPTER 4 *RESEARCH REPORTS*

## *PAPER ONE*

**Structural and Cellular Differences between Metaphyseal and Diaphyseal Periosteum in Different-aged Rats**

Wei Fan, Ross Crawford, Yin Xiao

**Suggested Statement of Contribution of Co-Authors for Thesis by Published Papers:**

| Contributors | Statement of contribution* |
|---|---|
| Wei Fan | Performed laboratory experiments, data analysis and interpretation. Wrote the manuscript. |
| | |
| | |
| Ross Crawford | Involved in the conception and design of the project. Assisted in reviewing the manuscript. |
| Yin Xiao | Involved in the conception and design of the project. Assisted in sample collection, technical guidance and reviewing the manuscript |

**Principal Supervisor Confirmation**

**I have sighted email or other correspondence from all co-authors confirming their certifying authorship**

**Name** **Signature** **Date**

**Abstract**

In both physiological and pathological processes, periosteum plays a determinant role in bone formation and fracture healing. However, no specific report is available so far focusing on the detailed structural and major cellular differences between the periostea covering different bone surface in relation to ageing. The aim of this study is to compare the structural and cellular differences in diaphyseal and metaphyseal periostea in different-aged rats using histological and immunohistochemical methods.

Four female Lewis rats from each group of juvenile (7-week old), mature (7-month old) and aged groups (2-year old) were sacrificed and the right femur of each rat was retrieved, fixed, decalcified and embedded. 5 μm thick serial sagittal sections were cut and stained with Hematoxylin and Eosin, Stro-1 (stem cell marker), F4/80 (macrophage marker), TRAP (osteoclast marker) and vWF (endothelial cell marker). 1mm lengths of middle diaphyseal and metaphyseal periosteum were selected for observation. The thickness, total cell number and positive cell number for each antibody were measured and compared in each periosteal area and different-aged groups. The results were subjected to two-way ANOVA and SNK tests.

The results showed that the thickness and cell number in diaphyseal periosteum decreased with age ($p<0.001$). In comparison with diaphyseal area, the thickness and cell number in metaphyseal periosteum were much higher ($p<0.001$). There were no significant differences between the juvenile and aged groups in the thickness and cell number in the cambial layer of metaphyseal periosteum ($p>0.05$). However, the juvenile rats had more $Stro1^+$, $F4/80^+$ cells and blood vessels and fewer $TRAP^+$ cells in different periosteal areas compared with other groups ($p<0.001$). The aged rats showed much fewer $Stro1^+$ cells, but more $F4/80^+$ ,$TRAP^+$ cells and blood vessels in the cambial layer of metaphyseal periosteum ($p<0.001$).

In conclusion, structure and cell population of periosteum appear to be both age-related and site-specific. The metaphyseal periosteum of aged rats seems more destructive than diaphyseal part and other age groups. Macrophages in the periosteum may play a dual important role in osteogenesis and osteoclastogenesis.

## Introduction

The periosteum is a type of connective tissue developed from mesodermal cells during the embryonic development. It is tightly attached to various bone surfaces through Sharpy's fibres, forming a thin but very tough membrane. In both physiological and pathological processes, periosteum plays a determinant role in both bone formation and fracture healing in addition to the involvement of other important factors such as growth factors and mechanical loading [9, 20, 35]. The periosteum contains progenitor cells both osteogenic and chondrogenic in nature, as well as other related bioactive factors, and is highly vascularised [9, 14, 23]. Transplantation of autogenous and allogenous periosteum have been applied successfully to repair various-sized bone or cartilage defects, in particular to large bone defects [7, 36-37, 130-131]. However, the availability of periosteum, morbidity associated with harvest and immunological concerns are still barriers against large scale *in vivo* application of periosteum transplantation. Interestingly, the progenitor cells in the bone marrow and periosteum have been successfully applied in bone tissue engineering with various scaffold materials [18, 115, 128, 132-135]. Some researchers have attempted to make artificial periosteum by seeding progenitor cells onto a membrane and achieved positive results in repairing bone defects *in vivo* [56-57]. However, current artificial periosteum, which is based on single type of cell structure, is still far from clinical application, primarily due to the questionable cell viability, stability and long-term function. One of the major challenges in tissue-engineered periosteum is to form the cellular structures similar to native periosteum, which can represent the stage of active bone formation. Therefore, it is imperative to understand the cellular structures of periosteum and their relationship during bone development and ageing. To date, however, no clear histological basis is available for the selection of donor-site or age-related periosteal grafts.

Previous studies have revealed that periosteum consists of two different layers [10]. The outer fibrous layer is composed of fibroblasts, collagen, elastin fibrers, nerve, and microvascular network. The inner cambial layer is highly cellular containing mesenchymal stem cells, fibroblasts, osteogenic progenitors and osteoblasts. However,

no study has documented the detailed structural and specific cellular differences between the periosteum on different bone surface, such as the difference between metaphyseal and diaphyseal periosteum.

Age is another important factor affecting the structure and function of periosteum. Some age-related changes in periosteum have been reported including decreased periosteal fibroblast number, fibrous layer thickness, osteoblast number, collagen formation, osteoid zones and vessel density throughout the periosteum [11, 136-138]. Depending on the locations of bone formation or resorption periosteum shows corresponding structural changes with ageing [136, 139]. However, the detailed information about the age-related structural and cellular changes in different periosteal areas is still unclear. We hypothesize that age-related changes in periosteum are also site-specific. Therefore, the distribution of mesenchymal stem cells, macrophages, osteoclasts, blood vessels and structural changes in metaphyseal and diaphyseal periostea from the femurs of different aged rats were investigated in this study.

## Materials and Methods

### Animal samples and slices

This study was carried out according to the guideline of the Animal Ethics Committee of the Queensland University of Technology. Three different aged groups of female Lewis rats were utilized with four rats in each group. The juvenile, mature, and aged groups were 7-week old, 7-month old, and two-year old rats respectively. The right femur of each rat was retrieved after the animals were sacrificed. The tissue samples were fixed with 4% paraformaldehyde for 12 hours at room temperature, then decalcified in 10% EDTA and embedded in paraffin. Serial sections of 5 μm thick sagittal slices were cut from the paraffin blocks using a microtome (Leica Microsystems GmbH Wetzlar, Germany). The slices near the central sagittal plane were used for subsequent experiments.

### Definition and selection of observed tissue areas

The diaphyseal and metaphyseal periostea were selected for the observation. The diaphyseal periosteum was selected from 1 mm length of periosteum in the middle of diaphyseal area and the metaphyseal periosteum was selected from 1 mm length of periosteum from metaphyseal area starting from the mesial border of growth plate on upper metaphysis.

**Structural observation**

Four slices from each rat sample were stained with Hematoxylin and Eosin (HD Scientific supplies Pty Ltd, Kings Park, NSW, Australia). The images were captured under ×200 magnification. The thickness of fibrous and cambial layers on the middle line perpendicular to the periosteum in each microscopic field and cell number of each layer throughout each periosteal area were measured using Axion software (Carl Zeiss Microimaging GmbH, Göttingen, Germany) under a microscope (Carl Zeiss Microimaging GmbH, Göttingen, Germany). The data from the four slices were averaged and recorded for subsequent analysis.

**Immunohistochemistry**

Four specific cell markers, Stro-1 (mouse anti-human, Chemicom International Inc., Temecula, CA, USA), F4/80 (Rat anti-mouse, ABR-Affinity BioReagents Inc., Golden, CO, USA), TRAP (tartrate-resistant acid phosphatase)(mouse anti-human, Lab Vision Co., Fremont, CA, USA) and vWF (mouse anti-human, Chemicom International Inc., Temecula, CA, USA), were utilized to identify mesenchymal stromal cells, monocytes/macrophages, osteoclasts and blood vessels in each periosteal sample of different-aged groups. To validate the results, each experiment was repeated at least three times.

Prior to immunoperoxidase staining, endogenous peroxidase activity was quenched by incubating the tissue sections with 3% $H_2O_2$ for 20 minutes. All sections were blocked with 10% swine serum for 1h. The enzymatic treatment was used to expose epitopes by incubating the slices with proteinase K (ready-to-use, DakoCytomation, CA, USA,) for 10 minutes at room temperature. Sections were then incubated with

optimal dilution of primary antibody Stro-1 (1:100), F4/80 (1:50), TRAP (1:20) and vWF (1:100) overnight at 4 $^{0}$C. Sections were then incubated with a biotinylated swine-anti-mouse, rabbit, goat antibody (DAKO Multilink, CA, USA) for 15 minutes, and then incubated with horseradish perioxidase-conjugated avidin-biotin complex (ABC) for 15 minutes. Antibody complexes were visualized after the addition of a buffered diaminobenzidine (DAB) substrate for 4 minutes. The reaction was stopped by immersion and rinsing of sections in PBS. Sections were then lightly counterstained with Mayer's haematoxylin and Scott's Blue for 40 seconds each, in between 3 minute rinses with running tap water. Following this, the sections were dehydrated with ascending concentrations of ethanol solutions, cleared with xylene and mounted with a cover slip using DePeX mounting medium (BDH Laboratory Supplies, England).

Controls for the immunohistological staining procedures included conditions where the primary antibody was omitted. In addition, an irrelevant antibody (IgG), which was not present in the test sections, was used as a control.

Under ×400 magnification, the positive cell number from each cell population in each periosteal area was counted using a microscope (Carl Zeiss Microimaging GmbH, Göttingen, Germany) and AxioVision software (Carl Zeiss Microimaging GmbH, Göttingen, Germany). Each measurement included three different slices and the average was recorded for subsequent analysis. To eliminate the effect of the difference in total cell number and periosteum thickness in different groups on the positive cell number and blood vessel counting, the Strol-1$^{+}$, F4/80$^{+}$, and TRAP$^{+}$ cell numbers were normalized to the cell number per 100 total cells in each specific group. The blood vessel number was normalized to the vessel number in 0.03mm$^{2}$ periosteal area.

**Statistical analysis**

All the data were analyzed according to the age of rats and the periosteal sites by two-way ANOVA using the General Linear Model and post-hoc testing performed using Student-Neuman-Keuls comparison (SNK) for group homogeneity. The

significance level was set at $p \leq 0.05$. Analysis was performed using SPSS software (SPSS Inc, Chicago Il).

## Results

### Structural differences in different periosteal areas and aged groups

The two-way analysis of variance model indicated that the age of rats and the periosteal sites both influenced, independently and interactively, the thickness and cell number in the periosteum ($p<0.001$). In diaphyseal periosteum, both thickness and cell numbers decreased with age in both cambial and fibrous layers (Fig.1). However, no significant differences were found in the thickness of the fibrous layer between juvenile and mature groups ($p=0.39$). There was no difference in cell numbers in the fibrous layer between mature and aged rats ($p= 0.07$) (Fig.1). Both the thickness and cell numbers in the cambial layer decreased significantly with age ($p<0.001$) (Fig.1). Compared to the diaphyseal area, the thickness and cell number in fibrous and cambial layers were significantly higher in metaphyseal periosteum ($p<0.001$) (Fig.1). In general，the metaphyseal periosteum of juvenile and aged animals was thicker and more cellular when compared with the mature group. Notably, there were no significant differences between the juvenile and aged groups in the thickness and cell numbers in the cambial layer of metaphyseal periosteum ($p=0.07$ for thickness and $p=0.14$ for cell number) (Fig.1). The mature rats had the thinnest and least cellular cambial layer in the metaphyseal area. The thickness of the fibrous layer in the metaphyseal periosteum from all three age groups was similar ($p=0.09$), while both mature and aged groups were much less cellular in this layer than the juvenile group ($p<0.001$) (Fig.1).

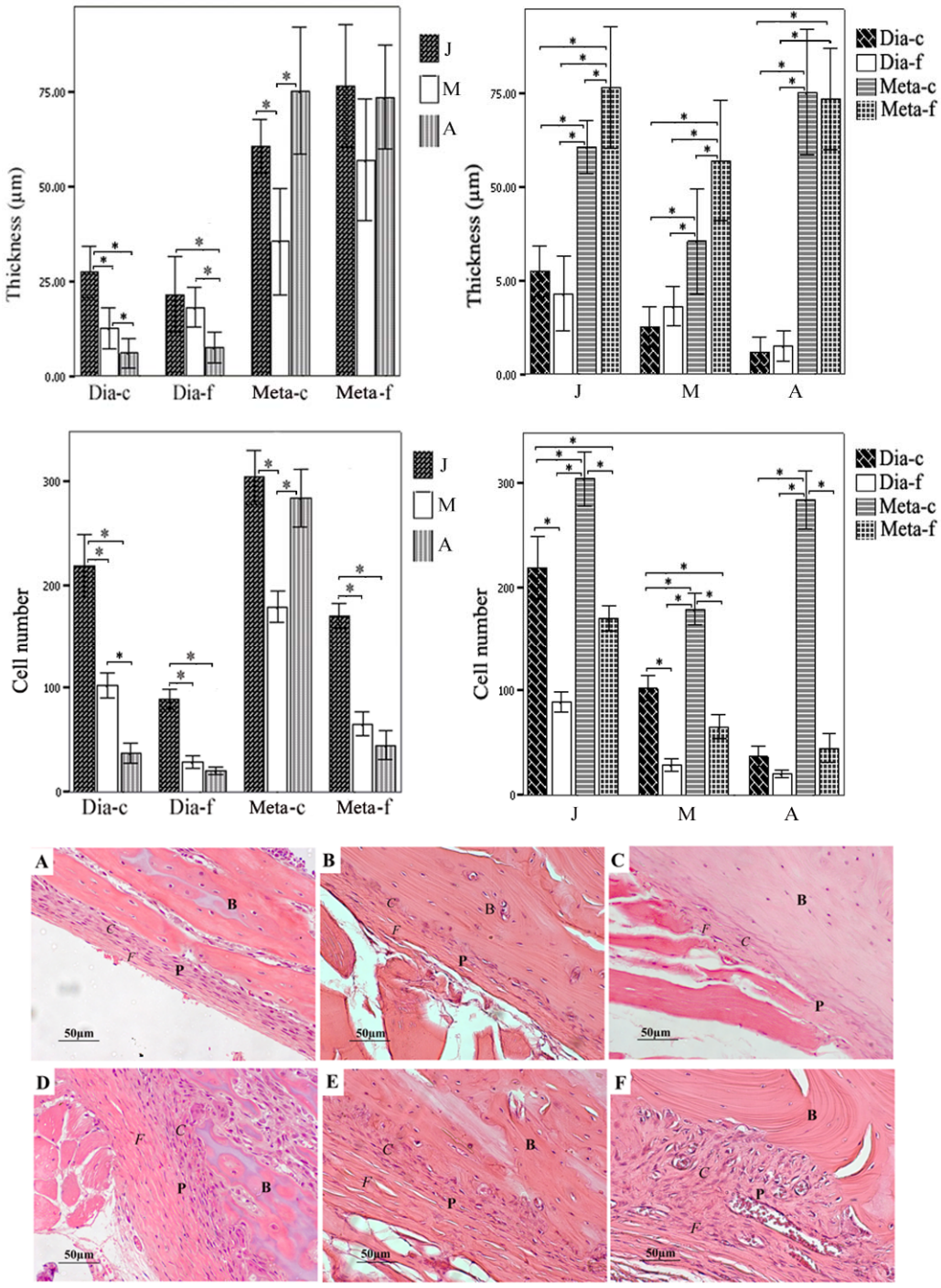


Figure 1. Diagrams and pictures (×200) of H&E observation of diaphyseal and metaphyseal periostea from different-aged groups. The thickness and cell number of the cambium layer in diaphyseal periosteum (Dia-c) decreased with age. No significant differences were found in the thickness of the diaphyseal fibrous layer (Dia-f) in juvenile and mature groups. There were no differences in cell numbers in the fibrous layer in mature and aged rats. There were no significant differences

between the juvenile and aged groups in the thickness and cell number in cambial layer of metaphyseal periosteum (Meta-c). The thickness of metaphyseal fibrous layer (Meta-f) from three aged groups was similar to one another, while both mature and aged groups were much less cellular in this layer than in the juvenile group. *: $p<0.05$. J: Juvenile; M: Mature; A: Aged..

A: diaphyseal periosteum from the juvenile group; B: diaphyseal periosteum from the mature group; C: diaphyseal periosteum from the aged group; D: metaphyseal periosteum from the juvenile group; E: metaphyseal periosteum from the mature group; D: metaphyseal periosteum from the aged group; (In pictures, B: bone tissue; P: periosteum; C: cambial layer; F: fibrous layer)

**Stro-1 expression in periosteum**

The normalized Stro-$1^+$ cell number was used in this analysis. Site ($p=0.04$), age ($p<0.001$) and the interactions between site/age were also significant ($p<0.001$) in the model for Stro1 expression. In diaphyseal periosteum, Stro-1 was broadly expressed in the cambial and fibrous layers in juvenile rats (Fig. 2). Very few Stro-1 positive cells were found in either cambial or fibrous layers from mature and aged rats compared to the juvenile group ($p<0.001$) (Fig. 2).

In the metaphyseal area, the juvenile rats had significantly more Stro-$1^+$ cells in both the cambial and fibrous layers compared with the mature and aged rats ($p<0.001$) (Fig. 2). In the fibrous layer of aged rats there were more Stro-$1^+$ cells compared with the cambial layer and the fibrous layer of mature group ($p<0.05$). The mature and aged groups had similar number of Stro-$1^+$ cells in the cambial layer. (Fig. 2).

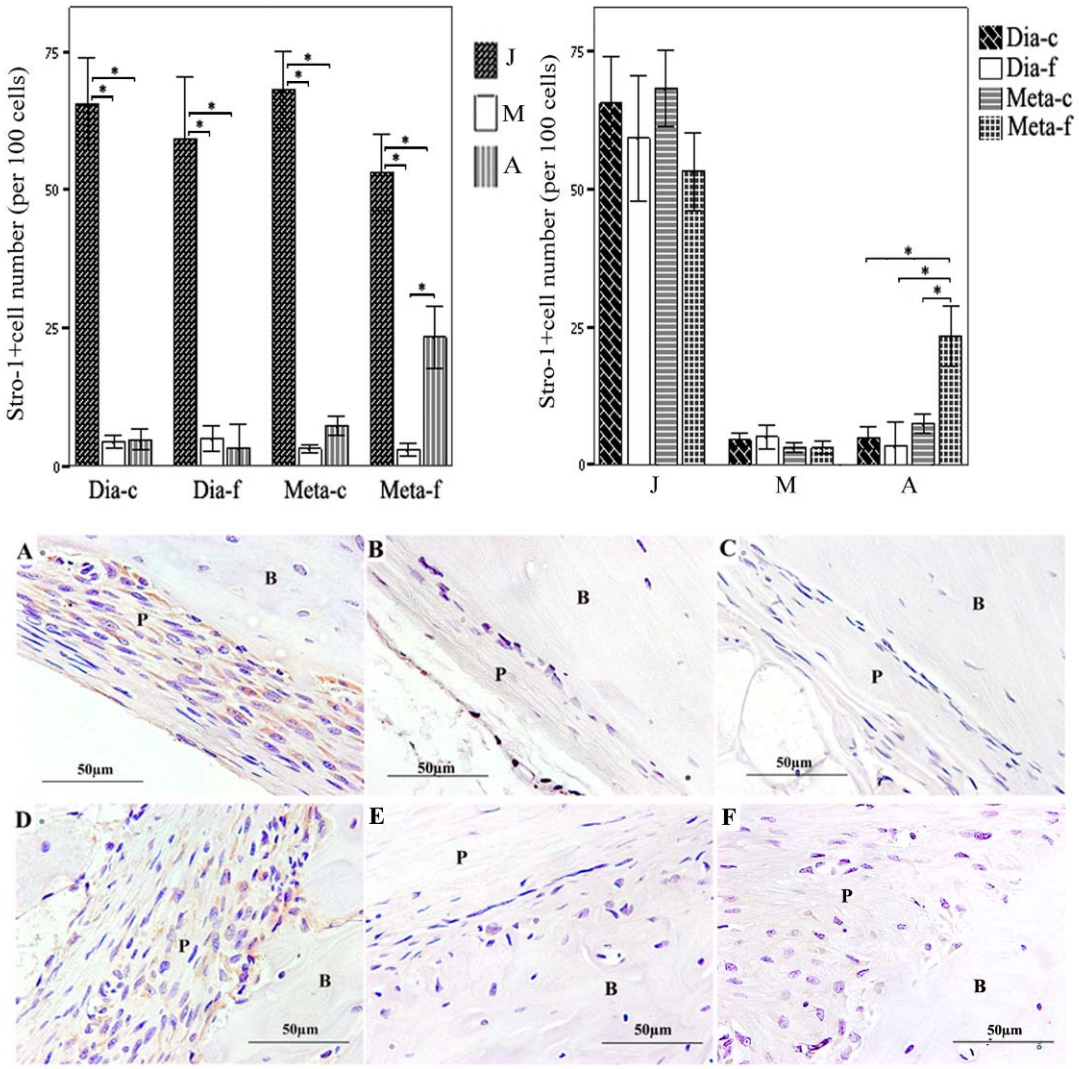


Figure 2. Diagram and pictures (×400) of Stro-1$^+$ cell distribution in different periosteal areas and age groups. Stro-1 was broadly expressed in both the cambial and fibrous layers of diaphyseal periosteum (Dia-c and Dia-f) from juvenile rats. Very few Stro-1$^+$cells were found in diaphyseal cambial and fibrous layers from mature and aged rats in comparison with the juvenile group. No significant difference was found in the Stro-1$^+$ cell numbers in metaphyseal periosteum (Meta-c and Meta-f) of the juvenile and mature rats when compared with the diaphyseal area, while both mature and aged groups had much fewer positive cells than the juvenile group in this area. *: $p<0.05$. J: Juvenile; M: Mature; A: Aged.

A: diaphyseal periosteum from the juvenile group; B: diaphyseal periosteum from the mature group; C: diaphyseal periosteum from the aged group; D: metaphyseal periosteum from the juvenile group; E: metaphyseal periosteum from the mature

group; D: metaphyseal periosteum from the aged group; (In pictures, B: bone tissue; P: periosteum)

**F4/80 expression in periosteum**

The normalized F4/80$^+$ cell number was used for this analysis. Periosteal sites and age were both significant ($p<0.001$) factors in the model as well as their interactions. The juvenile rats had significantly more F4/80$^+$ cells in both layers of the diaphyseal periosteum compared with the mature and aged groups ($p<0.001$) (Fig. 3). Nearly no F4/80$^+$ cells were detected in the diaphyseal periosteum in the mature and aged groups (Fig. 3).

In the metaphyseal area, the F4/80$^+$ cells were found mostly in the cambial and fibrous layers of aged periosteum as well as in the cambial layer of juvenile periosteum. Significantly fewer positive cells were identified in the mature periosteum ($p<0.001$) (Fig. 3).

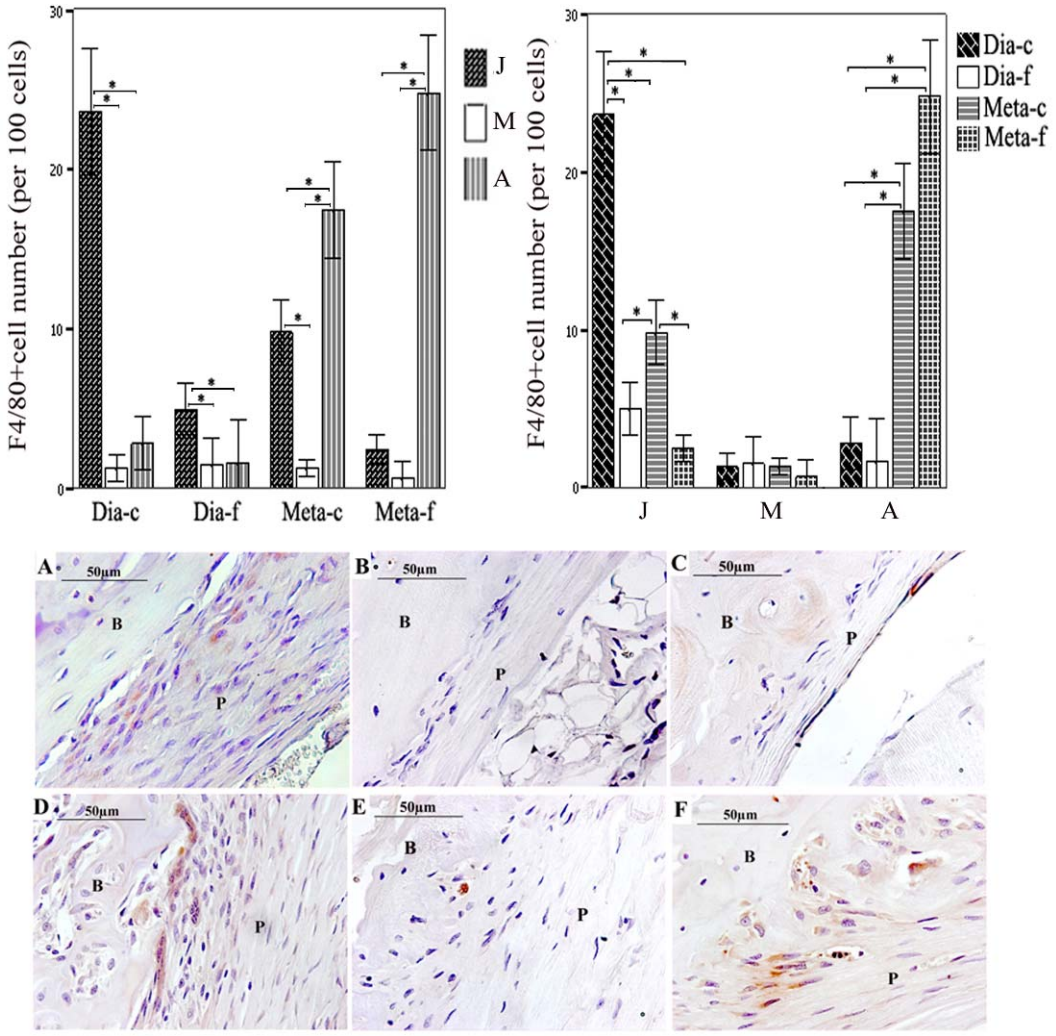


Figure 3. Diagram and pictures (×400) of F4/80$^+$ cell distribution in different periosteal areas and age groups. The juvenile rats had much more F4/80$^+$ cells in cambial layer of diaphyseal periosteum (Dia-c) compared with fibrous layer (Dia-f) and the other two groups. In metaphyseal area, the F4/80$^+$ cell number in both layers (Meta-c and Meta-f) from aged rats were more than other aged groups. *: $p<0.05$. J: Juvenile; M: Mature; A: Aged.

A: diaphyseal periosteum from the juvenile group; B: diaphyseal periosteum from the mature group; C: diaphyseal periosteum from the aged group; D: metaphyseal periosteum from the juvenile group; E: metaphyseal periosteum from the mature group; D: metaphyseal periosteum from the aged group; (In pictures, B: bone tissue; P: periosteum)

**TRAP expression in periosteum**

The normalized TRAP$^+$ cell number was used for this analysis. Site and age (both $p<0.001$) were significant factors in the model as well as the interaction between site/age ($p<0.001$). TRAP$^+$ cells were mostly detected in the both layers of the metaphyseal area in aged rats compared with the juvenile and mature rats ($p<0.001$) (Fig.4). Very few TRAP$^+$ cells were identified in diaphyseal periostum, although the cambial layer in the diaphyseal periosteum of aged rats had more positive cells than both the juvenile and mature aged groups ($p=0.004$) (Fig. 4). No difference was observed in the fibrous layer of diaphyseal periosteum in three age groups ($p=0.147$) (Fig. 4).

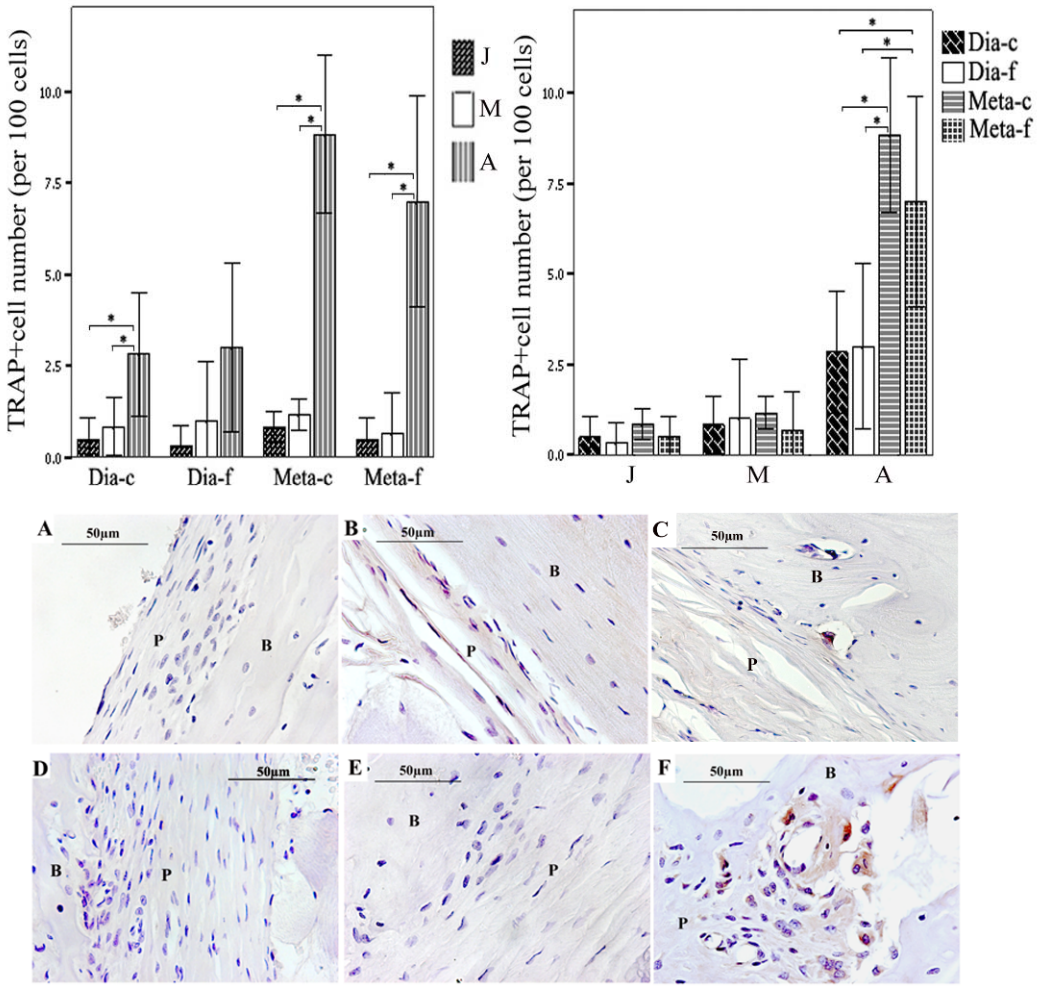


Fig.4 Diagram and pictures (×400) of TRAP$^+$ cell distribution in different periosteal areas and age groups. Few TRAP$^+$ cells were found in the diaphyseal periostum (Dia-c and Dia-f) in any of the three groups. In the metaphyseal area, the aged rats

had much more $TRAP^+$ cells in the cambial layer (Meta-c) than the fibrous layer (Meta-f) and the other two groups. *: $p<0.05$. J: Juvenile; M: Mature; A: Aged.

A: diaphyseal periosteum from the juvenile group; B: diaphyseal periosteum from the mature group; C: diaphyseal periosteum from the aged group; D: metaphyseal periosteum from the juvenile group; E: metaphyseal periosteum from the mature group; D: metaphyseal periosteum from the aged group; (In pictures, B: bone tissue; P: periosteum)

**vWF expression in periosteum**

The normalized vessel number was used in the analysis. Site and age (both $p<0.001$) were significant factors for vWF expression with the interaction of site/age also being significant ($p<0.001$). Blood vessels identified by the vWF staining in diaphyseal periosteum revealed that juvenile rats had a higher degree of vascularization in the cambial layer than the older age groups ($p<0.001$) with the exception of the fibrous layer ($p=0.77$)(Fig.5)..

In metaphyseal areas the juvenile and aged rats had the higher degree of vascularization in the cambial layer compared to the mature group ($p<0.001$) (Fig.5).. The degree of vascularization in the cambial layer of aged rats was also higher than the fibrous layer ($p<0.001$). The vessel number in the fibrous layer of mature rats was similar to that of juvenile rats ($p=0.154$), but greater than that of aged rats ($p<0.05$)(Fig.5).

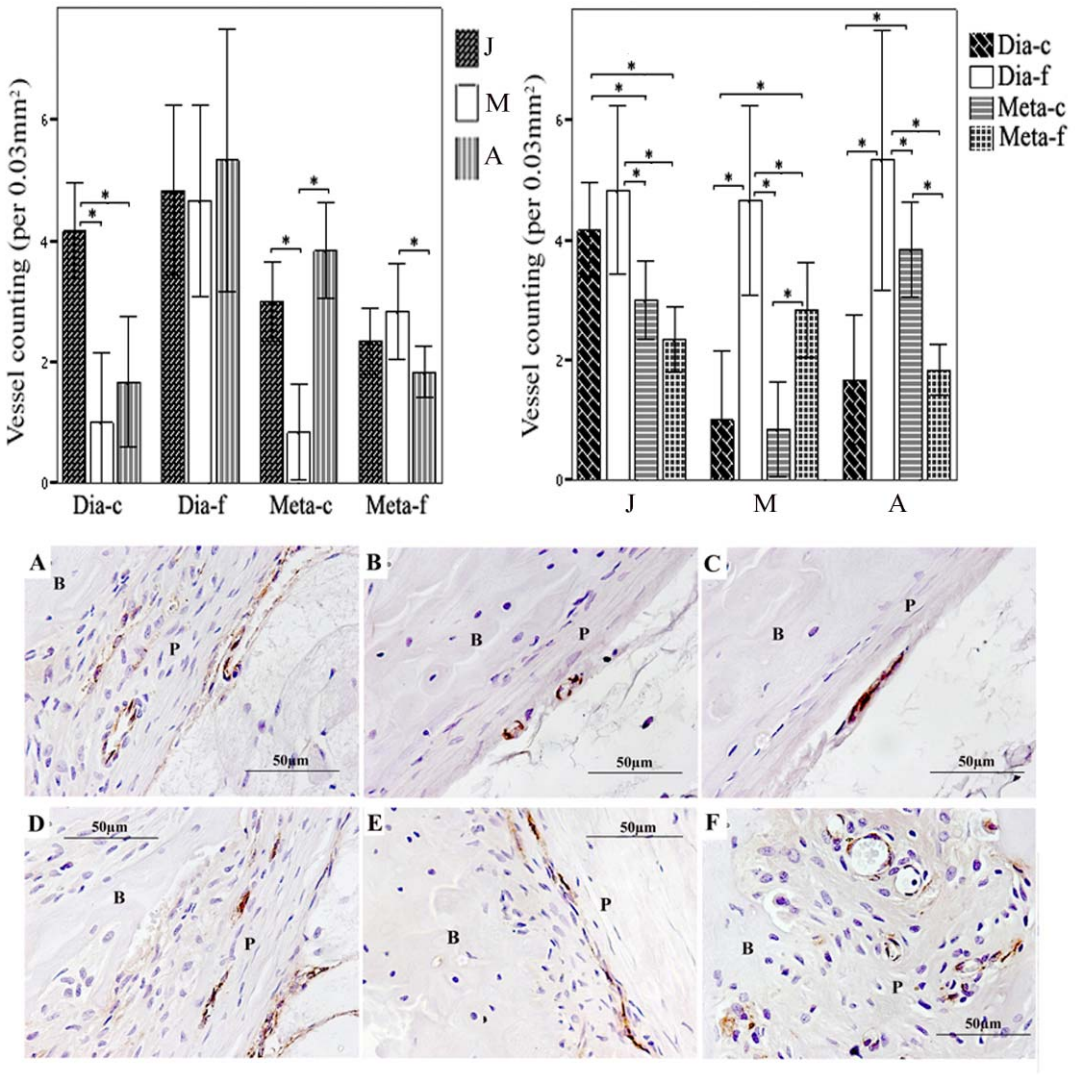


Fig.5 Diagram and pictures (×400) of $vWF^{+}$ blood vessel distribution in different periosteal areas and age groups. Juvenile rats had higher degree of vascularization in the cambial layer of diaphyseal periosteum (Dia-c) than the other two groups except in the fibrous layer (Dia-f). In metaphyseal area, the rats from aged group had highest degree of vascularization in cambial layer (Meta-c) among all three groups. The degree of vascularization in the cambial layer of aged rats was higher than the fibrous layer (Meta-f). The vessel number in the fibrous layer of mature rats was similar to that of juvenile rats, but more than that of aged rats. *: $p<0.05$. J: Juvenile; M: Mature; A: Aged.

A: diaphyseal periosteum from the juvenile group; B: diaphyseal periosteum from the mature group; C: diaphyseal periosteum from the aged group; D: metaphyseal periosteum from the juvenile group; E: metaphyseal periosteum from the mature

group; D: metaphyseal periosteum from the aged group; (In pictures, B: bone tissue; P: periosteum)

**Discussion**

The indispensable role of periosteum in both bone formation and fracture healing is well documented. When the periosteum is stripped off, the healing of bone defects and surrounding soft tissues is seriously compromised [20, 140]. This phenomenon has inspired many studies to focus on the application of periosteal grafts in bone and cartilage regeneration. It is known that periosteum is a thin membrane-like connective tissue covering the external surfaces of most bones and several studies have revealed the general histological and ultrastructural structures of periosteum from various bones [11, 141]. However, the detailed cellular structure of periosteum and its site specificity in relation to ageing are not well understood. In this study, the age-related degeneration (shown as decrease in thickness and cell number) was observed in the diaphyseal periosteum, especially the decrease in cell numbers in both cambial and fibrous layers in the aged group. However, in the metaphyseal areas, it is worth noting that the aged rats had thicker and more cellular cambial layer than the rats from the mature group although they were similar in the fibrous layer. There was also a noticeable change in cell populations within these areas, in particular an increased fractional number of osteoclasts. These observations would indicate aged-associated resorptive activity of cortical bone in metaphyseal areas, which in turn may have clinical relevance with more fractures reported in metaphyseal areas compared with diaphyseal areas in the elderly. In a recent study by Bliziotes M. et al.,[21] an increase in osteoclast numbers and eroded cortical bone surfaces was found more obvious at the femoral neck of nonhuman primates than at the shaft, especially in the castrated female animals. The nature of the regulation of periosteal bone turnover activity is not clear, but mechanical force and sex hormones are important modulators of periosteal activity. It has been found that low sex steroid levels in female animals are associated with an increase in periosteal resorptive activity [142] and the application of focal mechanical force results in an increase in local bone formation

[143].

Stro-1 is thought to be a pluripotent cell marker found highly expressed on various stromal cells [110, 144-145]. Stro-1 positive cells are capable of differentiating into multiple mesenchymal cell lineages including adipocytes, osteoblasts and chondrocytes, as well as hematopoiesis-supportive stromal cells, [144-145]. In this experiment, a higher percentage of Stro-1 positive cells were found in diaphyseal and metaphyseal periosteum in juvenile rats indicating the high osteogenic/chondrogenic nature of periosteum in this stage. In mature and aged groups, Stro-1 positive cells were significantly decreased and the intensity of Stro-1 staining was weaker in all periosteal areas compared with the juvenile group. In juvenile rats, the expression of Stro-1 was found in periosteal cells, pre-osteoblasts, osteoblasts and early osteocytes embedded in osteoid. Only mature osteocytes were negative for Stro-1. The broad expression of Stro-1 in both layers of juvenile periosteum suggests that both cambial and fibrous layers may be involved in the new bone formation.

To our knowledge no other study has documented the age-related distribution of monocytes/macrophages or osteoclasts in periosteum even though periosteal bone turnover activity and osteoclast distribution have recently been documented in the femoral neck in a series of adult rhesus and Japanese macaques [21]. In our study, periosteal monocytes/macrophages and osteoclasts were identified using F4/80 and TRAP as specific cell markers. F4/80 (or EMR1) is a specific monocyte/macrophage marker, while TRAP is mainly expressed by mature osteoclasts. Although both monocytes/macrophages and osteoclasts derive from the haemopoietic precursors and both can be multinucleate, there are still substantial differences existing between these two cell types [146]. The differentiation into the osteoclast lineage from haemopoietic precursors is found prior to macrophage commitment [147]. It has been reported that some growth factors produced by macrophages, such as BMP2 or TGF-β, could promote the osteogenesis and proliferation of osteoblasts and chondrocytes *in vitro* [148]. Macrophages can develop into osteoclasts only when certain stimuli exist, such as receptor activator of nuclear factor Kappa B ligand (RANKL), Macrophage-Colony Stimulating Factor (M-CSF) or inflammation factors [149]. In

this study numerous macrophages, but limited number of osteoclasts, were found in the diaphyseal and metaphyseal periosteum especially in the cambial layer of juvenile rats. In aged rats both macrophages and osteoclasts were increased in the metaphyseal area. Few macrophages and osteoclasts were found in mature rats and the diaphyseal periosteum of aged rats.

Blood vessels, identified by vWF staining, showed that both cambial and fibrous layers in different periosteal areas in juvenile rats were well vascularized while mature rats had blood vessels predominantly in the fibrous layer. In the juvenile rats more active periosteal osteogenic activity was found in both periosteal areas, which was demonstrated by increased cell numbers of mesenchymal stem cells and macrophages as well as increased thickness of the cambial layer. The high degree of vascularization in the periosteum of juvenile rats suggests a role in nutrient and osteoprogenitor cell supply. In diaphyseal periosteum, blood vessel numbers in the cambial layer decreased with age. However, in the metaphyseal region, the aged rats had more blood vessels in the cambial layer when compared to the juvenile and mature groups. The increase of periosteal vascularisation in aged rats could be related to increased bone resorptive activity. The increased number of blood vessels in the areas of osteoclastic bone resorption is also reported in bone metastasis [150] and ectopic bone resorption [151]. In bone development angiogenesis and bone resorption are closely associated with each other. Vascular endothelial growth factor (VEGF), the most critical growth factor for angiogenesis, has been found to stimulate osteoclast activity [152]. Therefore, osteoclast activity and angiogenesis can be regulated by the common mediators such as VEGF.

Based on the results obtained in this study, it could be concluded that the age-related periosteal structure and cell populations are site-specific. The diaphyseal periosteum showed age-related degeneration, whereas, the metaphyseal periosteum is more destructive in older age. Macrophages in the periosteum may play a dual, age dependent role in bone metabolism with osteogenesis in young rats and osteoclastogenesis in aged rats.

**Acknowledgements**

We would like to thank Ms Sarah Whitehouse, a statistician in our institute for assisting the statistic analysis of the data.

## *PAPER TWO*

**Structural and Cellular Features in Metaphyseal and Diaphyseal Periosteum of Osteoporotic Rats**

Wei Fan, Stefan AW Bouwense, Ross Crawford, Yin Xiao

**Suggested Statement of Contribution of Co-Authors for Thesis by Published Papers:**

| Contributors | Statement of contribution* |
|---|---|
| Wei Fan | Performed laboratory experiments, data analysis and interpretation. Wrote the manuscript. |
| | |
| | |
| Stefan Bouwense | Perform part of laboratory experiments and data collection |
| Ross Crawford | Involved in the conception and design of the project. Assisted in reviewing the manuscript. |
| Yin Xiao | Involved in the conception and design of the project. Assisted in sample collection, technical guidance and reviewing the manuscript |

**Principal Supervisor Confirmation**

**I have sighted email or other correspondence from all co-authors confirming their certifying authorship**

**Name** **Signature** **Date**

**Abstract**

Despite the important physiological role of periosteum in the pathogenesis and treatment of osteoporosis, little is known about the structural and cellular characteristics of periosteum in osteoporosis. To study the structural and cellular differences in both diaphyseal and metaphyseal periosteum of osteoporotic rats, samples from the right femur of osteoporotic and normal female Lewis rats were collected and tissue sections were stained with hematoxylin and eosin, antibodies or staining kit against tartrate resistant acid phosphatase (TRAP), alkaline phosphatase (ALP), vascular endothelial growth factor (VEGF), von Willebrand (vWF), tyrosine hydroxylase (TH) and calcitonin gene-related peptide (CGRP). The results showed that the osteoporotic rats had much thicker and more cellular cambial layer of metaphyseal periosteum compared with other periosteal areas and normal rats ($p<0.001$). The number of $TRAP^+$ osteoclasts in bone resorption pits, $VEGF^+$ cells and the degree of vascularization were found to be greater in the cambial layer of metaphyseal periosteum of osteoporotic rats ($p<0.05$), while no significant difference was detected in the number of $ALP^+$ cells between the two groups. Sympathetic nerve fibers identified by TH staining were predominantly located in the cambial layer of metaphyseal periosteum of osteoporotic rats. No obvious difference in the expression of CGRP between the two groups was found. In conclusion, periosteum may play an important role in the cortical bone resorption in osteoporotic rats and this pathological process may be regulated by the sympathetic nervous system.

## Introduction

The mineralization and development of bone tissue is a dynamic process determined by the balance between the bone formation and resorption occurring on periosteal and endosteal surfaces [153-155]. This modeling and remodeling process will alter the size, shape, internal structure, total mass, and finally the mechanical strength of bone. The thickness of cortical bone, a crucial feature in determining bending strength of bone, is defined both by periosteal and endosteal bone apposition and resorption. Osteoporosis is a metabolic disorder of the bone whereby the balance between bone formation and resorption has shifted such that the rate of bone resorption exceeds bone formation, resulting in net bone loss, trabecular and cortical thinning and porosity [156].

Periosteum is a dense connective tissue membrane covering the outer surface of all bones, except at the joint of long bones. In both normal and pathological processes the periosteum plays a pivotal role in both bone formation and fracture healing, in conjunction with the involvement of other important factors such as growth factors and mechanical loading [9, 20, 35]. Periosteum is a highly vascularized tissue which contains both osteogenic and chondrogenic progenitor cells, as well as other related bioactive factors [9, 14, 23]. The osteogenic function of periosteum determines the amount of *de novo* postnatal periosteal bone formation defining the thickness and strength of cortical bone. Previous researchers have revealed an age related structural and cellular degeneration in periosteum [11, 19, 136-138]. However, in osteoporosis, which is characterized by decreased bone strength and a high incidence of fractures, the changes occurring in the periosteum are not well characterized and require further investigation. Although estrogen deficiency is believed to be an intrinsic cause of osteoporosis, the process and mechanism of bone loss in osteoporosis remain unclear. Most researchers have emphasized the bone resorption activity occurring in the endocortical or intramedullary area, but there are no reports in the current literature describing the structural and cellular changes in periosteum of osteoporosis. The purpose of this study is therefore to characterize the structural and cellular differences in both diaphyseal and metaphyseal periosteum of osteoporotic

rats.

## Materials and Methods

### Animal samples and slices

This study was carried out in accordance with the guidelines of the University Animal Ethics Committee. Osteoporosis was induced by ovariectomy of three-month old female Lewis rats, followed by a 30% caloric reduced diet and four months to develop osteoporosis [19, 157]. The induced osteoporosis has been confirmed in our previous study [154]. Four osteoporotic rats and three normal female Lewis rats (sham-operated group in which ovaries were exposed but only equal volumes of fat tissue was excised), all in 7-months old, were utilized in this experiment. The right tibia and femur were retrieved for the following experiments. Tibia were scanned using a Micro CT machine (μCT 40, SCANCO Medical AG, Brüttisellen, Switzerland) to confirm the osteoporosis induced in rats. Then both tibia and femur were fixed in 4% paraformaldehyde for 12 hours at room temperature, then decalcified in 10% EDTA and embedded in paraffin. Serial sections of sagittal slices, 5 μm thick, were cut from the paraffin blocks with a microtome (Leica Microsystems GmbH, Germany). Only slices near the central sagittal plane were used for subsequent experiments.

### Structural observation

After Micro CT scanning, the three dimensional (3D) image of trabecular bone in proximal end of tibia from both normal and osteoporotic rats was reconstructed and related histomorphometrical parameters, such as normalized trabecular bone volume (BV/TV), trabecular bone thickness (Tb.Th), trabecular bone separation (Tb.Sp), trabecular bone number (Tb.N) and conectivity density (Conn.D), were calculated by the software package of the Micro CT machine. These images and parameters were compared between two groups to confirm the osteoporosis induced in rats. On the other hand, slices from tibia were stained with hematoxylin and eosin (H&E) (HD Scientific Supplies, Australia), and the trabecular bones in proximal end were

observed under a microscope (Carl Zeiss Microimaging GmbH, Germany) to further confirm the induced osteoporosis.

For periosteum observation, 1 mm lengths of periosteum from diaphyseal area and 1mm lengths of periosteum from proximal metaphyseal area were selected for analysis (Fig. 1). According to the difference of cell and fiber distribution in the periosteum, the cambial and fibrous layers were defined [59]. The thickness of fibrous and cambial layers on the middle line perpendicular to the periosteum surface in each microscopic field, as well as the cell number of each layer throughout each periosteal area, were measured using Axion software (Carl Zeiss) under a microscope (Carl Zeiss). Data from each animal of the osteoporotic and normal groups were recorded for further analysis.

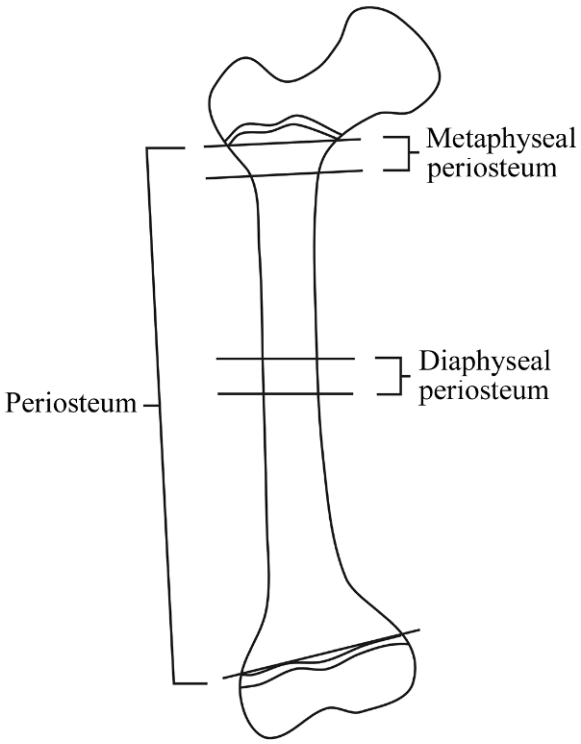


Figure 1: Illustration of the periosteal sites observed in this study

**Immunohistochemistry**

Osteoclasts were identified using a TRAP (tartrate-resistant acid phosphatase) staining kit (Sigma-Aldrich, Australia); ALP (Alkaline Phosphatase) specific antibody (Goat anti-mouse, Sigma-Aldrich, Australia) was used to identify osteogenic cells; VEGF

specific antibody (mouse anti-human, R&D System, Inc., USA) was used to identify VEGF positive cells; vWF specific antibody (mouse anti-human, Chemicom International Inc., USA) was used to identify blood vessels; TH (Tyrosine Hydroxylase) specific antibody (Rabbit anti-rat, Serotec, UK) was used to identify sympathetic nerve fibers; and CGRP (Calcitonin gene-related peptide) specific antibody (Goat anti-rat, Serotec, UK) was used to identify sensory nerve fibers. To validate the results, each experiment was repeated at least three times.

Prior to immunoperoxidase staining, endogenous peroxidase activity was quenched by incubating the tissue sections in 3% $H_2O_2$ for 20 minutes. All sections were blocked with 10% swine serum for 1 hr. The enzymatic treatment was used to expose epitopes by incubating the slices with proteinase K (DakoCytomation, USA,) for 10 minutes at room temperature. Sections were incubated with optimal dilution of primary antibody ALP (1:300), VEGF (1:300), vWF (1:500), TH (1:400) and CGRP (1:500) at $4^oC$ overnight, and the following day incubated for 15 minutes with a biotinylated swine-anti-mouse, rabbit, goat secondary antibody (DAKO Multilink, USA), followed by 15 minutes incubation with horseradish perioxidase-conjugated avidin-biotin complex (ABC). Antibody complexes were visualized after the addition of a buffered diaminobenzidine (DAB) substrate for 4 minutes; the reaction stopped by immersing and rinsing of sections in PBS. Sections were then lightly counterstained with Mayer's haematoxylin and Scott's Blue for 40 seconds each, in between 3 minute rinses with running tap water. Following this, the sections were dehydrated with ascending concentrations of ethanol solutions, cleared with xylene and mounted with a cover slip using DePeX mounting medium (BDH Laboratory Supplies, UK). Standard TRAP staining procedure was done according to the manufacturer's instructions. Controls for the immunohistochemical staining procedures included conditions in which (a) the primary antibody was omitted for staining procedure, and (b) an irrelevant antibody (IgG), not present in the test sections, was utilized.

At ×200 magnification and with the aid of the AxioVision software, the number of positive cells from each cell population in each periosteal area was counted. Three

different slices from each rat from the two groups were observed and the data recorded for subsequent analysis. The number of active $TRAP^+$ osteoclasts in bone resorption pits, $ALP^+$ and $VEGF^+$ cells were normalized against the total cell number and expressed as positive cell number per total of 100 cells from each sample in order to counter the effect that variations of total cell numbers from the two groups had on the positive cell counts. The blood vessel counts were normalized to the vessel number in a $0.03mm^2$ periosteal area. As for nerve staining, spatial distribution was observed and described.

**Statistical analysis**

The data from both normal and osteoporotic groups were compared using the Student's *t*-test. The data from different periosteum layers and periosteal areas of osteoporotic rats were subjected to one-way ANOVA and SNK tests and results were regarded as significance at $p \leq 0.05$. Data analysis was performed using the SPSS software (SPSS Inc, USA).

**Results**

**Structural differences between osteoporotic and normal rats**

Osteoporotic rat model was further confirmed by the significantly lower trabecular bone volume, thickness, number, connectivity density and higher trabecular bone separation when compared with normal rats ($p<0.05$)(Table 1, Fig. 2). Typical fenestrated trabeculae were demonstrated in the osteoporotic rat model (Fig. 2).

No statistically significant difference was found in the thickness and cell numbers between osteoporotic and normal rats of the diaphyseal periosteum, except for the thickness of the fibrous layer ($p<0.05$)(Fig. 3). In the metaphyseal periosteum, osteoporotic rats had thicker and more cellular cambial layers compared with normal rats ($p<0.001$) (Fig. 3). Although there was no significant difference in the thickness of the fibrous layer ($p>0.05$), the number of cells in the fibrous layer of osteoporotic rats in the metaphyseal area was higher than normal rats ($p<0.001$). In osteoporotic rats the metaphyseal periosteum was significantly thicker and more cellular than in

the diaphyseal periosteum, especially the cambial layer of metaphyseal periosteum ($p<0.05$) (Fig. 3).

Table 1 Histomorphometrical comparison of the tibia bone from osteoporotic and normal rats

| | BV/TV (%, x ±SD) | Tb.Th(mm, x ±SD) | Tb.Sp(mm, x ±SD) | Tb.N (1/mm, x ±SD) | Conn.D($1/mm^3$) (x ±SD) |
|---|---|---|---|---|---|
| Osteoporotic* | 6.24±0.2 | 0.07±0.02 | 1.36±0.16 | 0.78±0.08 | 15.85±0.51 |
| Normal | 20.5±1.4 | 0.1±0.02 | 0.3±0.05 | 3.11±0.35 | 51.02±10.49 |

*: $p<0.05$.

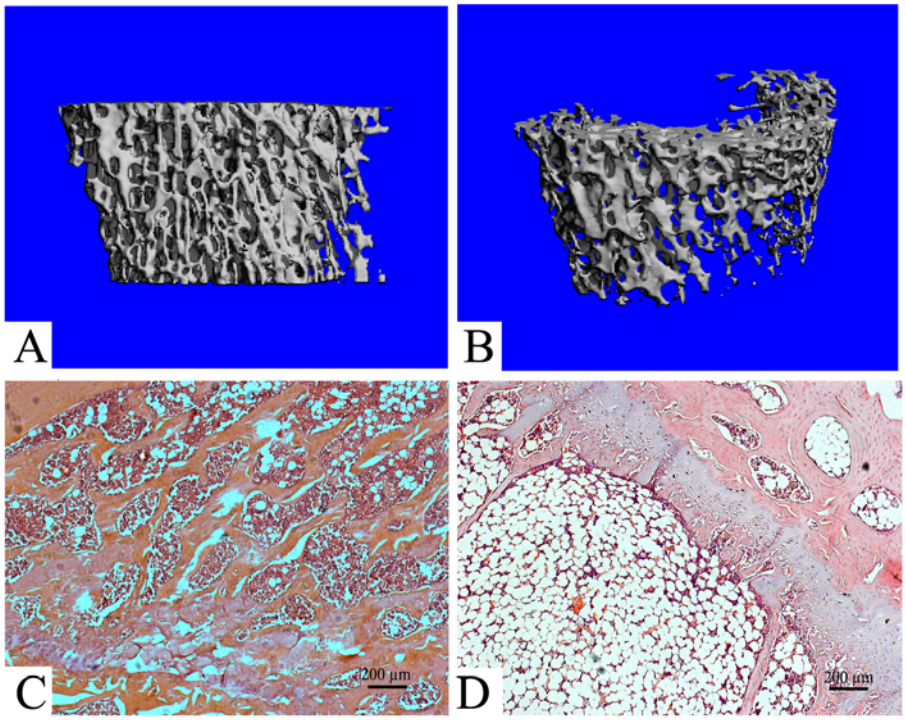


Figure 2: Histological validation of animal models

Osteoporotic rat model was confirmed by the significantly loss of trabecular bones (B)

compared with normal rats (A) in 3D reconstructed images; Typical fenestrated trabeculae were demonstrated in the osteoporotic rat model (D) in contrast to normal rats (C). H&E staining pictures (C&D) were taken at 40 × magnification.

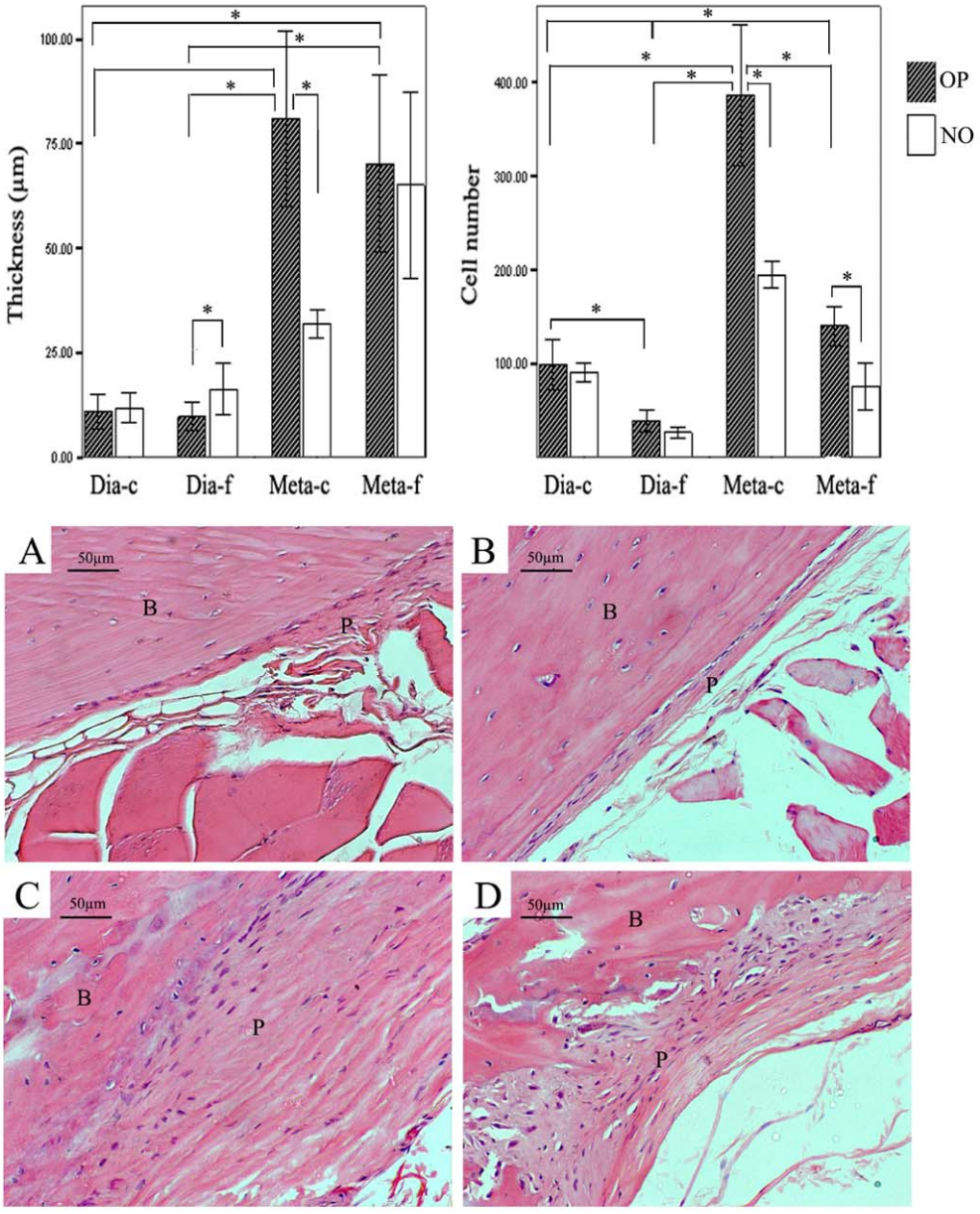


Figure 3: Diagrams and H&E staining (×200) of diaphyseal and metaphyseal periosteum from normal and osteoporotic rats. (A) diaphyseal periosteum from normal rats; (B) diaphyseal periosteum from osteoporotic rats; (C) metaphyseal

periosteum from normal rats; (D) metaphyseal periosteum from osteoporotic rats.
(NO: normal rats; OP: osteoporotic rats; Dia-c: cambial layer of diaphyseal periosteum; Dia-f: fibrous layer of diaphyseal periosteum; Meta-c: cambial layer of metaphyseal periosteum; Meta-f: fibrous layer of metaphyseal periosteum; * : $p<0.05$. In pictures: B: bone tissue; P: periosteum; C: cambial layer; F: fibrous layer.)

**$TRAP^+$ osteoclasts in periosteum**

The normalized cell number of active $TRAP^+$ osteoclast in bone resorption pits from the cambial layer was used for this analysis. The osteoporotic rats had significantly more active $TRAP^+$ osteoclasts in both diaphyseal and metaphyseal periosteal areas ($p<0.001$) compared to normal rats (Fig.4 & 5). In osteoporotic rats, the cambial layer of metaphyseal periosteum had similar $TRAP^+$ osteoclast density in bone resorption pits when compared with the cambial layer of diaphyseal periosteum ($p>0.05$) (Fig.4).

**ALP expression in periosteum**

The normalized $ALP^+$ cell count was used for this analysis. No significant difference was found in the ALP expression in either diaphyseal and metaphyseal periosteum of osteoporotic rats compared to normal rats ($p>0.05$) (Fig.4 & 5). No difference was detected between the cambial and fibrous layers in diaphyseal and metaphyseal periosteum respectively. Nor was there any significant difference to the ALP expression between different periosteal sites in osteoporotic rats ($p>0.05$) (Fig.4).

**VEGF expression in periosteum**

The normalized $VEGF^+$ cell count was used for this analysis. Significantly more $VEGF^+$ cells were found in the cambial layer of the metaphyseal periosteum of osteoporotic rats compared to normal rats ($p<0.001$) (Fig.4 & 5). No significant difference was found in other periosteal areas. In osteoporotic rats the cambial layer of both the metaphyseal and diaphyseal periosteum had more VEGF positive cells

than the fibrous layers in both periosteal areas, whilst the number of VEGF positive cells in the cambial layer of metaphyseal periosteum was higher than that in the cambial layer of diaphyseal periosteum ($p<0.001$) (Fig.4).

**Blood vessels revealed by vWF**

The normalized blood vessel count was used for this analysis. Osteoporotic rats had higher degree of vascularization in the cambial layers of both the diaphyseal and metaphyseal periosteum compared to normal rats ($p<0.001$), especially in the metaphyseal periosteum (Fig.4 & 5). No significant difference was found in the fibrous layer of either periosteal area between the two groups. In osteoporotic rats, the cambial layer of metaphyseal periosteum had a higher degree of vascularization than the fibrous layer ($p<0.001$) (Fig.4 & 5).

**Sympathetic nerves revealed by TH**

TH staining revealed that the distribution of sympathetic nerve fibers was mainly present in osteoporotic rats, predominantly in the cambial layer of periosteum (Fig. 5). A slight TH stain was observed in the cambial layer of metaphyseal area of normal rat. No obvious staining was detected in the fibrous layer or diaphyseal area.

**Sensory nerves revealed by CGRP**

Sensory nerve fibers identified by CGRP antibodies were found in both osteoporotic and normal rats (Fig. 5). There was no discernible difference in the expression of CGRP between the two groups in the different periosteal areas. However, in normal rats $CGRP^+$ nerve fibers appeared to be distributed in both fibrous and cambial layers, whereas in osteoporotic rats most $CGFP^+$ nerve fibers were present in the cambial layer of the metaphyseal area.

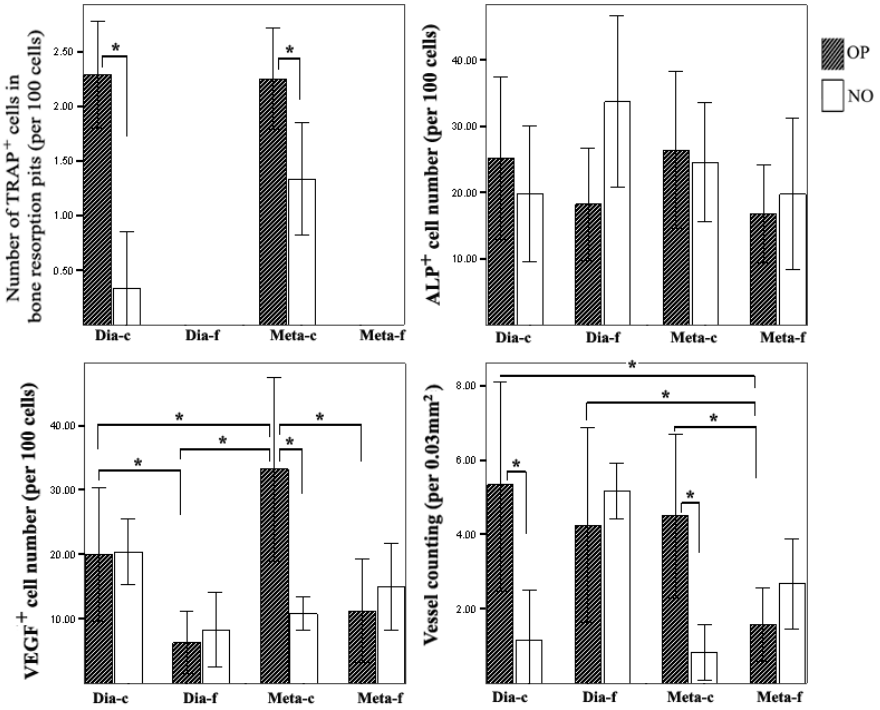


Figure 4: Cellular differences in diaphyseal and metaphyseal periosteum between osteoporotic and normal rats. (NO: normal rats; OP: osteoporotic rats; Dia-c: cambial layer of diaphyseal periosteum; Dia-f: fibrous layer of diaphyseal periosteum; Meta-c: cambial layer of metaphyseal periosteum; Meta-f: fibrous layer of metaphyseal periosteum; ∗:$p<0.05$)

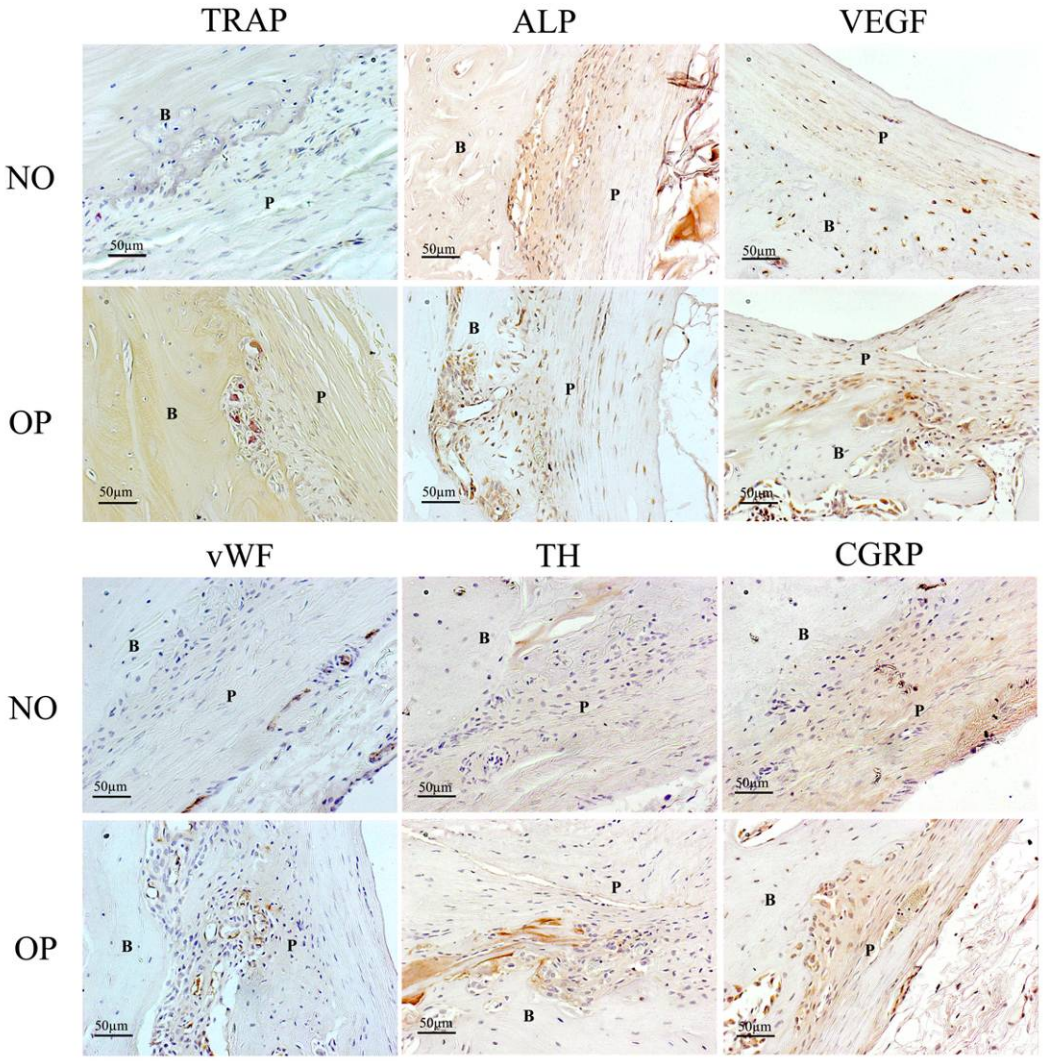


Figure 5: Immunohistochemical staining (×200) of metaphyseal periosteum from normal and osteoporotic rats. (NO: normal rats; OP: osteoporotic rats; B: bone tissue; P: periosteum)

**Discussion**

Osteoporosis is characterized by a negative balance of bone metabolism which leads to a decreased bone mass with subsequent thinning of the trabecular and cortical bone and a significantly greater risk of bone fractures. The cortical bone expansion through the periosteum is the most effective way to increase bone strength and protect against fractures. Despite the synergistical role and potential significance of periosteum in the pathogenesis and treatment of osteoporosis, little is known about this role of the periosteum in osteoporosis. Knowledge of periosteal structural and

cellular characteristics would greatly enhance our understanding of the disorder and aid in the development of more specific and effective treatments.

Osteoporosis patients are at a greater risk of bone fractures, and these fractures have different patterns compared with those in patients without osteoporosis [158]. Most fall related fractures in osteoporotic and elderly patients begin in the cortex of the metaphyses or former epiphyses, intertrochanteric, and femoral neck cortices; they never begin in metaphyseal spongiosa and rarely in the diaphyseal cortex [158]. This phenomenon indicates a fundamental difference in the mechanical environment and bone strength along the bone axis. It is known that endosteal or intramedullary bone resorption activity is greater in osteoporotic bone compared to normal bone, which is thought to be the main cause of net bone loss [159]. However, the synergic role of the periosteum in osteoporosis is not well understood. In an attempt to further the understanding of the function of periosteum at different periosteal sites in osteoporosis, we investigated the basic structure and related cell populations in the diaphyseal and metaphyseal periosteum of osteoporotic rats.

In the general H&E stain and histomorphometry observations, the thickness and cell numbers in the cambial layer of metaphyseal periosteum from osteoporotic rats were found to be much greater compared to normal rats, despite both groups being of similar age (7 months). This structural difference appears to be closely related to the different cell populations found in the two cohorts, an observation confirmed by the immunohistochemical staining.

To our knowledge, no previous studies have documented the distribution of active osteoclasts in the periosteum covering osteoporotic bones, although periosteal bone turnover activity and osteoclast distribution have recently been documented in the femoral neck in a number of adult rhesus and Japanese macaques [21]. In our study, periosteal osteoclasts were identified using TRAP specific cell markers. Immunohistochemical observations in this study found the evidence of a noticeable increased fraction of active osteoclasts in the cambial layer of both diaphyseal and metaphyseal periostea from osteoporotic rats. As these observed osteoclasts were found in bone resorption pits on eroded bone surfaces, which means they are active

osteoclasts, it might suggest more serious bone resorption activities on both diaphyseal and metaphyseal cortical bone surfaces of osteoporotic rats compared to the normal rats. As the thickness of cortical bone in metaphyseal area is thinner than the diaphyseal area [160], the metaphyseal bone could be more susceptible of bone fractures than the diaphyseal in osteoporosis conditions. This phenomenon could potentially have clinical relevance as more fractures are reported in the metaphyseal areas compared to the diaphyseal areas in osteoporotic patients [158]. Age-related bone loss often shows the following morphological changes including decreased periosteal apposition, endosteal bone loss, bone loss on the trabecular, endocortical and intracortical surfaces, although some controversies have been reported on periosteal apposition, which shows that periosteal apposition continues, even after menopause, and may partly offset the bone resorption on the endosteal surface [142]. However, the findings in our study suggest that bone resorption activity in the periosteum is greater in osteoporotic rats compared to normal rats and that the behavior of the osteoclast cells is destructive. On the other hand, osteogenic activity demonstrated by the ALP expression in this experiment revealed no significant difference was detected in either the different periosteal sites of osteoporotic rats or between the two groups of rats. Given the increased number of active osteoclasts in the periosteum of osteoporotic rats, the relatively stable osteogenic activity might therefore be inadequate to offset the bone resorption, which would consequently incur the net bone loss and strength decrease. This failed adaptation of bone to the bone resorption could be the result of the estrogen withdrawal in the osteoporotic rats since the estrogen is believed to be able to preserve the bone mass and decrease the bone resorption activity [161-162]. According to these findings, periosteum seems playing more destructive roles in osteoporosis, and new periosteum-targeting medicines or operations could be developed to suppress the bone resorption and enhance the osteogenic activities in periosteum, especially in metaphyseal area.

VEGF is an important growth factor which is reported to be involved in angiogenic, osteogenic and osteoclastogenic processes [152, 163-164]. Bone development, angiogenesis, bone formation and bone resorption are all closely associated processes

with VEGF known to stimulate osteoclast activity [152, 163-164]. Osteoclast activity and angiogenesis may therefore be regulated by a common mediator such as VEGF. The data in our study seems to support this view since a higher expression of VEGF, as well as more $vWF^+$ blood vessels, was found in the vicinity of active $TRAP^+$ osteoclasts in osteoporotic rats compared to normal rats. The increase of VEGF expression and periosteal vascularization in the periosteum of the osteoporotic rats may be related to the increased bone resorptive activity in these periosteal areas.

The reason for the increased expression of sympathetic nerve fibers in the periosteum in osteoporosis is unclear, although it is well documented that sympathetic nerve fibers are present in both the periosteum and bone [25-26]. Sympathetic innervation of periosteum and bone contributes to the regulation of bone cell activity and, therefore, the eqiulibrium between bone modeling and remodeling [27]. It is known that surgical and chemical sympathectomy can both modulate bone cell function. However, the sympathetic nervous system (SNS) can give rise to both anabolic and catabolic effects [28-31] and its role in regulating bone remodeling is, therefore, controversial. In this study, the distribution of sympathetic nerve fibers was demonstrated by employing an antibody against an SNS specific marker, tyrosine hydroxylase, which is expressed in adrenergic fibers. More sympathetic nerve fibers were found in the cambial layer of periosteum of osteoporotic rats compared to normal rats and this finding was also in accordance with the distribution of $TRAP^+$, $ALP^+$, $VEGF^+$ cells and blood vessels. The co-existence of nerve fibers and various cell populations indicates that sympathetic nerves in the periosteum are involved in the pathogenesis of osteoporosis by interacting with, and possibly regulating, osteogenic, osteoclastogenic and angiogenic factors. Sensory nerve fibers identified by CGRP antibody were found similarly expressed in both osteoporotic and normal rats, although the distribution is slightly different between the two groups. It is generally accepted that CGRP can promote osteogenesis and decrease bone resorption [32, 165]. CGRP has also been shown to inhibit osteoclastic resorption like calcitonin [165]. The similar expression of CGRP in both osteoporotic and normal rats suggests a similar osteogenesis-related role for CGRP in the two groups.

Based on the findings from this study, it could be concluded that the periosteum of osteoporotic rats differs from normal rats both in terms of structure and cell populations. This is especially evident in the cambial layer of metaphyseal periosteum. Bone resorption appears to be more active in the periosteum of osteoporotic rats compared to normal rats, whereas bone formation activity is comparable between the two groups. The dysregulation of bone resorption and formation in the periosteum, characteristic of the pathogenesis of osteoporosis, may therefore be the effect of the interaction between various neural pathways and the cell populations residing within it. The findings of this study were observed from rat osteoporosis model. It is known that there are some differences between human and rat in bone remodelling and fragility due to the differences in bone biology and physiology, therefore, these findings need to be further validated in mammal models to be relevant to human osteoporosis.

**Acknowledgments:**

We would like to thank Ms Wei Shi for her technique support in immunohistochemical work and Mr. Thor Friis for his proof reading of the entire manuscript. The Stichting Nijmeegs University Funds (SNUF) and the Reumastichting provided financial support for the internship of Stefan AW Bouwense. Wei Fan is on a Faculty Scholarship from the Queensland University of Technology

## *PAPER THREE*

**The ratio of VEGF/PEDF expression in bone marrow mesenchymal stromal cells regulates neovascularization**

Wei Fan, Ross Crawford, Yin Xiao

**Suggested Statement of Contribution of Co-Authors for Thesis by Published Papers:**

| Contributors | Statement of contribution* |
|---|---|
| Wei Fan | Performed laboratory experiments, data analysis and interpretation. Wrote the manuscript. |
| | |
| | |
| Ross Crawford | Involved in the conception and design of the project. Assisted in sample collection, reviewing the manuscript. |
| Yin Xiao | Involved in the conception and design of the project. Assisted in sample collection, technical guidance and reviewing the manuscript |

**Principal Supervisor Confirmation**

**I have sighted email or other correspondence from all co-authors confirming their certifying authorship**

**Name** **Signature** **Date**

**Abstract**

Angiogenesis is a well balanced process controlled by pro- and anti-angiogenic factors. Vascular endothelial growth factor (VEGF) is a major pro-angiogenic factor, while pigment epithelial-derived factor (PEDF) is the most potent natural angiogenesis inhibitor. In this study, BMSCs were isolated and cultured in angiogenic media containing 20ng, 40ng and 80ng/ml VEGF. The alterations of VEGF/PEDF expression pattern and endothelial cell differentiation of BMSCs were assessed. BMSCs cultured under cobalt chloride ($CoCl_2$)-induced hypoxia conditions with normal or angiogenic media were also investigated. To further test the ability of BMSC to induce vascularization in vivo, the treated cells were injected subcutaneously into SCID mice. Results showed that PEDF was more prominently expressed than VEGF in BMSCs ($p<0.05$), which was reverse to the expression in HUVECs. The ratio of VEGF/PEDF in BMSCs increased when VEGF concentration reached 40ng/ml in the culture media, but deceased at the 80ng/ml ($p<0.05$). Under $CoCl_2$-induced hypoxia conditions, the VEGF/PEDF ratio of BMSCs increased significantly in both normal and angiogenic media ($p<0.05$). No expression of endothelial cell markers was found in BMSCs cultured in either normxia or hypoxia conditions ($p>0.05$). In vitro and in vivo vascularization study showed that the $CoCl_2$-treated BMSCs could stabilize and induce much higher degree of vascularization than BMSCs or BMSCs treated with 20ng/ml VEGF ($p<0.01$). These results indicate that BMSCs are important regulators in angiogenesis, but unable to differentiate into endothelial cells under angiogenic or hypoxia culture conditions.

## Introduction

Angiogenesis is thought to be a process balancing between pro- and anti-angiogenic factors. Vascular endothelial growth factor (VEGF) is one of the most important pro-angiogenic factor and could initiate angiogenic differentiation of various endothelial progenitor cells (EPCs)[119]. VEGF could be expressed by a broad range of cells including bone marrow mesenchymal cells (BMSCs) [166]. On the other hand, pigment epithelial-derived factor (PEDF) which was initially purified from the conditioned media of human fetal retinal pigment epithelial (RPE) cells is the most potent natural angiogenesis inhibitor [167]. PEDF is also considered to be the key factor associated with avascularity of the cornea [167]. In the vascualrization of retina, the balance between VEGF and PEDF expression plays a very crucial role [168]. Despite the importance of VEGF and PEDF expression in the process of angiogenesis, very few information could be found in literatures about the VEGF/PEDF expression pattern in BMSCs in relation to angiogenesis. Furthermore, as the BMSCs are believed involved in the various angiogenic environments [169], whether VEGF/PEDF expression pattern could be influenced by the extracellular VEGF alone or together with oxygen stress and whether any changes in this expression pattern could influence the endothelial cell differentiation of BMSCs are all questions needing further investigations.

Bone marrow comprises a dual stem or progenitor cell system: the hematopoietic cell system and non-hematopoietic mesenchymal cell system [110-111]. When cultured in vitro, BMSCs rapidly adhere and can be easily separated from the non-adherent hematopoietic cells through repeated washing. Hematopoietic stem cells (HSCs) in bone marrow are the reservoir of various blood cells, such as erythrocytes, leukocytes, macrophages or platelets, and they also contain endothelial progenitor cells (EPCs) which can become mature endothelial cells when necessary [112-113]. BMSCs, when cultured in vitro, are negative for CD45, CD14, CD31 and CD34 but positive for CD105, CD 44, CD73 and CD90. They are a mixture of multipotent progenitor cells which can differentiate into various other mesodermal cells, such as osteoblasts, chondrocytes, fibroblasts or adipocytes [114]. However, whether the in vitro cultured

BMSCs could be differentiated into endothelial cells has long since been a controversial and unsettled question [170-171]. The information about the endothelial cell differentiation of BMSCs in hypoxia situations is also lacking.

In this study, the VEGF/PEDF expression pattern of BMSCs with or without supplementary VEGF and the effect of the VEGF/PEDF expression pattern on the endothelial cell differentiation of BMSCs under normoxia and cobalt chloride-induced hypoxia situations were investigated. The human umbilical vein endothelial cells (HUVECs) were used as the positive control when necessary.

## Materials and methods

### Cells and cell culture

Bone marrow was obtained from patients in orthopaedic department of Prince Charles Hospital with informed consent and ethics approval from the Ethics Committee of Queensland University of Technology. Mononuclear cells (MNCs) were isolated from the bone marrow by density gradient centrifugation over Lymphoprep (Axis-shield PoC AS, Oslo, Norway) according to the manufacturer's protocol. The MNCs were plated into the culture flasks and cultured in Dulbecco's Modified Eagle Medium (DMEM; Invitrogen Australia Pty Ltd., Mt Waverley, VIC, Australia) containing 10% (v/v) fetal calf serum (FCS; InVitro Technology, Noble Park, VIC, Australia) and 1% (v/v) penicillin/streptomycin (Invitrogen). The unattached hematopoietic cells were removed through changing media. When reaching the 70-80% confluence, the attached mesenchymal cells were subcultured after treatment with 0.25% trypsin (Invitrogen) and 1mM EDTA (Invitrogen). Only P2-P5 mesenchymal cells were used in this study. Human umbilical vein endothelial cells (HUVECs; Clonetics, San diego, CA, USA) were used as the positive control when necessary. HUVECs were cultured in a defined endothelial cell growth medium containing VEGF, FGF-2, IGF-1, EGF, ascorbic acid and hydrocortisone (EGM-2; Lonza Australia Pty Ltd., Mt Waverley, VIC, Australia) supplemented with 2% FCS. The medium was changed every three days until the cells were confluent.

**Endothelial cell differentiation of BMSCs under different extracellular VEGF concentrations**

BMSCs from five patients (one female and four male patients with the age ranging from 40y to 78y and averaging 61y) were included in this experiment. When BMSCs reached 80% confluence in the flask, angiogenic differentiation media with different VEGF (R&D Systems, Inc., Minneapolis, MN, USA) concentrations (DMEM supplemented with 5% FCS and 20ng, 40ng and 80ng VEGF per ml respectively) were added and changed every three days. After 6 days culturing, real time q-Polymerase Chain Reaction (real-time q-PCR), western blot, immunohistochemical staining and flow cytometry were conducted on these BMSCs. The ability to form vessel-like structures in vitro of these BMSCs was tested on Matrigel.

**Endothelial cell differentiation of BMSCs under cobalt chloride-induced hypoxia**

BMSCs from six patients (two female and four male patients with the age ranging from 47y to 76y and averaging 57y) were included in this experiment. When BMSCs reached 80% confluence in the flask, they were subcultured and equally allocated into following three groups: BMSCs cultured in normal DMEM containing 5% FCS; BMSCs cultured in DMEM containing 5% FCS and 100μM cobalt chloride; BMSCs cultured in DMEM containing 5% FCS, 100μM cobalt chloride and 20ng VEGF/ml. The media in each group were changed every three days and on the day 6, real-time q-PCR, western blot, immunohistochemical staining and flow cytometry were conducted on these BMSCs. The ability to form vessel-like structures in vitro of these BMSCs was tested on Matrigel.

**Real time q-Polymerase chain reaction**

On the day 6 of culturing, total RNA and cDNA of HUVECs and BMSCs cultured under different conditions were obtained using a cDNA reverse transcription kit (Invitrogen). The total cDNA were used to do the real time q-PCR. Briefly, a 12.5μl

SYBR green q-PCR master mix (AB Applied Biosystems, Melbourne, Australia) was mixed with 5 µl Ultrapure water (Invitrogen), 2.5 µl reverse and forward primers (Sigma-Aldrich Pty. Ltd**,** Castle Hill, NSW, Australia) and 2.5 µl cDNA to make a 25 µl final reaction system in a 96-well PCR clear plate. The gene expressions of PEDF, VEGF, CD31, VEGF receptor 2 (VEGFR2), von Willebrand factor (vWF), endothelium nitric oxide synthases (eNOS) were detected. The 18s gene was used as the house keeping gene. The sequences of forward and reverse primers of each gene observed are detailed in Table 1. Each sample was added in plates in triplicate and the PCR was run on a q-PCR machine (7300 sequence detection system, AB Applied Biosystems, Melbourne, Australia) according to the manufacturer's instruction. The final results came out as average cycle numbers (Cts) which was normalized against Cts of 18s by subtraction. The final relative expression of each target gene was calculated using the following formula: $2^{-(\text{normalized average Cts})} \times 10^4$.

Table 1 Primer sequences for the gene observed in this study

| genes | Primer seqences | Gene bank No. |
|---|---|---|
| PEDF | For.TTCAAAGTCCCCGTGAACAAG | AF400442 |
| | Rev.GGATCGCACCCGGTACAG | |
| VEGF | For.5'GCTGTCTTGGGTGCATTGG | E14233 |
| | Rev.5'GCAGCCTGGGACCACTTG | |
| VEGFR2 | For.5'CAAACGCTGACATGTACGGTCTA | AF063658 |
| | Rev.5'CCAACTGCCAATACCAGTGGAT | |
| CD31 | For. 5' TGGAGCACAGTGGCAACTACAC | M37780 |
| | Rev.5'CCACGATGCTGCTGACCTT | |
| vWF | For.5'AGCCCCACCACTCTGTATGTG | NM_000552 |
| | Rev.GTAGCCTGCTGCAGTAGAAATCG | |
| eNOS | For.5'CGGCATCACCAGGAAGAAGA | AF400594 |
| | Rev.5'CATGAGCGAGGCGGAGAT | |
| 18s | For.5'TTCGGAACTGAGGCCATGAT | M10098 |
| | Rev.5'CGAACCTCCGACTTCGTTC | |

**Western blot**

On the day 6 of culturing, total cell proteins were obtained using a cell lysis buffer supplemented with proteinase inhibitors (Roche Ltd., Dee Why, NSW, Australia). The protein concentration was determined by a BCA protein assay kit (Sigma) and 10μg proteins from each sample were used to do the western blot. Briefly, the protein samples were loaded onto SDS-page gels and run at 125V for 1h. Then the proteins were transferred to a nitric cellulous membrane (Pall corporation, East Hills, NY, USA) using semi-dry transfer method. The VEGF, PEDF and α-tubulin were recognized by VEGF (1:2000, rabbit anti-human, Thermo Fisher Scientific, Fremont, CA, USA), PEDF (1:2000, mouse anti-human Millipore, North Ryde, NSW, Australia) and α-tubulin (1:5000, rabbit anti-human, Abcom Inc., Cambridge, MA, USA) primary antibodies which then bound to the HRP-conjugated anti-mouse or rabbit secondary antibodies ($1:10^5$, Thermo Fisher Scientific, Fremont, CA, USA). Super-signal substrate (Thermo Fisher Scientific, Fremont, CA, USA) was used to visualize the band through eliciting green fluorescence which could leave band images on X-ray films. All operations were performed under the same conditions.

**Flow cytomytry and immunohistochemistry**

To detect endothelial cell markers, flow cytomytry and immunohistochemistry were performed. For the flow cytomtry, 105 cells were resuspended in 3% PBS/BSA at 4°C and incubated with CD31 (mouse anti-human, 1:100, Invitrogen, Mt Waverley, VIC, Australia) or VEGFR2 (goat anti-human, 1:100, R&D Systems, Inc., Minneapolis, MN, USA) primary antibody for 30mins on ice. After incubation and repeated wash for at least three times with 3% PBS/BSA, cells were resuspended and incubated with a biotinylated universal secondary antibody (swine-anti-mouse, rabbit and goat, ready to use, DAKO Multilink, CA, USA) for 30mins on ice. After washing away secondary antibody, the PE-conjugated anti-biotin antibody (1:200, Jackson ImmunoResearch Laboratories, Inc., West Grove, PA, USA) was added into the cell suspension and incubated for another 30mins. After totally removing the antibodies by repeated washing, cells were resuspended in 1ml 3% PBS/BSA and read through in a flow cytometry machine (Becton Dickinson, Cowley, Oxford, UK). Negative controls were

cell suspensions incubated with mouse IgG isotype as primary antibody, and HUVECs were used as positive controls. For the immunohistochemistry, cells were cultured in chamber slices and on the day 6 of culturing, the cells were fixed in 4% paraformaldehyde and washed with PBS for at least three times. After cell permeablization by 0.1% triton solution for 6mins, endogenous peroxidase activity was quenched by incubating the sample slices with 3% $H_2O_2$ for 15mins and then blocked with 10% swine serum for 1h. The cells were incubated with the vWF (Rabbit anti-human, 1:300, Millipore, North Ryde, NSW, Australia) and eNOS (goat anti-human, 1:100, R&D Systems, Inc., Minneapolis, MN, USA) primary antibodies overnight at 4°C, followed by incubation with the biotinylated swine-anti-mouse, rabbit, goat secondary antibody (DAKO Multilink, CA, USA )for 15mins, and then with horseradish peroxidase-conjugated avidin-biotin complex (DAKO Multilink, CA, USA) for another 15mins. The antibody complexes were visualized by the addition of a buffered diaminobenzidine (DAB) substrate for 4 mins. Mayer's haematoxylin (HD Scientific Pty Ltd., Kings Park, NSW, Australia) were used for counter staining.

**Matrigel Assay**

Aliquots (50µl) of growth factor-reduced phenol red free Matrigel matrix (BD biosciences, North Ryde, NSW, Australia) were added into individual wells of a 96-well cell culture plates and allowed to polymerize at 37°C for at lease 30min. 3 $\times 10^3$ BMSCs, HUVECs and BMSCs cultured under different conditions, i.e. with different VEGF concentrations or under cobalt chloride-induced hypoxyia, were added onto the matrigel matrix. The new vessel networks formed on the matrigel by different cells were observed using a microscope at 40× magnification after 6 hrs incubation under 37°C and 5% $CO_2$ condition. To investigate the interaction between the HUVECs and BMSCs cultured under different conditions, 3 $\times 10^3$ HUVECs were mixed with $CoCl_2$-treated BMSCs or untreated BMSCs in serum-free DMEM at the ratio of 1:1, and seeded onto the Matrigel. The unmixed HUVECs and $CoCl_2$-treated BMSCs were used as controls. The vessel networks formed on the matrigel by different cell combinations were observed after 24 hrs and 72hrs incubation. The total

number of vessels in five randomly selected areas from each sample was recorded using the Axion software (Carl Zeiss Microimaging GmbH, Göttingen, Germany). This experiment was repeated three times and the average was taken for statistical analysis.

**In vivo vascularization assessment**

To assess the angiogenesis of BMSCs treated in different ways, three SCID mice (Animal Resources Centre, Canning Vale, WA, Australia) were used with the ethics approval from QUT Animal Ethics Committee. The animals were anesthetized with 1ml of Katemine (100mg/ml) and 0.15ml of xylazine (20mg/ml) injected intraperitoneally. $5 \times 10^4$ resuspended BMSCs, HUVECs, BMSCs treated with 20ng/ml VEGF for 6 days, BMSCs treated with 100μM cobalt chloride for 6 days and BMSCs treated with both 20ng/ml VEGF and 100μM cobalt chloride for 6 days were mixed with matrigel at a ratio of 1:2 to a final volume of 300 μl before subcutaneous injection on the dorsal area of mice. Gels without cells were used as negative control. On each mouse, six gels, one from each group, were injected with approximate 1cm apart along the both sides of longitudinal middle line of dorsal area. All animals were sacrificed after 10 days and the implants were retrieved, photographed and fixed in 4% para formaldehyde. After being embedded in paraffin, the implants were sliced and three serial sagittal slices close to the centre of each implant were used to do the immunohistochemical staining. To detect the endothelial cells, vWF antibody was used. The staining method is the same as above described. All $vWF^+$ positive cells, capillaries or blood vessels were counted on each slice and normalized to the slice area ($mm^2$). The average from each group was used to do the statistical analysis. To confirm the relationship between the VEGF expression and vascularization, the same VEGF antibody (1:50) for the western blot was used to stain the harvested samples by the same immunohistochemical method described above.

**Statistical analysis**

Analysis was performed using SPSS software (SPSS Inc., Chicago, Il., USA). All the

data were analyzed using Student-*t*, one-way ANOVA or Friedman test. The significance level was set at $p \leq 0.05$.

## Results

### The original VEGF/PEDF expression pattern of BMSCs and HUVECs

Real time q-PCR revealed that both VEGF and PEDF gene expressions of BMSCs are significantly higher than those of HUVECs (Student-*t* test, $p<0.01$) (Fig. 1A) and the VEGF/PEDF expression pattern is also very much different between these two different cells. BMSCs have significantly higher PEDF expression compared with the VEGF (Student-*t* test, $p<0.05$) (Fig. 1A), while HUVECs have much lower PEDF expression than the VEGF (Student-*t* test, $p<0.05$) (Fig. 1A). The average VEGF/PEDF expression ratio of HUVECs is around 8.0 which is significantly higher than that (around 0.5) of BMSCs (Student-*t* test, $p<0.01$) (Fig. 1B). The western blot and immunohistochemical staining on the VEGF and PEDF proteins confirmed these differences between the two different cells (Fig. 1C, D).

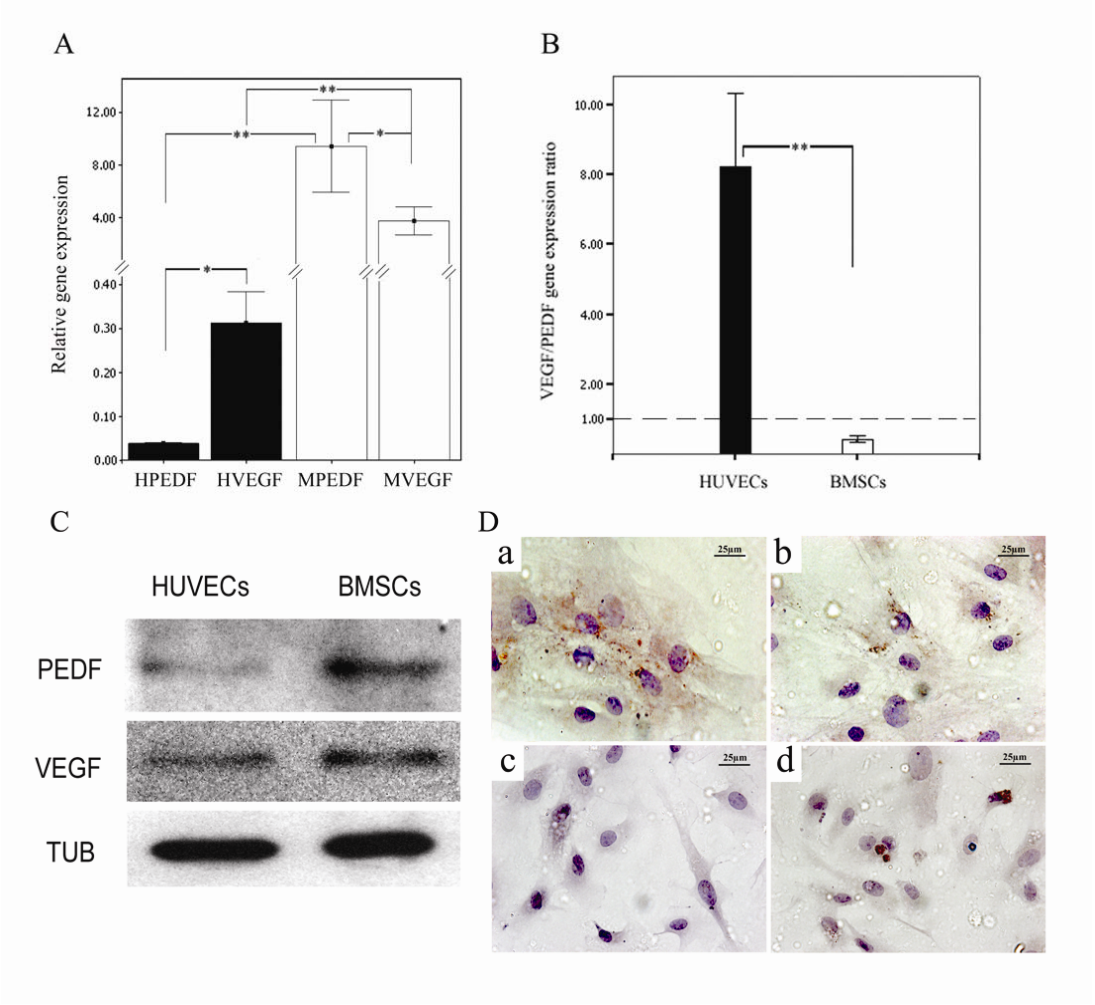


**Figure 1. The original VEGF/PEDF expression pattern of BMSCs and HUVECs**

A. Relative gene expression of VEGF and PEDF of BMSCs and HUVECs; B. VEGF/PEDF expression ratio of BMSCs and HUVECs; C. Western blot showing the PEDF and VEGF expressions on protein level in BMSCs and HUVECs. α-tubulin (TUB) used as control; D. Immunohistochemical staining (400×) showing the PEDF and VEGF expression of BMSCs and HUVECs (a. PEDF expression of BMSCs; b. VEGF expression of BMSCs; c. PEDF expression of HUVECs; d. VEGF expression of HUVECs.). *: $p<0.05$; **: $p<0.01$.

**The VEGF/PEDF expression pattern and endothelail cell differentiation of BMSCs under different extracellular VEGF concentrations**

When cultured in angiogenic media with upgrading VEGF concentrations, BMSCs showed different VEGF/PEDF gene expression pattern (Fig 2). When the extracellular

VEGF concentration was increased from “no added VEGF” through to 40ng/ml, the PEDF expression decreased by almost half of the original expression, but when the VEGF concentration reached 80ng/ml, the PEDF expression returned to almost 75% of its original expression (Friedman test, $p<0.05$) (Fig.2 B). The VEGF expression, on the other hand, increased to around 1.5 times as much as the original expression at the 20ng/ml extracellular VEGF concentration, and then fell back to almost its original expression as the extracellular VEGF concentration increased from 40ng/ml to 80ng/ml (Friedman test, $p<0.05$) (Fig.2 A). The VEGF/PEDF expression ratio reached its peak average value of around 0.8 at the 40ng/ml extracellular VEGF concentration (Friedman test, $p<0.05$) (Fig.2 D). These changes in VEGF/PEDF expression pattern were confirmed by western blot on those two proteins (Fig.2 C). The angiogenic differentiation of BMSCs under various extracellular VEGF concentrations was also tested using real time-qPCR against CD31, VEGFR2, vWF and eNOS III endothelial cell markers. The HUVECs were used as control. HUVECs showed significantly higher gene expression of those markers than BMSCs cultured in either normal DMEM or angiogenic media with different VEGF concentrations (one-way ANOVA, $p<0.01$) (Fig.3 A), while there were no significant differences among different BMSCs groups (one-way ANOVA, $p>0.05$) (Fig.3 A). Flowcytometry on CD31 and VEGFR2 revealed no expression differences between the undifferentiated and differentiated BMSCs (Fig.3 B). There were no obvious immunohistochemical staining against vWF and eNOS III on different BMSCs slices in contrast to the HUVECs (Fig.3 C). The Matrigel assay showed HUVECs formed much more new vessel-like structures within 6hrs compared with both undifferentiated and differentiated BMSCs (one-way ANOVA, $p<0.01$) (Fig.6), while there were no difference among BMSC groups in the ability to form vessel-like structures (one-way ANOVA, $p>0.05$) (Fig.6)

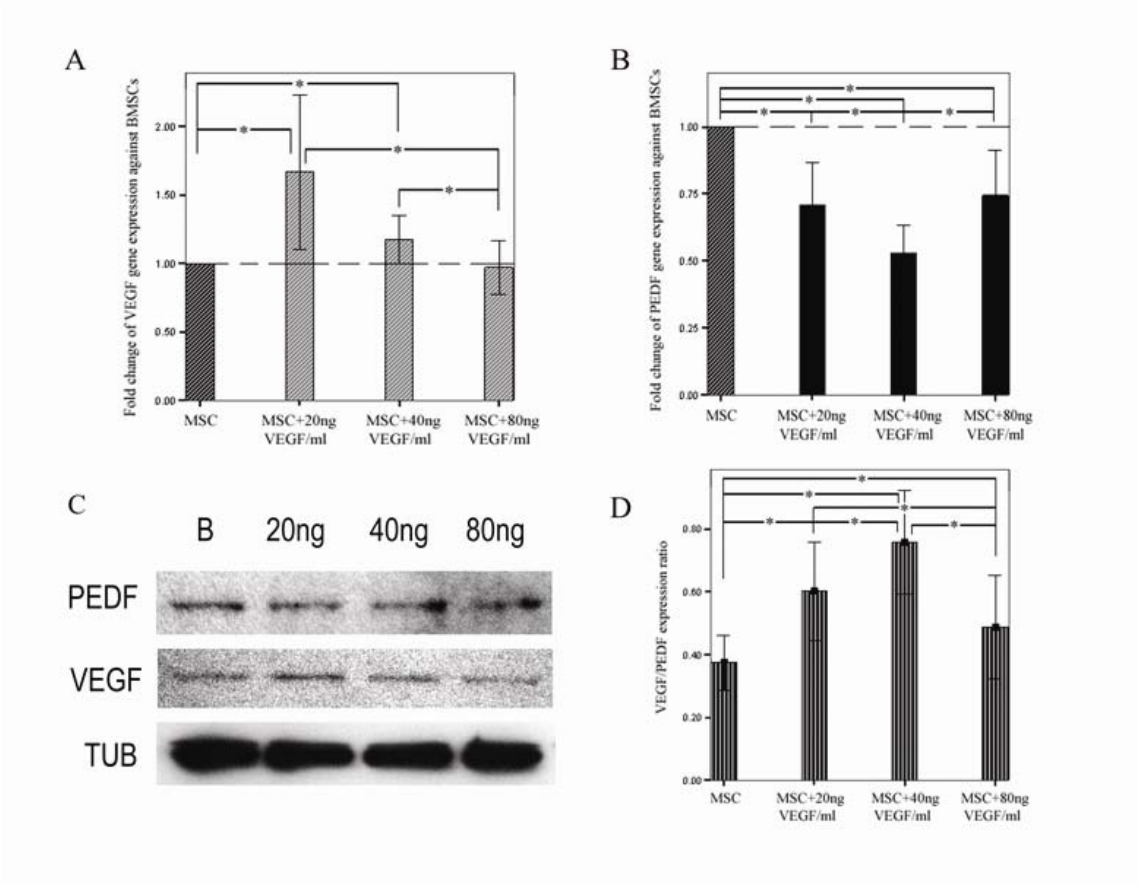


**Figure 2. The VEGF/PEDF expression pattern of BMSCs under different extracellular VEGF concentrations**

A. Fold change of VEGF gene expression of BMSCs cultured with different extracellular VEGF concentrations against BMSCs cultured in DMEM; B. Fold change of PEDF gene expression of BMSCs cultured in different extracellular VEGF concentrations against BMSCs cultured in DMEM; C. Western blot showing the alterations of PEDF and VEGF expression on protein level in BMSCs cultured under different conditions (B: BMSCs cultured in DMEM; 20ng: BMSCs cultured in DMEM plus 20ng/ml VEGF; 40ng: BMSCs cultured in DMEM plus 40ng/ml VEGF; 80ng: BMSCs cultured in DMEM plus 80ng/ml VEGF). α-tubulin (TUB) used as control; D. The alterations of VEGF/PEDF gene expression ratio in BMSCs cultured under different conditions. *: $p<0.05$.

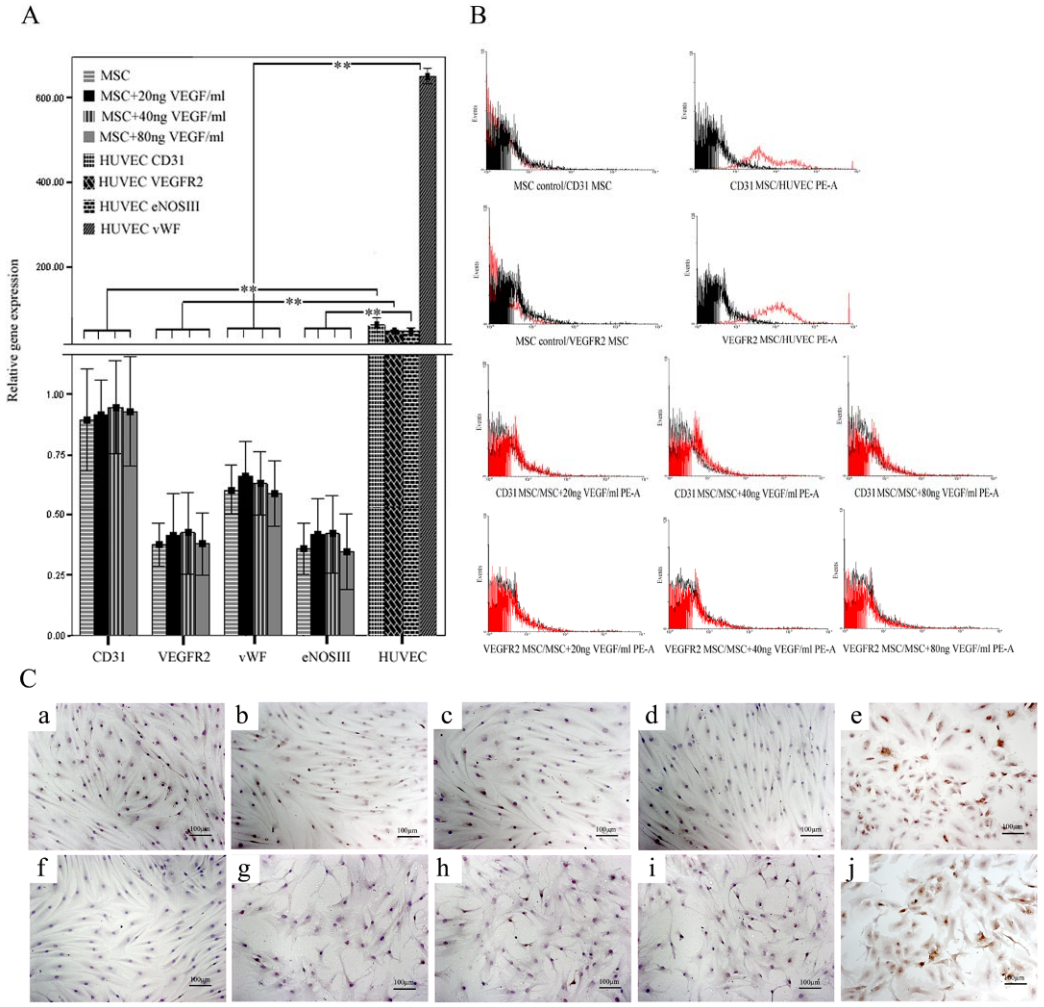


**Figure 3. Endothelial cell differentiation of BMSCs under different extracellular VEGF concentrations**

A. Relative gene expression of endothelial cell markers in BMSCs cultured under different conditions and HUVECs; B. Flow cytometry graphs showing the expression of CD31 and VEGFR2 on HUVECs and BMSCs cultured under different conditions; C. Immunohistochemical staining (100×) of vWF and eNOSIII on HUVECs and BMSCs cultured under different conditions (a-d. vWF staining on BMSCs cultured in DMEM or DMEM plus 20,40 or 80ng/ml VEGF; e. vWF staining on HUVECs; f-i. eNOSIII staining on BMSCs cultured in DMEM or DMEM plus 20,40 or 80ng/ml VEGF;j. eNOSIII staining on HUVECs.). **: $p<0.01$.

**The VEGF/PEDF expression pattern and angiogenic differentiation of BMSCs**

**under hypoxia induced by cobalt chloride**

When cultured under hypoxia induced by 100μM $CoCl_2$, BMSCs significantly increased the VEGF expression by almost 5 times on average and cut off the PEDF expression by nearly 50% (Friedman test, $p<0.05$) (Fig.4 A&B). The VEGF/PEDF expression ratio increased to about 4.0 (Fig.4 D). The addition of 20ng/ml VEGF did not significantly influenced the effect of CoCl2 on the VEGF/PEDF expression (Friedman test, $p>0.05$) (Fig.4 A,B&D). The endothelial cell differentiation of BMSCs under hypoxia situation was also investigated using real time q-PCR against CD31, VEGFR2, vWF and eNOS III endothelial cell markers. No significant differences were found in the expressions of these markers between BMSCs, BMSCs treated with 100μM $CoCl_2$ alone or with both 100μM $CoCl_2$ and 20ng/ml VEGF (one-way ANOVA, $p>0.05$) (Fig.5 A). Flowcytometry and immunohistochemical staining revealed no obvious expressions of those markers compared with HUVECs (Fig.5 B&C). Matrigel assay showed no difference in the ability to form vessel-like structures within 6hrs among different BMSCs groups (one-way ANOVA, $p>0.05$) (Fig.6).

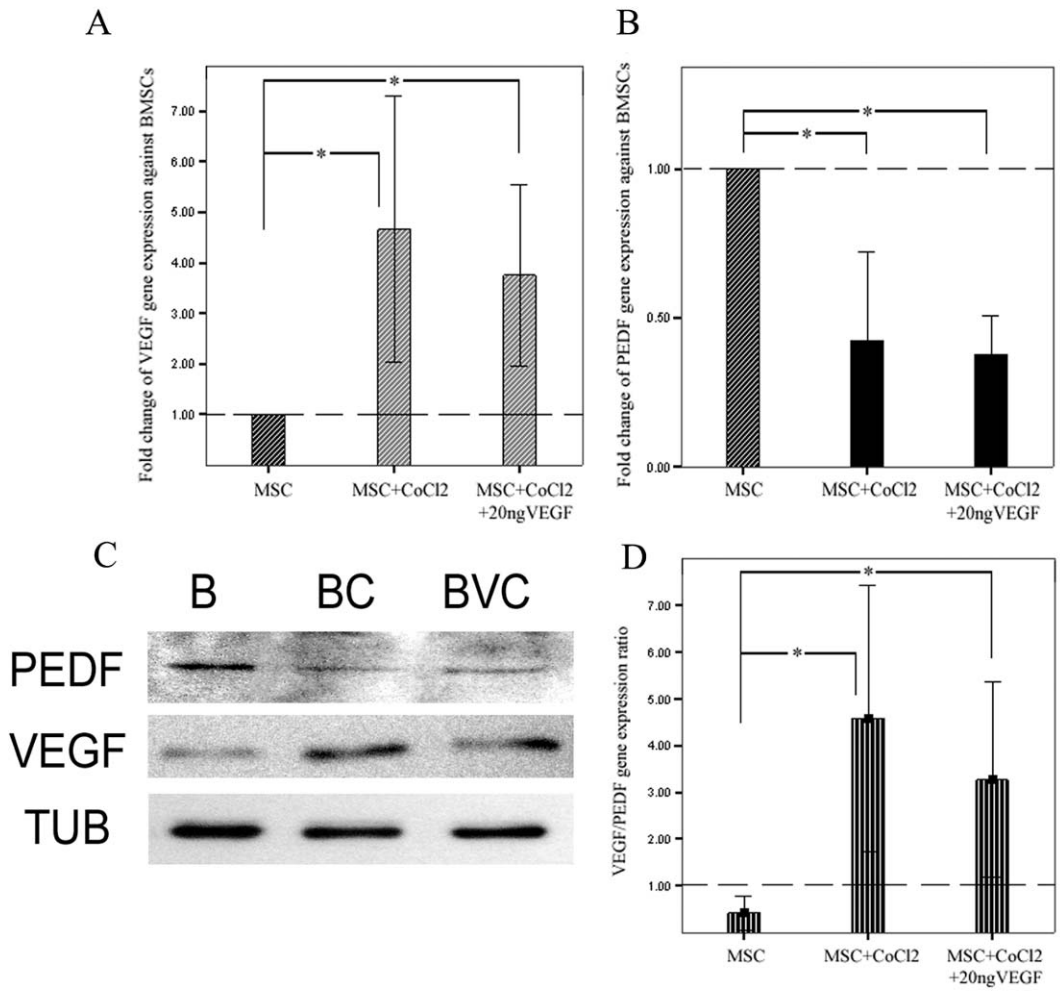


**Figure 4. The VEGF/PEDF expression pattern of BMSCs under hypoxia induced by cobalt chloride**

A, B&D. Bar graphs showing the relative gene expression and ratio of VEGF and PEDF of BMSCs cultured under different conditions; C. Western blot showing the alterations of PEDF and VEGF expression on protein level in BMSCs cultured under different conditions (B: BMSCs cultured in DMEM; BC: BMSCs cultured in DMEM plus 100μM $CoCl_2$; BVC: BMSCs cultured in DMEM plus both 20ng VEGF/ml and 100μM $CoCl_2$.) *: $p<0.05$.

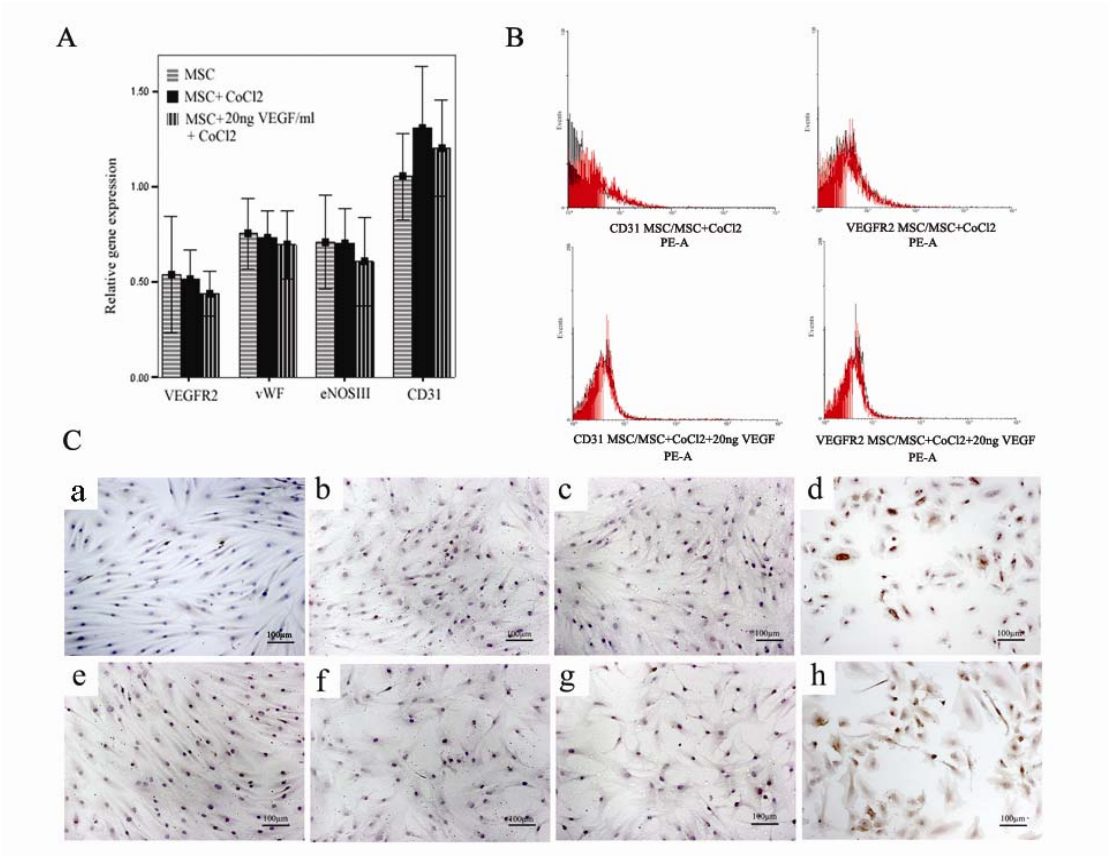


**Figure 5. Endothelial cell differentiation of BMSCs under hypoxia induced by cobalt chloride**

A. Relative gene expression of endothelial cell markers in BMSCs cultured under different conditions; B. Flow cytometry graphs showing the expression of CD31 and VEGFR2 on BMSCs cultured under different conditions; C. Immunohistochemical staining (100×) of vWF and eNOSIII on HUVECs and BMSCs cultured under different conditions (a-c. vWF staining on BMSCs cultured in DMEM or DMEM plus 100μM $CoCl_2$ or both 20ng VEGF/ml and 100μM $CoCl_2$; d. vWF staining on HUVECs; e-g. eNOSIII staining on BMSCs cultured in DMEM or DMEM plus 100μM $CoCl_2$ or both 20ng VEGF/ml and 100μM $CoCl_2$; h. eNOSIII staining on HUVECs.)

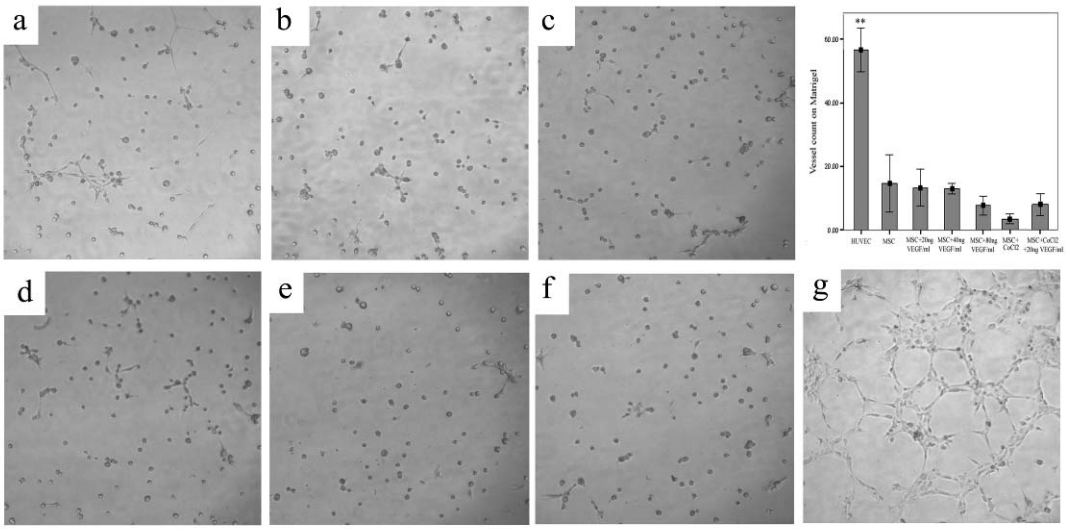


**Figure 6. Vessel-like structure formation on the Matrigel by HUVECs and BMSCs cultured under different conditions.**

a-d. vessel-like structures formed by BMSCs cultured in DMEM or DMEM plus 20, 40 or 80ng/ml VEGF; e-f. vessel-like structures formed by BMSCs cultured in DMEM plus 100μM $CoCl_2$ or both 20ng VEGF/ml and 100μM $CoCl_2$; g. vessel-like structures formed by HUVECs; bar graph showing the number and statistical analysis of vessel-like structures formed by HUVECs and BMSCs cultured under different conditions. **: $p<0.01$

**The enhanced vessel formation of HUVECs on Matrigel by $CoCl_2$-treated BMSCs**

HUVECs, when mixed with $CoCl_2$-treated BMSCs in serum-free DMEM, formed more stable vessel-like strucutures after both 24hrs and 72hrs incubation on the Matrigel than HUVECs alone or with untreated BMSCs (one-way ANOVA, $p<0.001$) (Fig.7). The number of vessel-like structures formed by HUVECs- $CoCl_2$-treated BMSCs mixture was more than other groups after both 24hrs and 72hrs incubation (one-way ANOVA, $p<0.001$) (Fig.7).

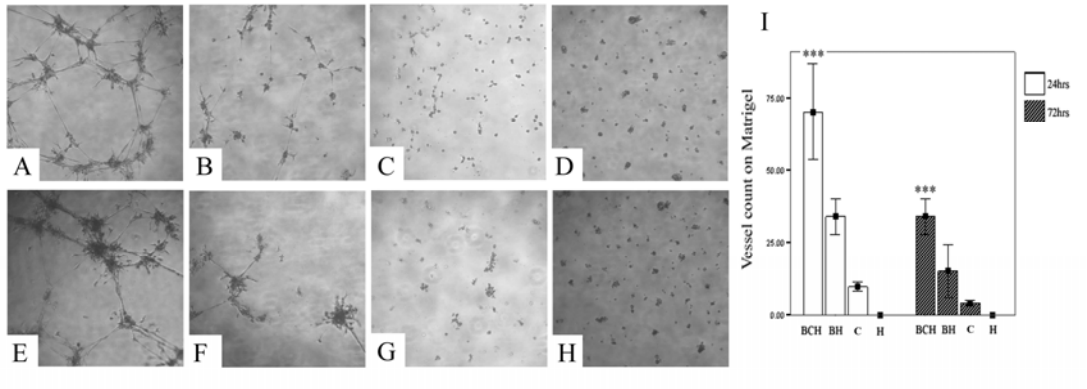


**Figure 7. The enhanced vessel formation of HUVECs on Matrigel by $CoCl_2$-treated BMSCs.**

A-D. vessel-like structures formed by HUVECs plus $CoCl_2$-treated BMSCs or untreated BMSCs, $CoCl_2$-treated BMSCs alone and HUVECs alone after 24hrs incubation in serum-free DMEM; E-H. vessel-like structures formed by HUVECs plus $CoCl_2$-treated BMSCs or untreated BMSCs, $CoCl_2$-treated BMSCs alone and HUVECs alone after 72hrs incubation in serum-free DMEM; I. bar graph showing the number and statistical analysis of vessel-like structures formed by different groups; In bar graph, BCH: HUVECs plus $CoCl_2$-treated BMSCs; BH: HUVECs plus untreated BMSCs; C: $CoCl_2$-treated BMSCs only; H: HUVECs only;***: $p<0.001$.

**In vivo vascularization ability of BMSCs cultured under different conditions**

After being retrieved from the SCID mice, the Matrigel implants were observed under a stereomicroscope and the images were taken (Fig.8 a-f). No obvious vascularization could be seen in the negative control, Matrigels carrying BMSCs or BMSCs treated with VEGF, while in the Matrigel carrying HUVECs, BMSCs treated with $CoCl_2$ alone or together with VEGF, blood vessels could be seen (Fig.8 a-f). After Staining with the vWF antibody, positive cells and blood vessels on each slice were counted and normalized against the area of each slice. Results showed that Matrigels carrying HUVECs, BMSCs treated with $CoCl_2$ alone or together with VEGF had much more $vWF^+$ cells and blood vessels than the negative control, Matrigels carrying BMSCs or BMSCs treated with VEGF (Friedman test, $p<0.01$) (Fig.8 g-p). Further VEGF and PEDF staining revealed that non-vascularized areas in Matrigels containing untreated BMSCs showed much stronger expression of PEDF compared to

the highly vascularized areas in Matrigels carrying CoCl2-treated BMSCs (Fig.9 A-D). On the other hand, in the Matrigel containing $CoCl_2$-treated BMSCs, very strong VEGF expression was identified in both newly formed blood vessel wall and the surrounding cells (Fig. 9 E-H).

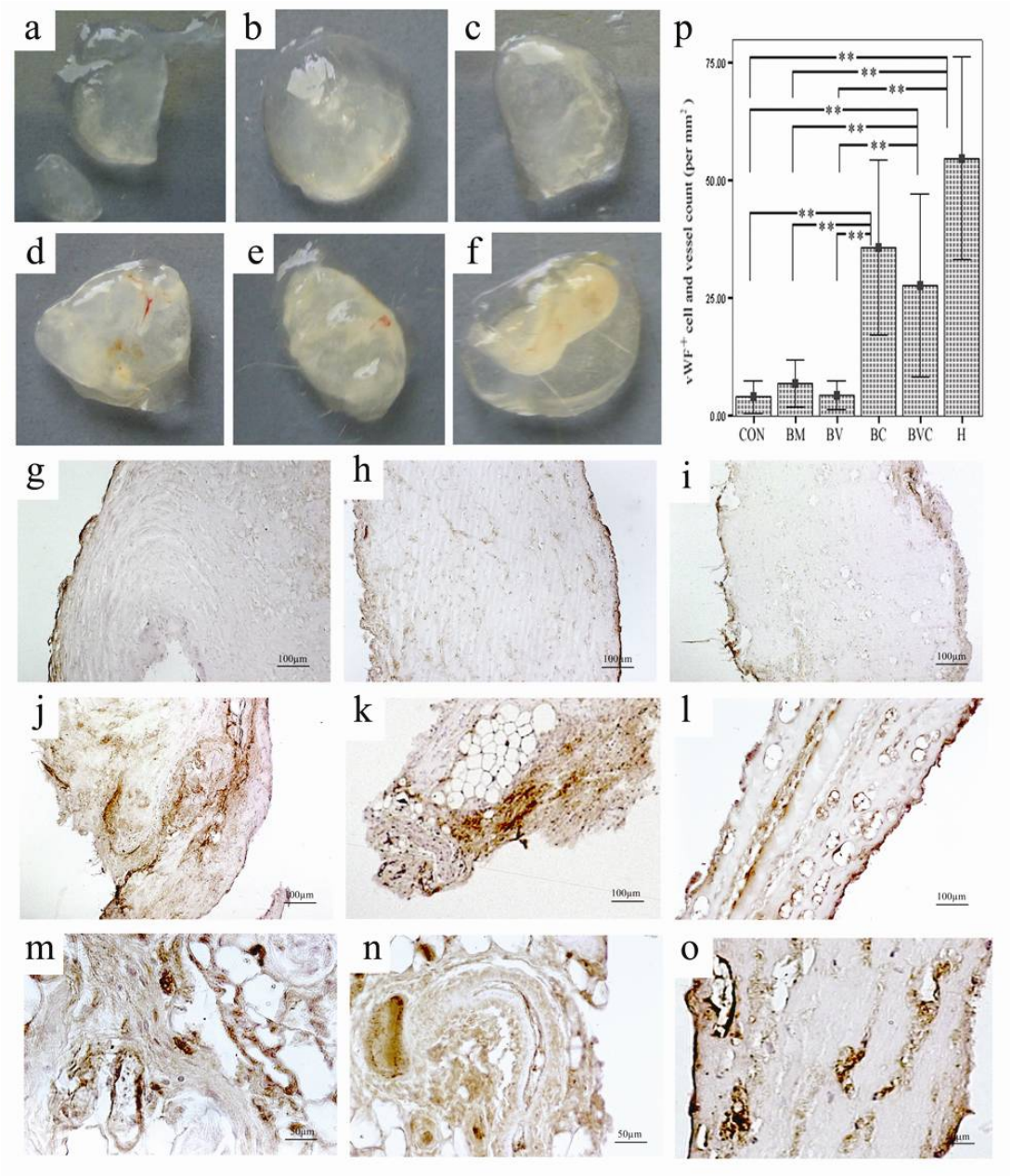


**Figure 8. In vivo vascularization ability of BMSCs cultured under different conditions**

a.Matrigel without pre-mixed cells; b. Matrigel with untreated BMSCs; c. Matrigel with BMSCs treated with 20ng/ml VEGF; d. Matrigel with BMSCs treated with

100μM $CoCl_2$; e. Matrigel with BMSCs treated with both 100μM $CoCl_2$ and 20ng/ml VEGF; f. Matrigel with HUVECs; g. vWF staining (100×) of Matrigel without cells; h. vWF staining (100×) of Matrigel with untreated BMSCs; i. vWF staining (100×) of Matrigel with BMSCs treated with 20ng/ml VEGF; j. vWF staining (100×) of Matrigel with BMSCs treated with 100μM $CoCl_2$; k. vWF staining (100×) of Matrigel with BMSCs treated with both 100μM $CoCl_2$ and 20ng/ml VEGF; l. vWF staining (100×) of Matrigel with HUVECs; m. Higher magnification (400×) of vWF staining of Matrigel with BMSCs treated with 100μM $CoCl_2$ showing blood vessels and capillaries; n. Higher magnification (400×) of vWF staining of Matrigel with BMSCs treated with 100μM $CoCl_2$, showing a small artery growing into the gel; o. Higher magnification (400×) of vWF staining of Matrigel with HUVECs, showing positive capillaries; p. Bar graphs showing the differences in vascularization among different matrigel groups (CON: Matrigel without cell; BM: Matrigel with untreated BMSCs; BV: Matrigel with BMSCs treated with 20ng/ml VEGF; BC: Matrigel with BMSCs treated with 100μM $CoCl_2$; BVC: Matrigel with BMSCs treated with both 100μM $CoCl_2$ and 20ng/ml VEGF; H: Matrigel with HUVECs.). **: $p<0.01$.

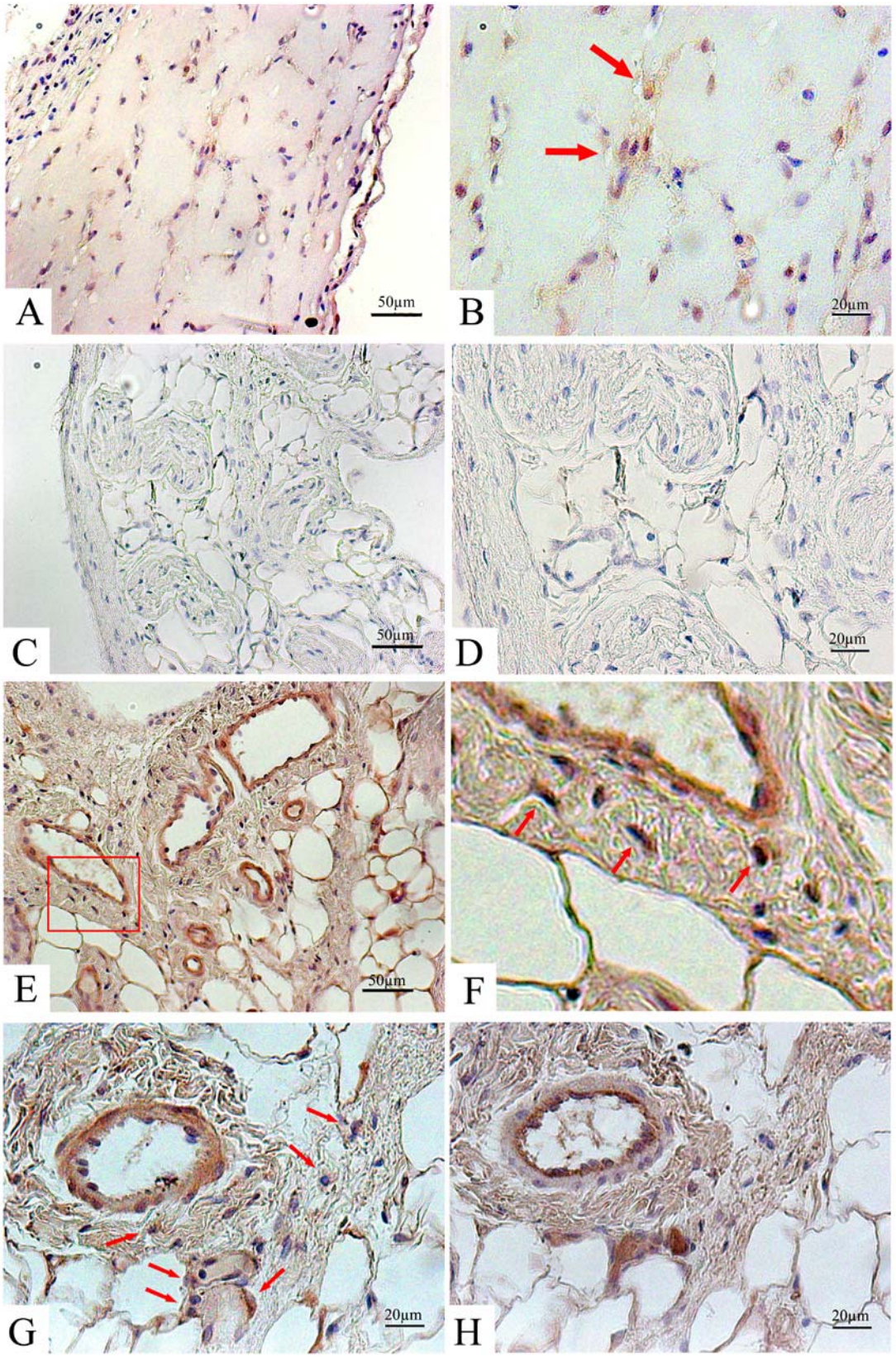


**Figure 9. VEGF/PEDF expressions in Matrigels containing untreated or $CoCl_2$-treated BMSCs.**

A. PEDF highly expressed in non-vascularized areas of Matrigel containing untreated

BMSCs (200×); B. A higher magnification (400×) of a local area in A (arrows indicating PEDF positive cells); C. Almost no PEDF expressed in highly-vascularized areas of Matrigel containing $CoCl_2$-treated BMSCs (200×); D. A higher magnification (400×) of a local area in C; E. VEGF highly expressed on blood vessel walls and some surrounding cells (200×); F. Zoom-in image of the selected area in A (within red square frame) showing VEGF positive cells around the blood vessel; G&H. Higher magnification (400×) showing the VEGF (G) and vWF (H) expressions on two consecutive slices (arrows indicating VEGF positive cells).

**Discussion**

BMSCs are the cells isolated from the bone marrow mononuclear cells and attaching to the plastic cell culture surfaces. Whether those in vitro cultured BMSCs could be differentiated into endothial cells, or in the other word, whether in vitro cultured BMSCs contain EPCs, has long since been a controversy [170-171]. Multipotent adult progenitor cells (MAPCs), a recently identified elusive stem-cell population from bone marrow mononuclear cells, are reported to be able to differentiate into endodermal, mesodermal and ectodermal cells including endothelial cells[172]. To purify the MAPCs, fibronectine-coated cell culture surfaces and growth factors (platelet-derived growth factor-BB and Epidermal growth factor) are needed, which is different from that used for BMSCs isolation[172]. As MAPCs have not been well characterized against BMSCs and the modified purification method for MAPCs may be more favorable for different cell populations to attach, it is possible that MAPCs might be a mixture of BMSCs and HSCs. To simplify the question and investigate the endothelail cell differentiation ability of BMSCs, the traditional BMSCs isolation and expansion methods were used in this study, and only P2-P5 cells were included to make sure there is no HSCs contamination.

BMSCs have been reported involved in various tissue development and regeneration processes, such as osteogenesis, chondrogenesis and angiogenesis[173-177]. In angiogenesis, what roles BMSCs are playing is not clear yet although some studies showed that BMSCs could support and help stabilize new-formed blood vessels as

pericytes [175-177]. In angiogenic environment, VEGF is a major pro-angiogenic growth factor that can help endothelial cell differentiation, migration and blood vessel formation [178-180], and its concentration is always increased in the angiogenic areas [181]. On the other hand, PEDF is the most potent natural angiogenesis inhibitor that can prevent vascularisation and induce the apoptosis of endothelial cells[167, 182]. The ratio or balance between these two antagonistic factors (VEGF/PEDF) in a local environment will affect the angiogenesis and vascularization in that area despite other pro- and anti-angiogenic factors[168]. Based on the findings in this study, the regulatory roles of BMSCs in neovascularization through adjusting VEGF/PEDF ratio could be illustrated in Fig.10. Although the VEGF expression of BMSCs has been investigated and reported [183-185], studies about the PEDF expression and the VEGF/PEDF expression pattern of BMSCs can hardly be found in literatures. The findings from this study reveal for the first time that PEDF is much more strongly expressed by BMSCs than the VEGF and other anti-angiogenic factors such as endostatin or chondromodulin (data not shown). Interestingly, HUVECs have much higher VEGF expression than the PEDF, which is exactly reverse to the BMSCs. These phenomena indicate that the BMSCs, when in a neutral environment, may not necessarily be an angiogenesis-promoting cell population. To be differentiated into endothelial cells, the VEGF/PEDF ratio of BMSCs should be reversed besides the expression of endothelial cell markers.

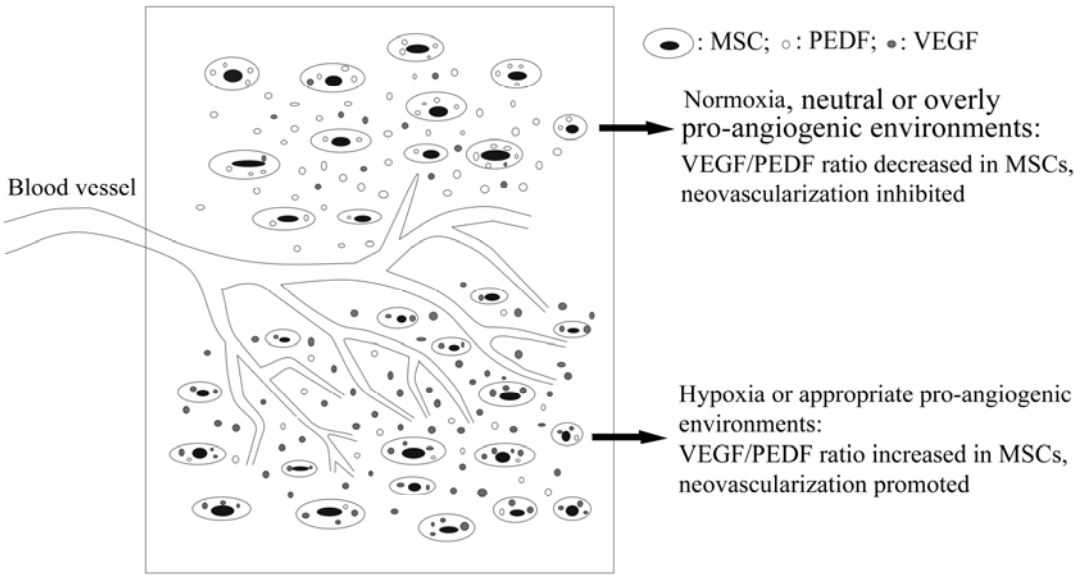

**Figure 10. Illustration showing the regulatory role of MSCs in different situations.**

In pro-angiogenic environment, the extracellular VEGF concentration will be increased and varying during the angiogenic process[181]. No information could be found in literatures so far regarding alterations of the pro- and anti- angiogenic factor expression of BMSCs in pro-angiogenic environment with varying VEGF concentrations. In this study, the alterations of VEGF/PEDF expression under different extracellular VEGF concentrations were investigated. The findings showed that VEGF/PEDF expression ratio of BMSCs will increase as the extracellular VEGF concentration increases to 40ng/ml. If the extracellular VEGF concentration becomes more than 40ng/ml, the VEGF/PEDF ratio will fall back. These alterations in VEGF/PEDF expression pattern may indicate that when the environmental VEGF concentration is at an appropriate level, BMSCs will become more supportive in the angiogenic process; when there is too much VEGF in a local area, BMSCs may become less supportive. These findings may be useful in the application of BMSCs to help control angiogenesis or vascularization in vivo. As for the endothelial cell differentiation under various extracellular VEGF concentrations, BMSCs did not show any sign of differentiation towards endothelial cells, which means BMSCs cannot directly get involved in the blood vessel formation through the way of endothelial cell differentiation.

Cobalt chloride is a hypoxia mimicking agent often used to activate hypoxia-related responses in cells[186]. The biochemical and molecule mechanisms of the hypoxia induced by $CoCl_2$ are proven similar to that of the real hypoxia induced by low oxygen tension [186]. Although the gene expression alterations of BMSCs under the hypoxia condition have been reported [187], very few information could be found in literatures about the hypoxia effect on the VEGF/PEDF expression pattern of BMSCs. On the other hand, whether the endothelial cell differentiation ability of BMSCs will be improved under hypoxia conditions is still unknown. In this study, hypoxia induced

by $CoCl_2$ increases the VEGF expression and suppresses the PEDF expression significantly, which means the hypoxia drives the BMSCs to favor angiogenesis and vascularisation. Unfortunately, no signs of differentiation towards endothelial cells were found in BMSCs cultured under hypoxia induced by $CoCl_2$.

To further investigate the role of BMSCs in angiogenesis, especially the BMSCs cultured in hypoxia conditions, the HUVECs were mixed with $CoCl_2$-treated BMSCs or untreated BMSCs in serum-free media and seeded onto the Matrigel. $CoCl_2$-treated BMSCs significantly enhanced and stabilized the vessel-like structure formation on the Matrigel. As the media is serum free, the upregulated VEGF expression in $CoCl_2$-treated BMSCs could account for this phenomenon. For in vivo vascularization analysis, SCID mice were used and BMSCs cultured under various conditions were injected subcutaneously. The implant with BMSCs treated with $CoCl_2$ showed much higher degree of vascularizton than the BMSCs cultured in nomoxia despite whether the extracellular VEGF was added or not, which could be attributed to the significantly increased VEGF/PEDF expression ratio in $CoCl_2$-treated BMSCs. The VEGF/PEDF staining further revealed that VEGF/PEDF expression in a local area is closely linked with the neovascularization.

Based on the findings in this study, it is reasonable to conclude that BMSCs involve in the angiogenesis as regulators rather than endothelial cell progenitors under both nomoxia and hypoxia conditions. BMSCs treated by hypoxia conditions can promote the vascularization in local areas and consequently be very useful in ischemia treatment and vascularized-tissue engineering.

## *PAPER FOUR*

**Cobalt chloride-treated bone marrow mesenchymal stem cells (BMSCs) enhance in vivo osteogenesis of BMSCs-derived osteoblasts and vascularization in a tissue engineered periosteum model**

Wei Fan, Ross Crawford, Yin Xiao

**Suggested Statement of Contribution of Co-Authors for Thesis by Published Papers:**

| Contributors | Statement of contribution* |
|---|---|
| Wei Fan | Performed laboratory experiments, data analysis and interpretation. Wrote the manuscript. |
| | |
| | |
| Ross Crawford | Involved in the conception and design of the project. Assisted in sample collection, reviewing the manuscript. |
| Yin Xiao | Involved in the conception and design of the project. Assisted in sample collection, technical guidance and reviewing the manuscript |

**Principal Supervisor Confirmation**

**I have sighted email or other correspondence from all co-authors confirming their certifying authorship**

**Name** **Signature** **Date**

**Abstract**

The periosteum plays an indispensable role in both bone formation and defect healing. Developing a tissue engineered bi-layered periosteum may throw a new light on critical-sized bone defect restoration. This study constructed in vitro an artificial periosteum by incorporating BMSCs-derived osteoblasts alone or together with $CoCl_2$ pre-treated BMSCs or HUVECs, then the engineered periostea were implanted both subcutaneously (for two weeks) and into skull bone defects (for four weeks) of SCID mice to investigated ectopic and orthotopic osteogenesis and vascularisation. Micro-CT, histological and immunohistochemical methods were used to assess the ectopic and orthotopic osteogenesis and vascularisation after implants harvest. The results showed that $CoCl_2$ pre-treated BMSCs and HUVECs induced a higher degree of vascularisation in implants ($p<0.05$). $CoCl_2$ pre-treated BMSCs significantly enhanced the ectopic and orthotopic osteogenesis of BMSCs-derived osteoblasts ($p<0.05$), while HUVECs promoted orthotopic new bone formation after a four-week observation ($p<0.05$). No signs of new bone tissues but calcium precipitation were found in subcutaneously implanted scaffolds. Based on the findings of this experimental study, it could be concluded that $CoCl_2$ pre-treated BMSCs can enhance both ectopic and orthotopic osteogenesis of BMSCs-derived osteoblasts and vascularization at an early osteogenic stage. Subcutaneous areas of mice may not be appropriate for assessment of new bone formation on collagen scaffolds. This study demonstrated the potential application of $CoCl_2$ pre-treated BMSCs in tissue engineering not only for periosteum but also bone or other vascularized tissues.

## Introduction

Bone defects, especially large bone defects, remain a major challenge in orthopedic surgery [188]. Autologous bone transplantation is considered the most effective treatment, but insufficient donor tissue, coupled with concerns about donor site morbidity, has hindered this approach in large-scale applications. On the other hand, immunological reactions that would occur in recipients against allo or xenogeneic bone grafts impose a major restriction on the clinical application of these approaches.

In both physiological and pathological processes, the periosteum plays an indispensable role in both bone formation and defect healing alongside the involvement of various growth factors and mechanical loading [9, 20, 35]. Periosteum is a dense, dual-layered and highly vascularized connective tissue membrane covering cortical bone surfaces [9, 14, 23]. The cambial layer of periosteum contains osteoblasts and osteogenic progenitor cells, whereas in the fibrous layer there are collagen fibers, fibroblasts and blood vessel networks. It is the osteogenic function of periosteum that determines the rate of *de novo* postnatal periosteal bone formation and consequently the bone strength during the process of growth or defect healing [35]. Transplantation of autogenous or allogenous periosteum has been applied successfully in the restoration of various-sized bone defects, especially large bone defects [131, 189]. Bone healing induced by periosteum has several advantages compared to direct bone or bone substitute transplantation, such as healing with a natural bone structure, optimal bone integrity in the defect area, appropriate degree of vascularization, and minimal ectopic ossification through the defect encasement [131, 189]. However, major concerns in the case of autogenous periosteum transplantation include insufficient autologous donor tissues and donor site morbidity; and in the case of allogenous transplants, immunological rejection reactions.

*In vitro* tissue-engineered periosteum, designed to mimic the anatomical structure of real periosteum, may provide a novel approach in the treatment of large bone defects.

Bone marrow-derived mesenchymal stem cells (BMSCs) are a widely used progenitor cell source and are believed to be able to differentiate into osteogenic progenitor cells

and finally osteoblasts following ex vivo expansion under certain conditions. These osteoblasts are reportedly able to regenerate bone tissues lost in trauma or diseases by direct orthotopic placement in conjunction with appropriate scaffolds, most commonly those containing hydroxyapatite/tricalcium phosphate (HA/TCP)[190]. However, whether and how the in vitro differentiated BMSCs maintained the osteogenic phenotype on collagen scaffolds in vivo is still elusive although a lot of researches had used collagen as the cell carrier to restore bone defects[75]. On the other hand, as periosteum is a highly vascularized tissue, introducing new blood vessels into the engineered periosteum to form a dual-layered structure is essential for the function of engineered periosteum. Hypoxia will increase the expression of pro-angiogenic factors, such as VEGF, by BMSCs, and BMSCs pre-treated with hypoxia conditions can help restore the vascularization in ischemic tissues[191-192]. But on the other hand, whether these hypoxia-pre-treated BMSCs could enhance osteogenesis of BMSCs-derived osteoblasts as well as vascularisation needs further investigation.

In this study, the concept of tissue engineered periosteum was investigated by combining BMSCs-derived osteoblast and endothelial cells or BMSCs pre-treated with cobalt chloride ($CoCl_2$) -induced hypoxia on both sides of a collagen I membrane. The osteogenesis and vascularization of the tissue engineered periosteum were evaluated in both the subcutaneous area and skull defects of mice.

## Materials and methods

### Cells and cell cultures

Bone marrow was obtained from hip and knee replacement patients in orthopedic department of the Prince Charles Hospital, Brisbane with informed consent and ethics approval from the Ethics Committee of Queensland University of Technology. Mononuclear cells (MNCs) were isolated from the bone marrow by density gradient centrifugation over Lymphoprep (Axis-shield PoC AS, Oslo, Norway) according to the manufacturer's protocol. The MNCs were plated into the culture flasks and

cultured in Dulbecco's Modified Eagle Medium (DMEM; Invitrogen Pty Ltd., Mt Waverley, VIC, Australia) containing 10% (v/v) fetal calf serum (FCS; InVitro Technology, Noble Park, VIC, Australia) and 1% (v/v) penicillin/streptomycin (Invitrogen). The unattached hematopoietic cells were removed through media changes. When reaching the 70-80% confluence, the attached mesenchymal cells were subcultured using 0.25% trypsin (Invitrogen) with 1mM EDTA (Invitrogen). Only passages 2 to 5 (P2-P5) mesenchymal cells were used in this study. Human umbilical vein endothelial cells (HUVECs; Clonetics, San diego, CA, USA) were cultured in a defined endothelial cell growth medium containing VEGF, FGF-2, IGF-1, EGF, ascorbic acid and hydrocortisone (EGM-2; Lonza Australia Pty Ltd., Mt Waverley, VIC, Australia) supplemented with 2% FCS. The medium was changed every three days until the cells were confluent.

**In vitro osteogenic differentiation and cobalt chloride treatment of BMSCs**

For the in vitro osteogenic differentiation, BMSCs were firstly seeded onto one side of collagen membrane and cultured in normal DMEM for 24hrs, then the DMEM was changed to osteogenic differentiation medium (10mM β-glycerophosphate, 50μM ascorbic acid and 100nM dexamethasone; Sigma Aldrich Pty Ltd, Castel Hill, NSW, Australia) 2 weeks prior to in vivo implantation. For the cobalt chloride-induced hypoxia treatment, BMSCs were firstly cultured in DMEM until reaching 70-80% confluence on cell culture flask surface, then the media was changed to the DMEM containing 10% (v/v) FCS and 100μM $CoCl_2$ one week before the implantation.

**Periosteum tissue engineering**

Collagen membrane scaffolds were fashioned from a 1mm-thick bovine type I collagen sheet (Medtronic Australia Pty Ltd, North Ryde, NSW, Australia) using a hole puncher 5mm across and sterilized by soaking in 75% ethanol for 10mins, then washed at least three times in PBS prior to cell seeding. The scaffold was fitted into a well of 96-well cell culture plate before 6 x $10^4$ BMSCs were seeded on top of the

scaffolds and incubated in osteogenic differentiation media at 37°C and in 5% $CO_2$ for 2 weeks prior to implantation (Fig.2 A-F). For the scaffolds carrying both osteogenesis-committed BMSCs and HUVECs or $CoCl_2$ pre-treated BMSCs or untreated BMSCs, 1 x $10^5$ HUVECs or $CoCl_2$ pre-treated BMSCs or untreated BMSCs were seeded onto the other side of scaffolds 3hrs prior to implantation (Fig.2 A-F). For the scaffolds carrying only untreated BMSCs, 6 x $10^4$ cells were seeded on top of the scaffold 2 weeks before the implantation. Scaffolds without cells were used as negative control.

To find out cell seeding efficiency and ascertain cell attachment to the scaffolds, the cells that fell off the scaffold (n=3) were trypsinized and collected 3hrs after initial cell seeding or secondary cell seeding. Then the cell number was counted using a NucleoCounter (ChemoMetec A/S, DK-3450 Allerød, Denmark) and the seeding efficiency was calculated as the percentage of cells remaining on the scaffold to the total cells seeded. To observe the cell attachment and distribution on scaffolds after initial cell seeding, the scaffold was fixed in 4% paraformaldehyde, embedded in paraffin and 5μm-thick serial sections were cut perpendicular to the cell seeding surface using a microtome (Leica Microsystems GmbH, Wetzlar, Germany). Cell nuclei were stained with DAPI (Molecular Probes, Invitrogen) and observed under a microscope (Carl Zeiss Microimaging GmbH, Gottingen, Germany) at 100 x magnification. To observe the cell attachment and distribution on scaffolds after secondary cell seeding, BMSCs labelled with intra-cellular green fluorescent nano-particles (Q-tracker 565; Invitrogen) were seeded onto the scaffolds carrying osteogenesis-committed BMSCs, and a 60μm thick slice from cryosectioning was stained with DAPI and observed directly under a fluorescent microscope (Carl Zeiss Microimaging GmbH, Göttingen, Germany) at 100 x magnification.

**Subcutaneous implantation of tissue engineered periosteum in SCID mice**

Animal ethics approval for the use of severe combined immunodeficient (SCID) mice in this experiment was granted by the QUT Animal Ethics Committee. A total of four

5-week old male SCID mice (Animal Resources Centre, Canning Vale, WA, Australia) were used. The animals were anesthetized with 1mL of ketamine (100mg/mL) and 0.15 mL of xylazine (20mg/mL) injected intraperitoneally. Three small incisions were made longitudinally along the central line of the shaved dorsal area, approximately 1cm apart, and subcutaneous pockets were made on each side of the incision with a pair of surgical scissors. Each individual pocket had in it one scaffold with different cell seeding strategy. Then the incisions were closed with surgical clips. All animals recovered fully from the surgery by the following day and were sacrificed after two weeks. The implants were retrieved and pictures were taken using a digital camera.

**Skull defect implantation of tissue engineered periosteum in SCID mice**

A total of twenty-eight 5-week old male SCID mice (Animal Resources Centre, Canning Vale, WA, Australia) were used. The animals were anesthetized with 1mL of ketamine (100mg/mL) and 0.15 mL of xylazine (20mg/mL) injected intraperitoneally. One small incision was made longitudinally along the centre line of the shaved skull skin area (Fig.1 A). After the skull bone surface was exposed, the periosteum covering the bone surface was totally removed using a dental scraper (Fig.1 B). A Ø2.5mm defect was then made through the skull using a dental bur driven by a dental drilling machine (Fig.1 C-F). Care was taken during the drilling to avoid entering the dura. The phosphate buffered saline (PBS) was applied regularly onto the drilling site to prevent overheating-related damages to local tissues. The defect was then managed in the following seven different ways with four mice in each: i.e. empty defect, defect filled with collagen only or collagen plus BMSCs, Bost, Bost plus BMSCs or HUVECs or $CoCl_2$ treated BMSCs. For the defect filled with scaffolds, one scaffold with different cell seeding strategy was gently inserted into the defect (Fig.1 G). Then the skin was replaced and the incision was closed with surgical clips (Fig.1 H). All animals recovered fully from the surgery by the following day and were sacrificed after four weeks. The skull defect area together with implants was harvested and pictures were taken by a digital camera.

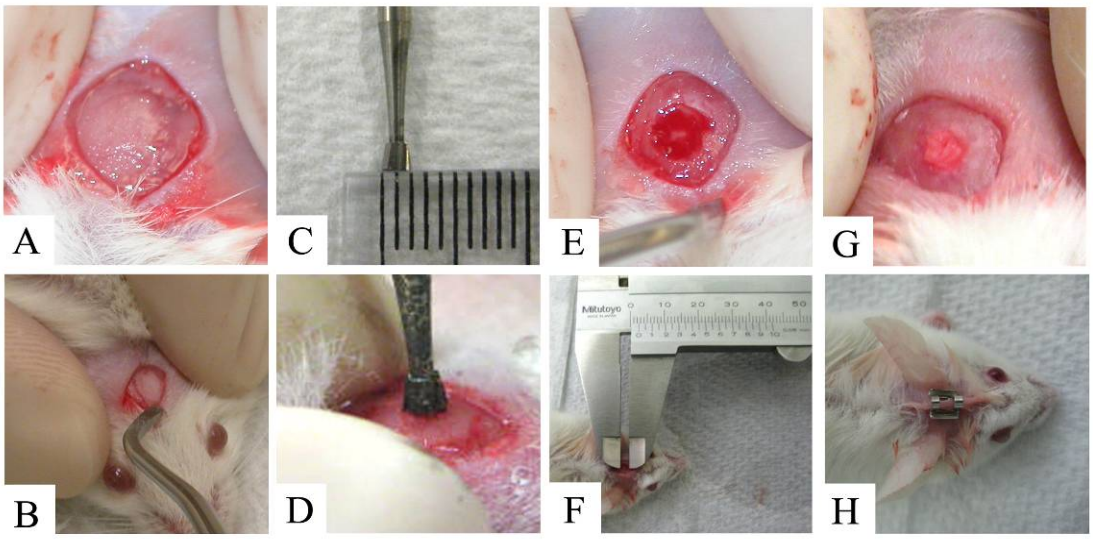


**Fig.1 Skull defect implantation of tissue engineered periosteum in SCID mice.** (A. an incision made on the skull skin; B. periosteum was removed by a scraper; C. measurement of the dental bur diameter; D. drilling a hole defect on the skull; E. a defect made on the skull; F. measurement of the defect size; G. a defect filled with scaffold; H. incision closed with a clip.)

**Assessment of calcification by micro-CT scanning**

All implants were fixed in 4% paraformaldehyde solution overnight at room temperature and then washed in PBS. Cross-sectional scans parallel to the cell seeding surface of subcutaneous or skull defect implants were performed in a micro-CT scanner (μCT40, SCANCO Medical AG, Brüttisellen, Switzerland) at a resolution of 12μm and three dimensional (3D) images of implants were reconstructed from the scans by the micro-CT system software package. To validate the in vivo calcification, scaffolds without cells or carrying untreated BMSCs or BMSCs-derived osteoblasts in vitro were fixed and scanned as well. For in vitro or subcutaneously implanted scaffolds, total volume and average density against hydro-apatite (HA) of calcification were measured and recorded by the micro-CT system software package for statistical analysis. For scaffolds in the skull defect, volume and average density against hydro-apatite (HA) of calcification within the defect area (defined by encircling the defect area on each micro-CT slice as area of interest) were measured and recorded for statistical analysis (Fig. 7 A-C).

**Von Kossa staining for calcification in subcutaneous implants**

Following micro-CT scanning the subcutaneous implants were embedded in paraffin and 5μm-thick serial sections were cut perpendicular to the implants using a microtome (Leica Microsystems GmbH, Wetzlar, Germany). Slices near the central area of the implants were used for Von Kossa staining. In brief, after slice dewaxing and hydration, Mayer's haematoxylin (HD Scientific Pty Ltd., Kings Park, NSW, Australia) were used for nuclear staining. 5% silver nitrate (Sigma-Aldrich) was added onto each slice and exposed to light for at least 30 minutes. Then the slices were briefly washed in distilled water and dehydrated in ethanol before being mounted with cover slides. The calcification was observed under a microscope (Carl Zeiss Microimaging GmbH, Göttingen, Germany) and images were taken.

**Assessment of new bone formation by histological H&E staining**

Following micro-CT scanning the skull defect implants were decalcified in 10% EDTA and embedded in paraffin as subcutaneous implants and 5μm-thick serial sections were cut perpendicular to the implants using a microtome (Leica Microsystems GmbH, Wetzlar, Germany). Slices near the central area of the implants were used for the H&E staining. Briefly, following slice dewaxing and hydration, Mayer's haematoxylin (HD Scientific Pty Ltd., Kings Park, NSW, Australia) was used for nuclear staining. After dehydration in alcohol with up-grading concentrations, cell plasma and extracellular matrix were stained by eosin (HD Scientific Pty Ltd., Kings Park, NSW, Australia). Based on H&E staining, *de novo* bone formation within the implants was observed and the area of new bone tissues on each slice was measured using AxioVision software (Carl Zeiss Microimaging GmbH, Göttingen, Germany). Three measurements from each implant were averaged and used for statistical analysis.

**Assessment of vascularization and new bone formation using immunohistochemical staining**

Slices near the central area of the implants were used for the immunohistochemical staining. A von Willebrand factor (vWF) antibody (mouse anti-human, Chemicom International Inc., Temecula, CA, USA) was used to identify the presence of endothelial cells in the implants. An alkaline phosphatase (ALP) antibody (Santa Cruz Biotechnology, Inc., Santa Cruz, CA) was used to confirm newly formed bone in implants. In brief, following slice dewaxing and hydration, endogenous peroxidase activity was quenched by incubating the sample slices with 3% $H_2O_2$ for 20 minutes then blocked with 10% swine serum for 1 hour. The samples were incubated with the vWF primary antibody (1:300) or ALP antibody (1:200) overnight at 4$^{o}$C, followed by incubation, at room temperature, with a biotinylated swine-anti-mouse, rabbit, goat secondary antibody (DAKO Multilink, CA, USA) for 15 minutes, and then with horseradish perioxidase-conjugated avidin-biotin complex (DAKO Multilink, CA, USA) for another 15 minutes. The antibody complexes were visualized by the addition of a buffered diaminobenzidine (DAB) substrate for 4 minutes. Mayer's haematoxylin (HD Scientific Pty Ltd., Kings Park, NSW, Australia) was used for counter staining. The number of $vWF^{+}$ blood vessels were counted and normalized to the area of the implant on each slice. Three measurements from each implant were averaged and used for statistical analysis.

**Double staining of both vWF and calcium on subcutaneous implants**

Double staining with vWF antibody and von Kossa method (calcium staining) was performed on subcutaneous implants to determine the distribution of and relationship between osteogenesis and vascularization. In brief, following vWF staining, 5% silver nitrate (Sigma-Aldrich) was added onto each slice and exposed to light for at least 30 minutes and the slices briefly washed in distilled water and dehydrated in ethanol before being mounted with cover slides.

## Statistical analysis

Analysis was performed using SPSS software (SPSS Inc, Chicago, Il, USA). All the data were analyzed using one-way ANOVA or Friedman test for group differences. The significance level was set at $p \leq 0.05$.

## Results

### In vitro Cell seeding efficiency and attachment in engineered periosteum

As the bar graph in Fig.2 shows, the cell seeding efficiency was 92.3 ± 2.5% for the first cell seeding and 85.3 ± 5.0% for the second seeding. Paraffin slices stained by DAPI revealed that after initial cell seeding the cells attached to the collagen fibres and distributed evenly within the scaffold (Fig. 2G). Slices from cryosectioning revealed that most fluorescence-labelled BMSCs attached and distributed on the seeding side of scaffold (Fig. 2H).

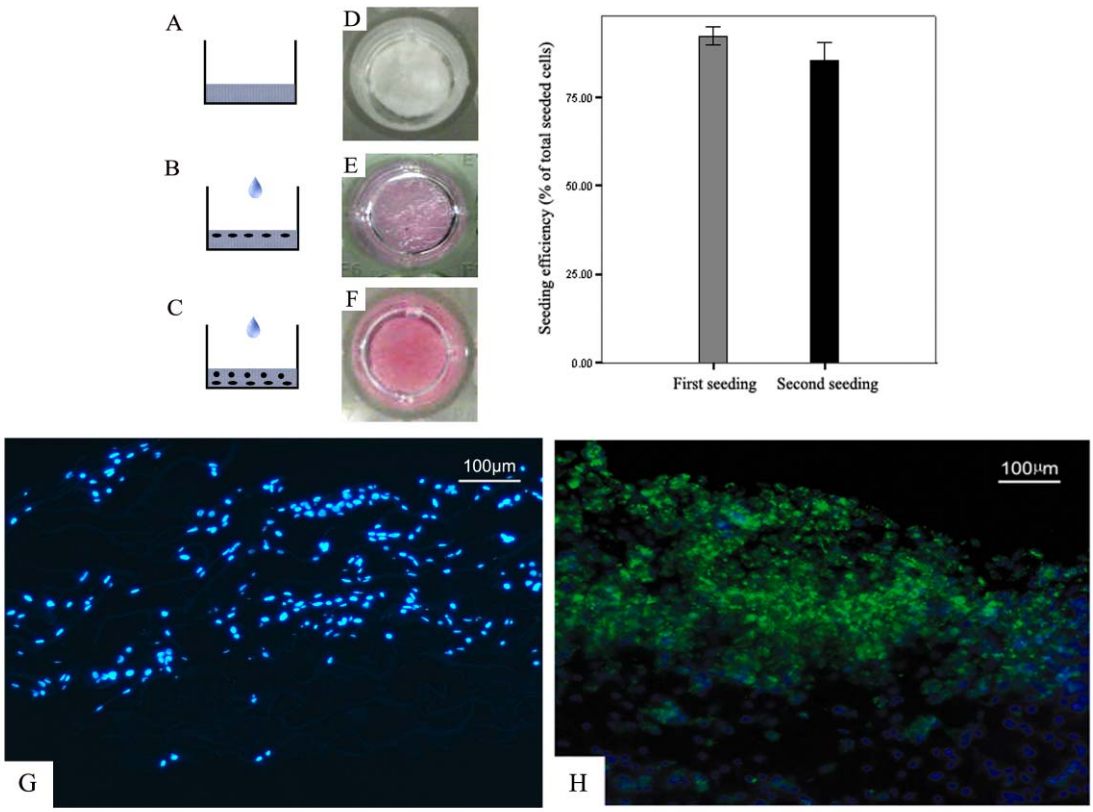


**Fig.2 Cell seeding on collagen scaffolds.** (A. illustration of a collagen membrane in

96-well plate; B. illustration of first cell seeding on one side of the collagen membrane; C. illustration of second cell seeding on the other side of the collagen membrane; D. actual image of a collagen membrane in 96-well plate; E. actual image of first cell seeding on one side of the collagen membrane; F. actual image of second cell seeding on the other side of the collagen membrane; G. paraffin slice stained with DAPI showing cell attachment and distribution on scaffolds after first seeding; H. Cryosectioned slice showing the distribution of secondarily seeded cells (with green fluorescence) on scaffolds.

**Osteogenesis in the subcutaneously implanted tissue engineered periosteum**

Upon general observation on the harvested implants, scaffolds carrying BMSCs-derived osteoblasts (Bost) alone or together with untreated BMSCs, HUVECs or $CoCl_2$-treated BMSCs seemed denser and more opaque compared with scaffolds in vitro or seeded with no cells or with untreated BMSCs (Fig.3A-G). After micro-CT scanning and 3D reconstruction, total volume and average density of the calcified areas in different scaffolds were calculated automatically by the micro-CT software (Fig. 3H-N). At the two week time point studied in this experiment, there was no calcification found in the naked scaffold or scaffold seeded with untreated BMSCs (Fig.2I-J); Very little calcification was identified in the scaffold carrying BMSCs and cultured in vitro in osteogenic media for two weeks (Fig.3H). Substantial amount of calcification was found in scaffolds seeded with Bost alone or together with untreated BMSCs, HUVECs or $CoCl_2$-treated BMSCs (Fig.3K-N), and the combination of Bost and $CoCl_2$-treated BMSCs showed the highest volume of calcified areas (Fig.3, $p<0.05$, Friedman test). No significant differences were found in the average density of calcified areas among scaffolds seeded with Bost alone or together other cells (Fig.3, $p>0.05$, Friedman test). Upon H&E and Von Kossa staining on paraffin slices, no bone tissue formation was found in all different scaffolds (Fig.4 A-C & G-I), while calcium precipitation along collagen fibres (shown as black dots or areas on slices) was far more evident in subcutaneously implanted scaffolds carrying Bost alone or together with other cells

(Fig.3F & J-L) than the in vitro Bost-carrying scaffolds (Fig.4D). The slices from Bost plus $CoCl_2$-treated BMSCs group showed more extensive calcification compared with other groups (Fig.4L).

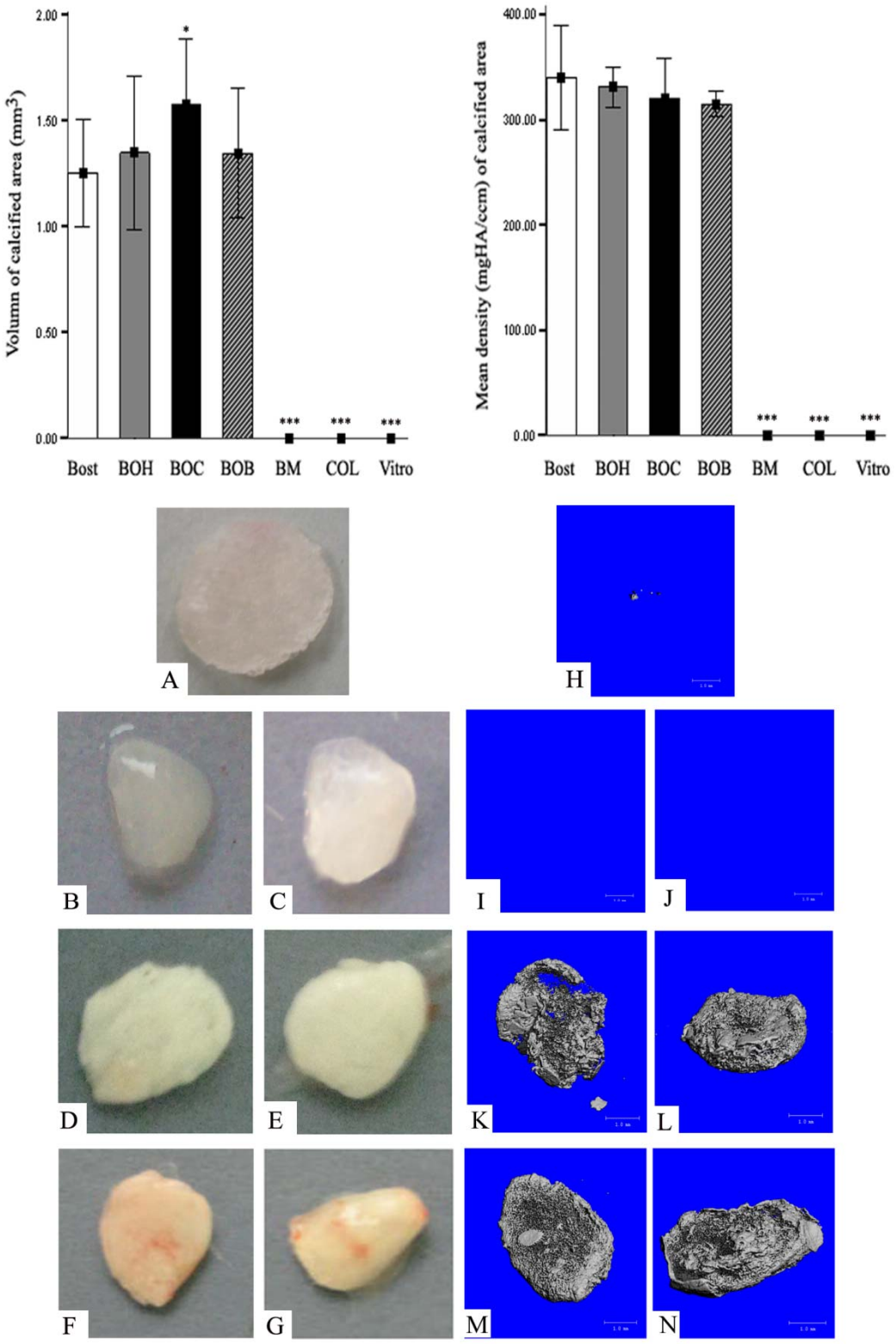

**Fig.3 In vitro scaffold, subcutaneous implants and Micro-CT scanning analysis.** (A. in vitro Bost-carrying scaffold; B. harvested scaffold without seeding cells; C. harvested scaffold carrying BMSCs; D. harvested scaffold carrying Bost only; E. harvested scaffold carrying Bost plus BMSCs; F. harvested scaffold carrying Bost plus HUVECs; G. harvested scaffold carrying Bost plus $CoCl_2$-treated BMSCs; H-N. 3D reconstruction images corresponding to the scaffolds shown in A-G; Bost: BMSCs-derived osteoblasts; BOH: Bost plus HUVECs; BOC: Bost plus $CoCl_2$-treated BMSCs; BOB: Bost plus BMSCs; BM: BMSCs only; COL: collagen scaffold only; Vitro: Bost-carrying scaffolds prior to implantation; *: $p<0.05$;***: $p<0.001$)

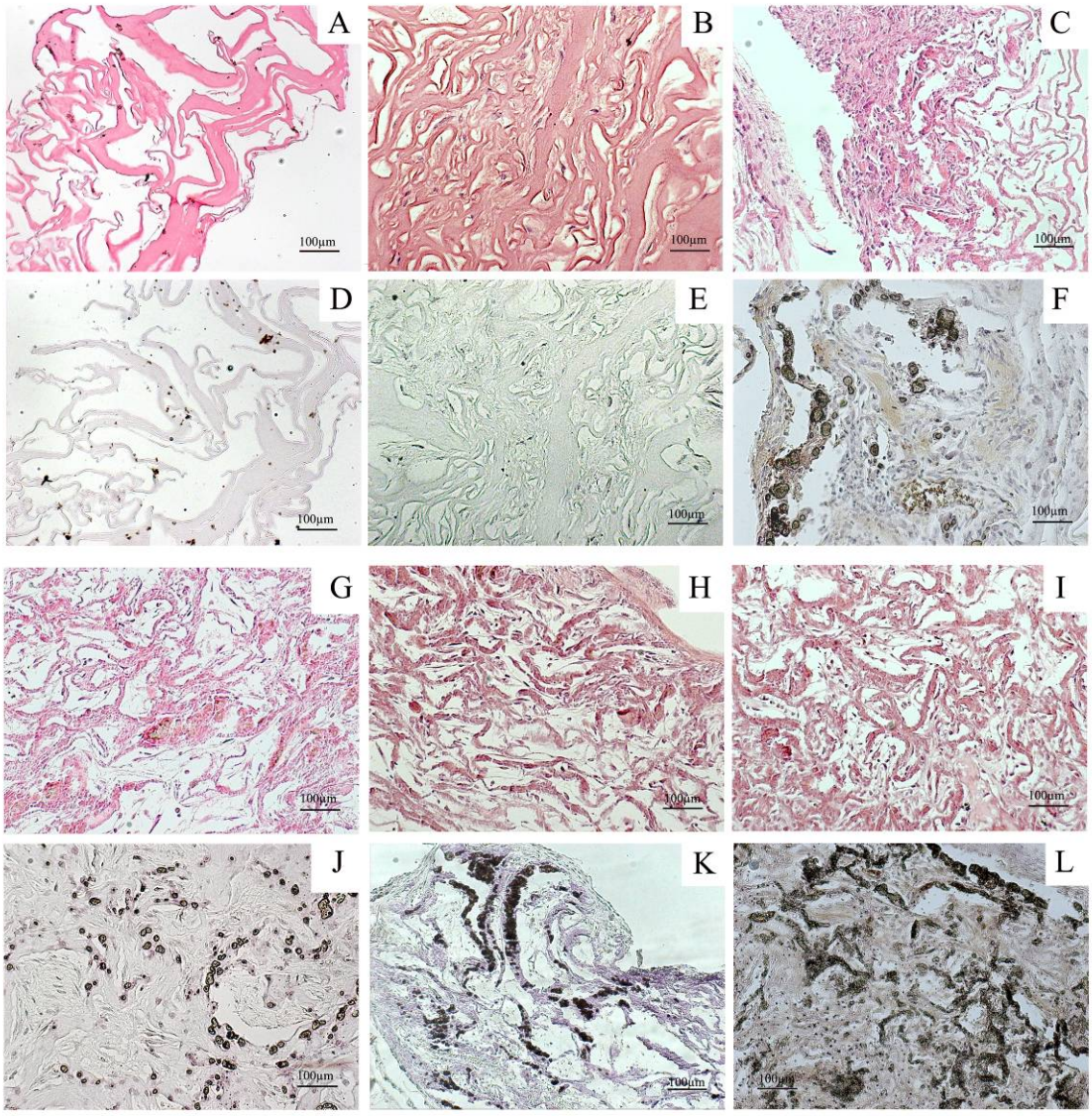


**Fig.4 H&E and von Kossa staining on in vitro and subcutaneous implants (100×).**

(A. H&E staining on in vitro Bost-carrying scaffold; B. H&E staining on harvested scaffold carrying BMSCs only; C. H&E staining on harvested scaffold carrying Bost only; G. H&E staining on harvested scaffold carrying Bost plus BMSCs; H. H&E staining on harvested scaffold carrying Bost plus HUVECs; I. H&E staining on harvested scaffold carrying Bost plus CoCl2-treated BMSCs; D-F & J-L. von Kossa staining on the slices from the same groups as A-C & G-I.)

**Vascularisation in the subcutaneously implanted tissue engineered periosteum**

Upon general observation on the harvested implants,, scaffolds carrying both Bost and HUVECs or $CoCl_2$-treated BMSCs seemed to have more blood vessels growing around and into the scaffold compared with other scaffolds (Fig.3F, G). Immunohistochemical staining against vWF showed that scaffolds carrying both Bost and HUVECs or $CoCl_2$-treated BMSCs had more micro-blood vessels and higher degree of vascularisation than other scaffolds (Fig.5A-H, $p<0.05$, Friedman test). Although scaffolds seeded with Bost or plus untreated BMSCs had higher average of vessel density than the scaffolds without seeding cells or seeded with BMSCs only, the difference was not statistically significant (Fig.5, $p>0.05$, Friedman test). Calcium-vWF double staining revealed that $vWF^+$ blood vessels distributed closely to the calcium precipitation areas (Fig.5 I).

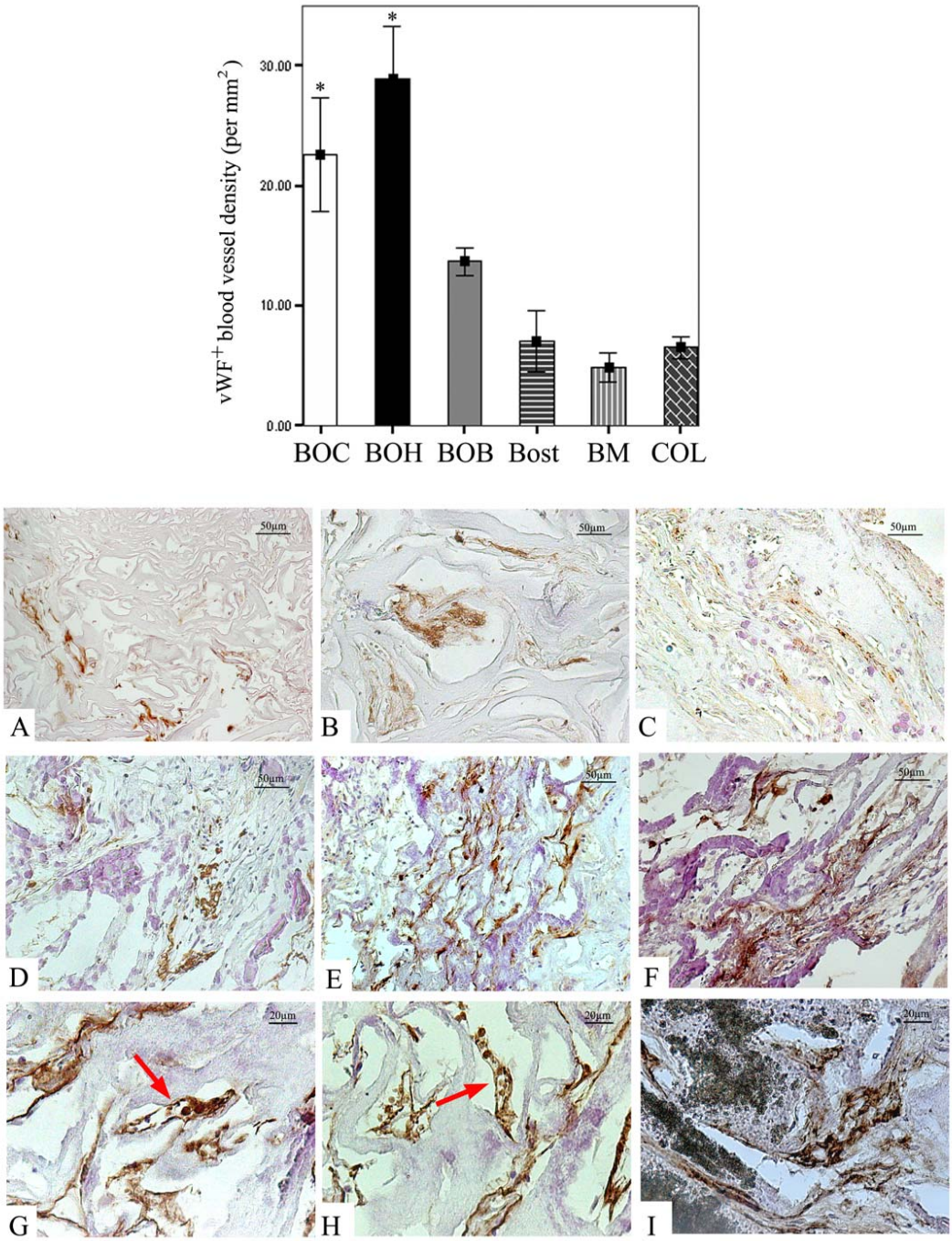


**Fig.5 Vascularisation in the subcutaneously implanted tissue engineered periosteum. (A.** $vWF^+$ blood vessels in harvested scaffold without seeding cells (200×); B. $vWF^+$ blood vessels in harvested scaffold seeded with BMSCs only (200×); C. $vWF^+$ blood vessels in harvested scaffold carrying Bost only (200×); D. $vWF^+$ blood vessels in harvested scaffold carrying Bost plus BMSCs (200×); E. $vWF^+$ blood vessels in harvested scaffold carrying Bost plus CoCl2-treated BMSCs (200×); F. $vWF^+$ blood vessels in harvested scaffold carrying Bost plus HUVECs (200×); G&H. $vWF^+$ blood vessels (arrows) in harvested scaffolds at higher magnification (400×); I.

Calcium-vWF double staining showing $vWF^+$ blood vessels distributed closely to the calcium precipitation areas (400×); Bost: BMSCs-derived osteoblasts; BOH: Bost plus HUVECs; BOC: Bost plus $CoCl_2$-treated BMSCs; BOB: Bost plus BMSCs; BM: BMSCs only; COL: collagen scaffold only; *: $p<0.05$ )

**Osteogenesis in the skull-defect implanted tissue engineered periosteum**

Upon general observation of the harvested skull defect-implant complex, the defects without implants or filled with collagen sponge alone or plus BMSCs showed very limited repair compared with the defects filled with scaffolds carrying Bost or together with other cells (Fig.6 A-G). The collagen sponge without pre-seeded cells or with only BMSCs was almost degraded and absorbed in the defect area (Fig.6 B-C). After micro-CT scanning and 3D reconstruction, total volume and average density of the calcified areas within defects were calculated. The implants carrying Bost plus HUVECs or $CoCl_2$-treated BMSCs showed significantly higher volume of calcified areas than other implants (Fig.7, $p<0.001$, one-way ANOVA test), while no significant difference was found in the average density among different groups (Fig.7, $p>0.05$, one-way ANOVA test). The top-bottom view of 3D reconstructed defect areas (Fig.7 D-J) showed that the defects filled with implants carrying Bost plus HUVECs or $CoCl_2$-treated BMSCs healed much better than other groups. H&E staining on slices revealed evident new bone formation within the implants carrying Bost alone or plus other cells (Fig.8 A-H), while very little bone formation was found in the defects without implants or filled with collagen sponge alone or plus BMSCs (Fig.8 A,D,G). The area of new bone tissues within implants on each slice was measured and the implants carrying Bost plus HUVECs or $CoCl_2$-treated BMSCs had significantly more new bone tissues than other implants (Fig.8, $p<0.001$, one-way ANOVA test). The defects filled with these two kinds of implants were almost bridged by the newly formed bone tissues (Fig.8 E-H). Interestingly, the *de novo* bone tissue formed along and incorporated the collagen fibers into the newly formed bone (Fig.8 I-J). Immunohistochemical staining against alkaline phosphatase (ALP) further confirmed the newly formed bone tissue within implants was surrounded by $ALP^+$ osteoblasts

(Fig.8 K).

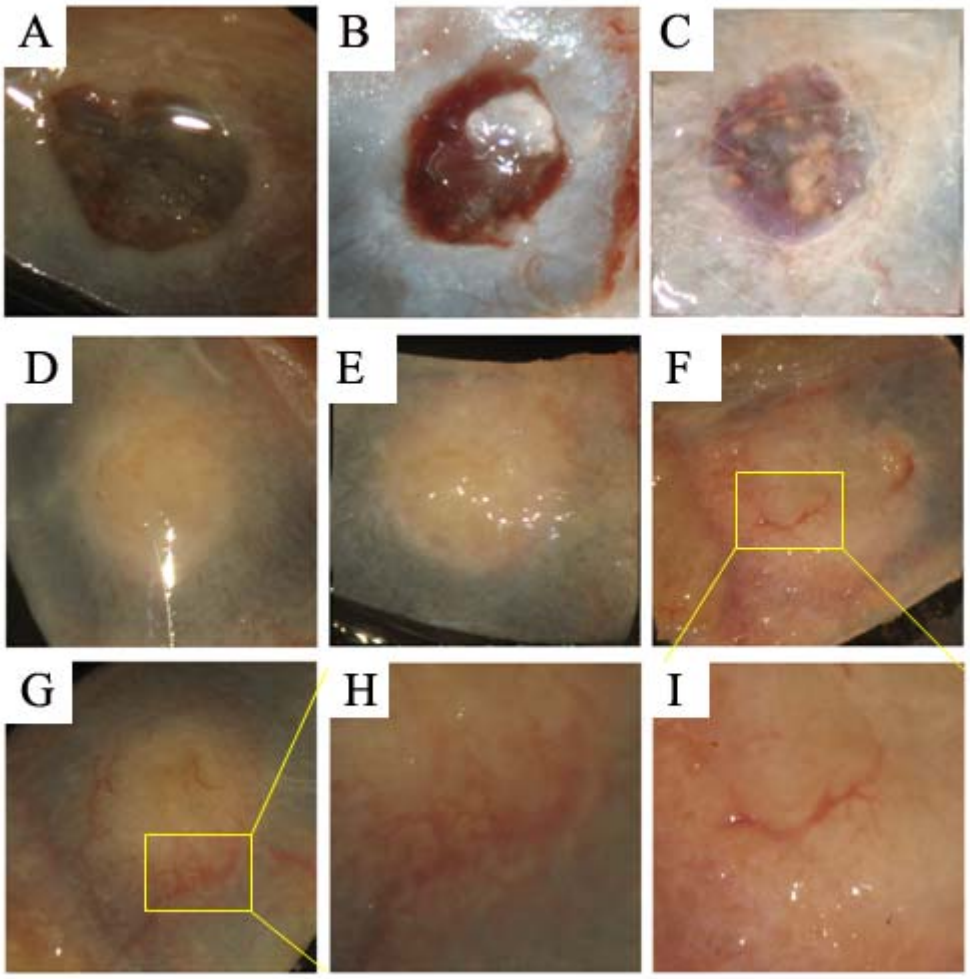


**Fig.6 General observation on the harvested skull defect-implant complex.** (A. defect without implant; B. defect filled with collagen only; C. defect filled with collagen plus BMSCs; D. defect filled with implant carrying Bost only; E. defect filled with implant carrying Bost plus BMSCs; F. defect filled with implant carrying Bost plus $CoCl_2$-treated BMSCs; G. defect filled with implant carrying Bost plus HUVECs; H. Zoom in image of the selected area in G showing blood vessel ingrowth; I. Zoom in image of the selected area in F showing blood vessel ingrowth.)

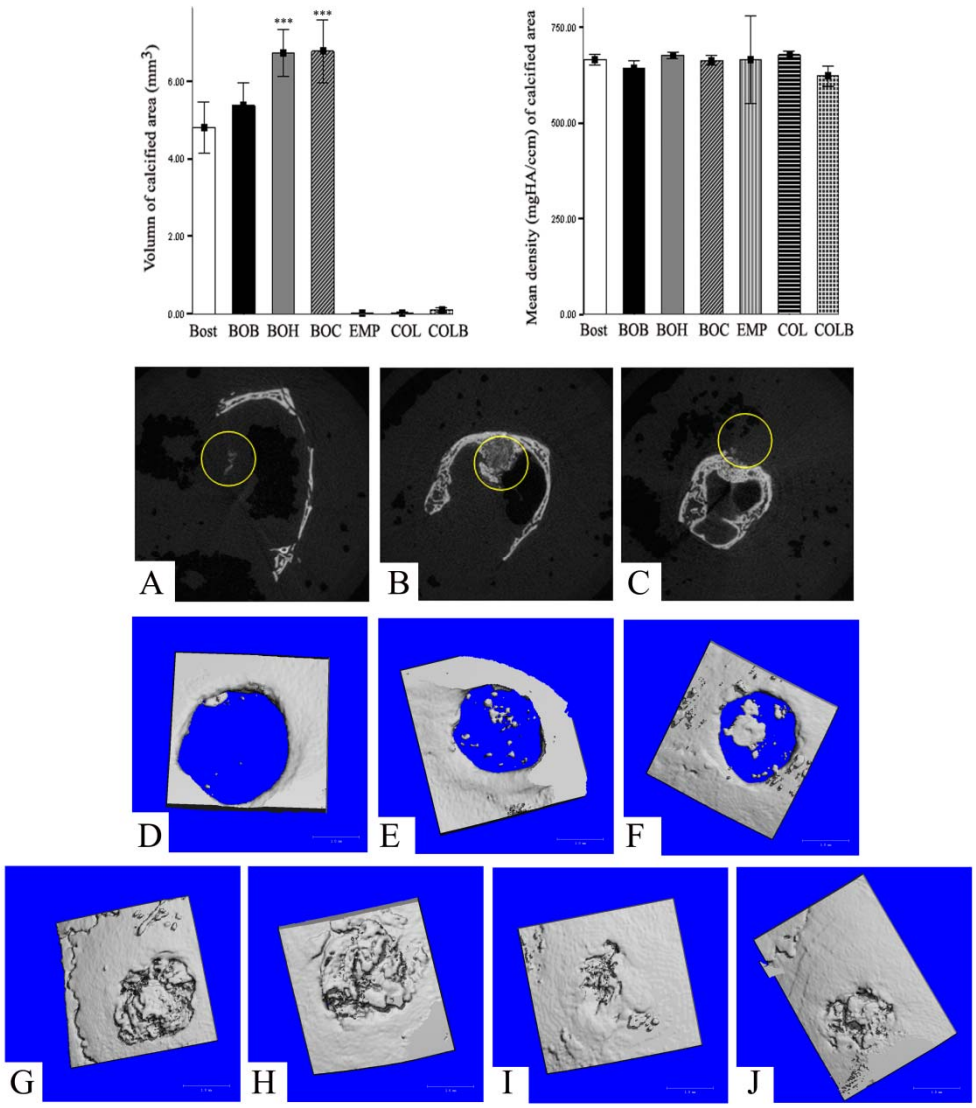


**Fig.7 Micro-CT scanning analysis on the harvested skull defect-implant complex.** (A. encircling the implant on the CT slice where it just appears; B. encircling the implant on the CT slice when the scanning is through the centre of implant; C. encircling the implant on the CT slice where it just disappears; D. top-bottom view of the 3D reconstructed image of the defect without implant; E. top-bottom view of the 3D reconstructed image of the defect filled with collagen only; F. top-bottom view of the 3D reconstructed image of the defect filled with collagen plus BMSCs; G. top-bottom view of the 3D reconstructed image of the defect filled with implants carrying Bost; H. top-bottom view of the 3D reconstructed image of the defect filled with implants carrying Bost plus BMSCs; I. top-bottom view of the 3D reconstructed image of the defect filled with implants carrying Bost plus $CoCl_2$ treated BMSCs; J.

top-bottom view of the 3D reconstructed image of the defect filled with implants carrying Bost plus HUVECs; Bost: BMSCs-derived osteoblasts; BOH: Bost plus HUVECs; BOC: Bost plus $CoCl_2$-treated BMSCs; BOB: Bost plus BMSCs; EMP: defect without implant; COLB: collagen plus BMSCs only; COL: collagen scaffold only; ***: $p<0.001$)

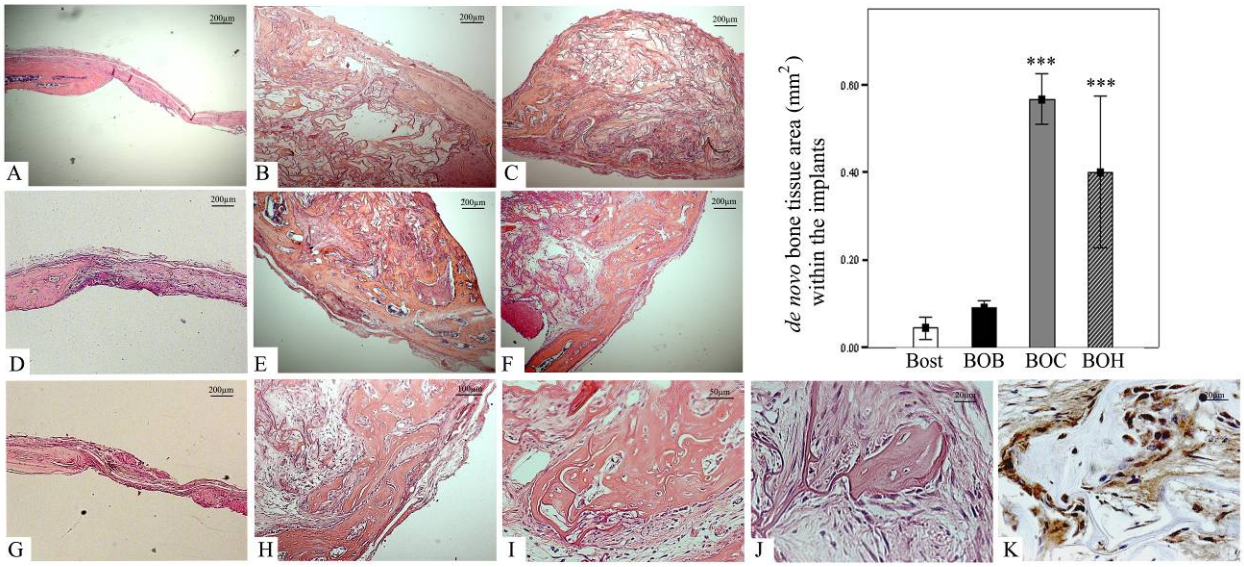


**Fig.8 H&E and ALP staining on the harvested skull defect-implant complex.** (A. H&E staining on defect without implant (40×); B. H&E staining on defect filled with implant carrying Bost only (40×); C. H&E staining on defect filled with implant carrying Bost plus BMSCs(40×); D. H&E staining on defect filled with collagen only (40×); E. H&E staining on defect filled with implant carrying Bost plus HUVECs (40×); F. H&E staining on defect filled with implant carrying Bost plus $CoCl_2$-treated BMSCs (40×); G. H&E staining on defect filled with collagen plus BMSCs (40×); H. A higher magnification showing the *de novo* bone formation in the defect area (100×); I & J. higher magnifications (200× and 400×) showing the *de novo* bone formed along and incorporated the collagen fibre; K. ALP staining showing $ALP^+$ osteoblast surrounding the *de novo* bone tissue (400×); Bost: BMSCs-derived osteoblasts; BOH: Bost plus HUVECs; BOC: Bost plus $CoCl_2$-treated BMSCs; BOB: Bost plus BMSCs; ***: $p<0.001$)

**Vascularisation in the skull-defect implanted tissue engineered periosteum**

Upon general observation on the harvested skull defect-implant complex, the defects filled with implants carrying Bost plus HUVECs or $CoCl_2$-treated BMSCs showed more blood vessels growing into the defect area than other defects (Fig.5 F-I). Immunohistochemical staining against vWF revealed significantly more blood vessels and higher degree of vascularization in implants carrying Bost plus HUVECs or $CoCl_2$-treated BMSCs than in other implants (Fig.9, $p<0.001$, one-way ANOVA test). $vWF^+$ micro blood vessels were found gathering around the *de novo* bone tissues and penetrating into the newly formed bone tissues (Fig.9 G-L).

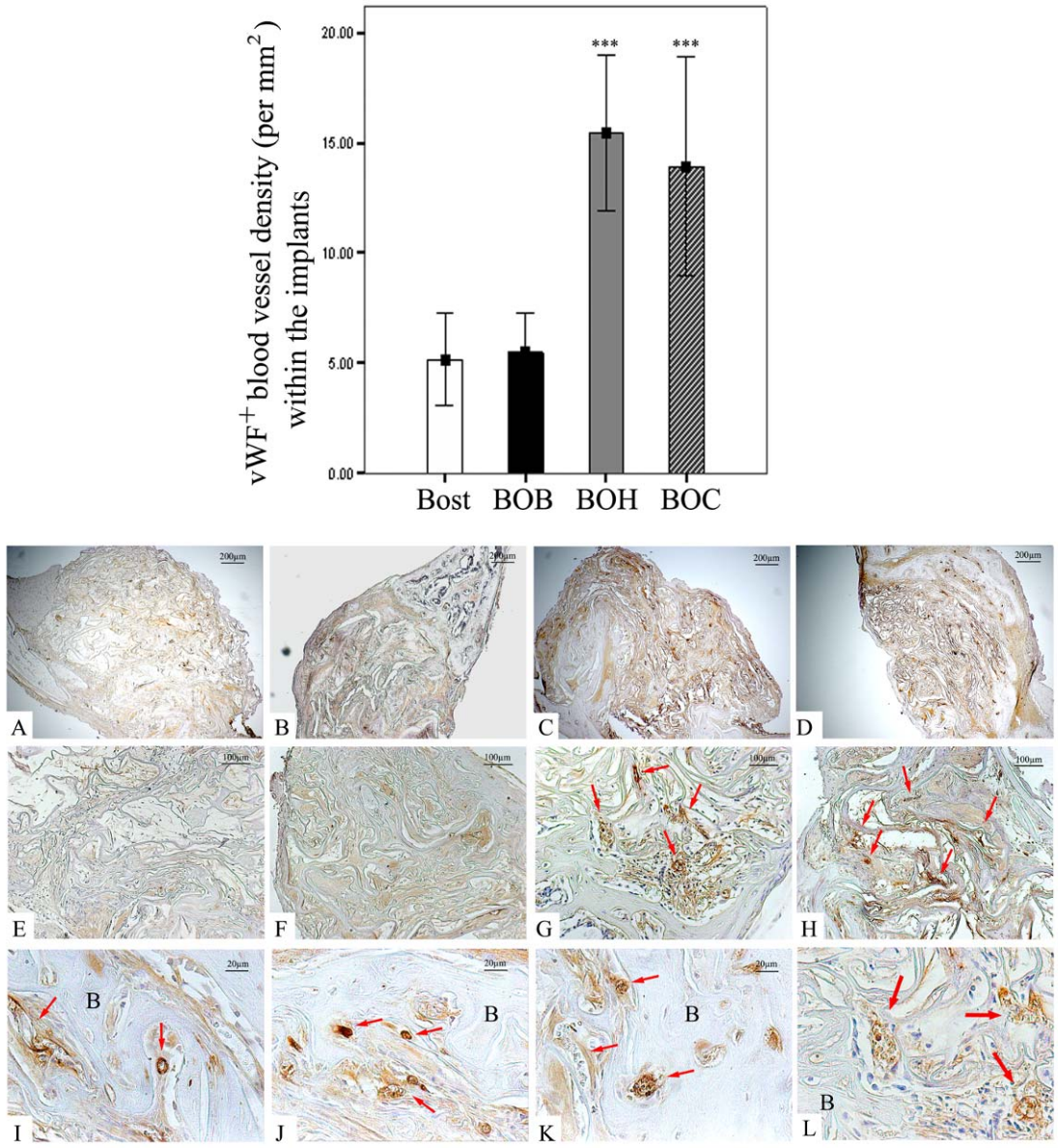


**Fig.9 Vascularisation in the skull-defect implanted tissue engineered periosteum. (A.** vWF staining on harvested implant carrying Bost only (40×); B. vWF staining on

harvested implant carrying Bost plus BMSCs (40×); C. vWF staining on harvested implant carrying Bost plus CoCl2-treated BMSCs (40×); D. vWF staining on harvested implant carrying Bost plus HUVECs (40×); E-H. higher magnification (100×) of the vWF staining on harvested implants from the same groups as A-D; I-L. higher magnification (400×) of the vWF staining showing the $vWF^+$ micro blood vessels gathering around and penetrating into the newly formed bone tissues; Arrows pointing to $vWF^+$ micro blood vessels; Bost: BMSCs-derived osteoblasts; BOH: Bost plus HUVECs; BOC: Bost plus $CoCl_2$-treated BMSCs; BOB: Bost plus BMSCs; ***: $p<0.001$)

**Discussion**

As recently pointed out in a review by Zhang et el, periosteum engineering could assist in structural *de novo* bone formation and is therefore a promising method for bone defect restoration [55]. Although much work has focused on the structure, cell populations and osteogenic mechanisms within the periosteum [18-19, 35, 59], few, if any, references were found which addresses engineered periosteum containing different cell populations such as osteogenic and pro-angiogenic cells, not to mention an *in vivo* assessment of any such constructs. As far as we can ascertain, this is the first attempt to construct an artificial bi-layered periosteum with two different cell populations – osteogenic and pro-angiogenic cells – modeled on the natural structure of real periosteum. Previous studies concerning artificial periosteum have described structures with a single cell population, and therefore differ considerably from the natural structure of real periosteum; the cell viability, stability, long-term function and clinical applicability of these artificial periostea are therefore questionable [56-58]. For example, in one study a collagen sponge composite was seeded with only osteogenic cells in order to form a bio-artificial periosteum – vascularization was therefore not even considered [57]. Another study used an acellular periosteum replacement membrane to wrap the defect areas and could therefore not be considered as a tissue engineered periosteum [56]. In a third study submucosa from the small intestine was used to mimic periosteum onto which bone marrow stromal cells

(BMSCs) were seeded [58]. The obvious drawback of this latter approach is that scaffold materials have to be sourced from the small intestine necessitating the need for an operation to harvest donor materials. In the experiment presented here, both osteogenic (BMSCs derived osteoblasts) and pro-angiogenic cells (endothelial cells or $CoCl_2$-pre-treated BMSCs) were seeded onto either side of a collagen membrane, trying to reflect the basic cellular and structural features of real periosteum.

Although there are many other cell populations residing within the real periosteum, osteogenic and endothelial cells are the major and most important populations [11] and the interactions between the osteogenesis and vascularisation determine the osteogenic function of periosteum to a large extent. To enhance the vascularisation of an engineered tissue or organ, there are many different methods and three of them are most often used: i) add autogenous or allogenous endothelial cells which could be directly incorporated into the host blood vessel networks[6, 74]; ii) impregnate pro-angiogenic growth factors, such as VEGF, bFGF, PDGF ect., into the scaffold to incur the new blood vessel ingrowth[8, 119]; iii) incorporate gene vectors (plasmid or virus) encoding pro-angiogenic growth factors or cells transfected by those gene vectors with scaffolds to attract new blood vessels[185]. Unfortunately, the drawbacks of these methods are as evident as their believed advantages, such as immunological reactions when using allogenous endothelial cells, the low in vitro growth rate of autologous endothelial cells, biological safety concerns about the gene vectors or transfected cells and unstable temporal and spatial release of pro-angiogenic growth factors in defect areas. Some studies had tried to induce autologous bone marrow-derived mesenchymal stem cells to differentiate towards endothelial cells, but the results so far are still elusive and uncertain[170-171]. On the other hand, it has been reported that either low oxygen pressure or hypoxia-mimicing agents, such as $CoCl_2$ or hydrogen peroxide ($H_2O_2$), can upregulate the expression of pro-angiogenic growth factors, VEGF in particular, in a variety of cells including BMSCs[187, 193]. The hypoxia pre-treated BMSCs had been successfully used to help re-vascularize the ischemic or infarcted muscles in animal models[191-192]. In this experimental study, BMSCs were pre-treated with the hypoxia-mimicing agent $CoCl_2$ and the VEGF

expression after treatment was found to be increased by around 5 fold in our previous studies. As VEGF is an important growth factor which has been reported closely involved in both angiogenic and osteogenic processes [152, 163-164], the $CoCl_2$ pre-treated BMSCs were incorporated together with BMSCs-derived osteoblasts into the engineered periosteum model to see whether they could enhance both osteogenesis and vascularization in vivo.

Two different animal models are often used to assess the in vivo osteogenic ability of engineered tissues: subcutaneous (ectopic) and bone defect (orthotopic) osteogenesis models. In this study, both models were included. During pathological and normal physiological osteogenesis, two distinct patterns of bone formation are involved – intramembranous and endochondral ossification. Intramembranous ossification predominantly takes place in the periosteum during normal bone formation in which osteoprogenitor cells differentiate directly into osteoblasts laying down new bone tissues [194]. Although much has been reported about both *in vivo* and *in vitro* interactions between osteogenesis and vascularization [6, 8], the knowledge of *in vivo* interactions between osteogenesis and vascularisation, especially those during early osteogenic stages and related to periosteal intramembranous ossification, is still very much patchy. Early stage histological and ultrastructural changes in microvessels of periosteal calluses after bone facture, using the light and electron microscope, has been described previously, but no quantitative data about the interaction between osteogenesis and vascularization was provided [49]. In the present study, observations and assessments about the osteogenesis and vascularisation at a relatively early stage in the engineered periosteum were performed two weeks after subcutaneous implantation and four weeks after skull defect implantation. Osteogenesis and vascularization were then quantified using micro-CT scanning, histological and immunohistochemical methods [195]. Our findings showed that subcutaneously implanted scaffolds presented no signs of new bone formation despite more extensive calcification compared with scaffolds prior to in vivo implantation, while in skull defects *de novo* bone tissues were evident. Although the observation time for subcutaneously and skull defect implanted scaffolds was different, no signs

of new bone tissues in the subcutaneously implanted scaffolds might still indicate that the differences in micro-environment at different implantation sites may determine different pattern of osteogenesis. Another noteworthy point is that in the skull defect naked collagen implants or implants carrying only BMSCs were almost bio-degraded and generated very limited new bone tissue within the defect when compared with implants carrying BMSCs-derived osteoblasts (Fig.8 A,D,G). This phenomenon suggests that new bone formation may require the orchestration of an osteogenesis-favouring environment, appropriate calcium precipitation on the collagen fibres and osteogenic cells.

As for the vascularisation, HUVECs and $CoCl_2$ pre-treated BMSCs helped increase blood vessel density in both subcutaneously and skull defect implanted scaffolds compared with others without these two kinds of cells. Interestingly, the addition of HUVECs only enhanced the osteogenesis in skull defect-filling implants but not in subcutaneously implanted scaffolds. It is different from $CoCl_2$ pre-treated BMSCs which enhanced the osteogenesis in both situations. This difference could be accounted for in terms of the mechanisms these two different cells exploit to enhance osteogenesis. The upregulated VEGF expression by $CoCl_2$ pre-treated BMSCs could start to stimulate the osteogenesis of BMSCs-derived osteoblasts as soon as the cells are seeded and this osteogenic process could be even more enhanced by subsequently enhanced vascularization. Alternatively, HUVECs might promote osteogenesis only after the supportive role of enhanced vascularization occurs as the natural VEGF expression of HUVECs was found to be quite low according to our previous studies. The calcium-vWF double staining and $vWF^+$ micro blood vessels surrounding *de novo* bone tissues also revealed the close relationship between osteogenesis and vascularization. To confirm the pro-osteogenic and angiogenic effects of $CoCl_2$ pre-treated BMSCs, untreated BMSCs were used together with BMSCs-derived osteoblasts as an internal control. The findings in this study showed that the addition of untreated BMSCs would not significantly help the in vivo ectopic or orthotopic osteogenesis by BMSCs-derived osteoblasts and vascularization. The roles of undifferentiated BMSCs in osteogenic environments need further investigation.

Based on the findings of this experimental study, it could be concluded that $CoCl_2$ pre-treated BMSCs can enhance both ectopic and orthotopic osteogenesis of BMSCs-derived osteoblasts and vascularization at an early osteogenic stage, while endothelial cells can promote osteogenesis only after four-weeks. Subcutaneous areas of mice may not be appropriate for assessment of new bone formation on collagen scaffolds. This study demonstrated the potential application of $CoCl_2$ pre-treated BMSCs in the tissue engineering not only for periosteum but also bone or other vascularized tissues.

**Acknowledgements**

We would like to thank the Built Environment & Engineering Faculty of Queensland University of Technology for its support in this project. The collagen sponge was kindly provided by Prof. Dietmar Hutmacher.

# CHAPTER 5 *SUMMARY AND DISCUSSION*

Many Bone substitute materials have been developed in recent years. However, blood supply in large bone defects is still one of the unsolved major challenges after these bone substitute materials are filled into defect areas. Periosteum plays an important and indispensable role in forming vascularized bone not only in bone development but also in bone defect healing. The initial rationale for this project was to construct a functional *in vitro* periosteum and then test its ability to aid the repair of critical-sized bone defect in animal models. In spite of the many efforts by other researchers, the actual construction of a functional and highly vascularized periosteum using autologous single stem cell source is still a considerable challenge. In an effort to construct a bio-mimetic tissue engineered periosteum, this project was designed with three separate but closely-linked experiments, which in the end led to four independent papers summarized in this thesis. The thought behind the design was that before commencing the periosteum engineering, it was important to better understand the structures and cell populations in the physiological periosteum, as well as the changes of periosteum in active stage of osteogenesis and physiological conditions such as ageing and oeteoporosis. Subsequently, a dual layered periosteum was constructed to induce or enhance the vascularization. Since the blood supply is one of the major part in the process of *de novo* bone formation *in vivo*, this project investigated the regulatory role of BMSCs in blood vessel formation. BMSCs are considered to play the primary role in inducing both osteogenesis and vascularization in the engineered periosteum since BMSCs are a source rich in stem cells and easy to obtain in terms of future clinical applications. To achieve this purpose, the focus was set upon the endothelial cell differentiation potential of BMSCs or the use of BMSCs to regulate vascularization as the osteogenic differentiation of BMSCs has been well established. The tissue engineered periosteum was further evaluated by the in vivo tissue formation after implantation of the construct into SCID mice subcutaneously and into a skull bone defect model.

To construct the periosteum which is mimicking the physiological periosteum not

only anatomically but also functionally and applicable in vivo, the structure and cell populations in physiological periosteum have been firstly investigated in depth and formed the basis of knowledge for the tissue engineered periosteum construction. Although the general structural and cell populations in periosteum have been well studied and established, the specific information about the site- and age-related alterations in periosteum anatomy and physiology is still lacking. On the other hand, whether the bone health status has the influence on the periosteum and its function is not known either. To answer these questions, the periostea on both diaphyseal and metaphyseal bone surfaces of femurs from rats of different ages or with induced osteoporosis were observed. Our findings revealed for the first time that despite the diaphyseal periosteum showed age-related degeneration which is indicated by the decrease in both the thickness and cell number in the periosteum, the metaphyseal periosteum from aged rats became thicker, more cellular but also more destructive as more osteoclasts were identified within the periosteum. Macrophages in the periosteum, as were found to be high in cell density in both young and aged rats, may in effect have a dual, age dependent role in bone metabolism: in young rats that of osteogenesis, and in aged rats that of osteoclastogenesis. The periosteum from osteoporotic bones differs from normal bones both in terms of structure and cell populations. This is especially evident in the cambial layer of metaphyseal periosteum. Bone resorption appears to be more active in the periosteum from osteoporotic bones, whereas bone formation activity is comparable between the osteoporotic and normal bone. The dysregulation of bone resorption and formation in the periosteum, characteristic of the pathogenesis of osteoporosis, may also be the effect of the interaction between various neural pathways and the cell populations residing within it. All these findings are indicating that the structure and cell population in periosteum are closely linked with bone metabolism and health status which are varying with age and different between bones or bone portions. Young and fast growing bone or bone portions with normal calcium metabolism would have thicker and more osteogenic periosteum, while periostea from elder or osteoporotic patients, especially those from the metaphyseal area of long bone, would be less osteogenic or even bone resorptive.

This phenomenon is of significance in guiding clinical periosteum transplantation as well as the periosteum engineering. Despite the findings from this project, further investigations about the structure and cell populations on different bones, especially weight-bearing and non-bearing bones, should be performed to help understand how mechanical stresses affect the structure and cell populations in periosteum.

As revealed in the investigation on periosteum anatomy, the active osteogenesis in periosteum requires higher degree of vascularization. To achieve both osteogenesis and vascularization in the constructed periosteum, different cell sources have been used, such as osteoblasts and endothelial cells. In this PhD project, the novel concept of using a single adult stem cell source (BMSCs) to achieve both osteogenesis and vascularization in the constructed periosteum was tested. As the osteogenic differentiation ability of BMSCs has been well proved, the focus of this project was set upon the endothelial cell differentiation of BMSCs and how to use BMSCs to induce higher degree of in vivo vascularization. The endothelial cell differentiation of BMSCs has long since an unsettled controversy and a lot of conflicting reports can often be found in published literatures. This project provided a complete investigation on both endothelial cell differentiation and pro-/anti-angiogenic factor expression of BMSCs under both normoxia and hypoxia conditions. Our findings revealed that BMSCs most likely cannot be differentiated into endothelial cells through the application of pro-angiogenic growth factors or by culturing under hypoxic conditions. However, they may involve in angiogenesis as regulators under both nomoxic and hypoxic conditions. Two major angiogenesis-related growth factors, VEGF (pro-angiogenic) and PEDF (anti-angiogenic) were found to have altered expression in accordance with the extracellular environment. BMSCs treated with the hypoxia-mimicking agent $CoCl_2$ expressed more VEGF and less PEDF and enhanced the vascularization of subcutaneous implants *in vivo.* These findings tried for the first time to settle the controversy about the physiological role of mesenchymal stem cells in angiogenesis and vascularization, and confirmed that BMSCs are important regulators rather than endothelial cell progenitors in the angiogenic process. BMSCs

regulate the angiogenic process through adjusting the expression of pro- and anti-angiogenic factors in different extracellular micro-environments. These findings throw a new light on the application of BMSCs in controlling angiogenesis in vivo and constructing vascularized tissues. The molecular mechanism lying behind the regulatory role of BMSCs in different extracellular micro-environments needs to be further investigated. For example, how does the extracellular VEGF affect the VEGF/PEDF expression of BMSCs? Is there any specific cell surface receptor or intracellular signal pathway involved in the regulatory role of BMSCs in vascularization? The hypoxia was induced by $CoCl_2$ in this project, and the effect of real hypoxia induced by low oxygen partial pressure on BMSCs should be investigated in the future as well as underlying molecular mechanisms.

Since the hypoxia can boost the VEGF expression in BMSCs and VEGF is a coupling factor between the osteogenesis and vascularization, it should be of great significance to use hypoxia pre-treated BMSCs to induce or enhance both osteogenesis and vascularization in engineered periosteum. $CoCl_2$ is a proven hypoxia mimicking reagent as well as a FDA approved medicine for the anemia treatment, and can significantly increase the VEGF expression of BMSCs as confirmed in this project. Using $CoCl_2$ to increase the VEGF expression of BMSCs is much easier and simpler than the real hypoxia which normally needs special incubator or chamber with lowered oxygen partial pressure. Although there had been reports testing the ability of hypoxia pre-treated MSCs to help revascularize ischemic tissues in vivo, very few trials, if any, can be found in literatures about the application of hypoxia pre-treated BMSCs in engineering vascularized tissues, such as bone and periosteum. The findings of this study revealed in the animal model that BMSCs pre-treated with $CoCl_2$ could enhance both ectopic and orthotopic osteogenesis of BMSCs-derived osteoblasts and vascularization at the early osteogenic stage, and that endothelial cells were only capable of promoting osteogenesis after an extended period of four-weeks. The interaction between the endothelial cells and osteogenic cells should be further investigated in the future. On the other hand, the subcutaneous area of the mouse is

most likely inappropriate for assessing new bone formation on collagen scaffolds as no new bone formation was observed in the subcutaneous area. The local microenvironment seems playing significant roles in determining the mineralization pattern of transplanted BMSCs: clacification or new bone formation. Besides, although these findings revealed the close relationship between the vascularization and osteogenesis at an early osteogenic stage, how the vascularization and osteogenesis interact with each other at later osteogenic stages would be of great interest and should also be investigated. This study demonstrated the potential application of $CoCl_2$ pre-treated BMSCs in the tissue engineering not only for periosteum but also bone or other vascularized tissues. Whether the real hypoxia-treated BMSCs could play a similar role is a question as well that needs to be answered in my future studies.

In summary, periosteum is actually a highly complex organ containing different cell populations, extracellular matrix and bioactive molecules. In this PhD project, I have investigated the cellular structure of physiological periosteum and focused on potential cell application in vascularization. The tissue engineered periosteum is in many ways comparable to the actual physical periosteum, in both structural and functional aspects, however it is not a trivial undertaking and much future effort is still required to create a synthetic periosteum that truly mimics the function of physiological periosteum.

# References


1. Parikh, S.N., *Bone graft substitutes in modern orthopedics.* Orthopedics, 2002. **25**(11): p. 1301-9; quiz 1310-1.
2. Kim, S.S., et al., *Poly(lactide-co-glycolide)/hydroxyapatite composite scaffolds for bone tissue engineering.* Biomaterials, 2006. **27**(8): p. 1399-409.
3. Nishikawa, M., et al., *Bone tissue engineering using novel interconnected porous hydroxyapatite ceramics combined with marrow mesenchymal cells: quantitative and three-dimensional image analysis.* Cell Transplant, 2004. **13**(4): p. 367-76.
4. Yoshikawa, H. and A. Myoui, *Bone tissue engineering with porous hydroxyapatite ceramics.* J Artif Organs, 2005. **8**(3): p. 131-6.
5. Premaraj, S., et al., *Collagen gel delivery of Tgf-beta3 non-viral plasmid DNA in rat osteoblast and calvarial culture.* Orthod Craniofac Res, 2005. **8**(4): p. 320-2.
6. Rouwkema, J., J. de Boer, and C.A. Van Blitterswijk, *Endothelial cells assemble into a 3-dimensional prevascular network in a bone tissue engineering construct.* Tissue Eng, 2006. **12**(9): p. 2685-93.
7. Knothe, U.R. and D.S. Springfield, *A novel surgical procedure for bridging of massive bone defects.* World J Surg Oncol, 2005. **3**(1): p. 7.
8. Kaigler, D., et al., *VEGF scaffolds enhance angiogenesis and bone regeneration in irradiated osseous defects.* J Bone Miner Res, 2006. **21**(5): p. 735-44.
9. Malizos, K.N. and L.K. Papatheodorou, *The healing potential of the periosteum molecular aspects.* Injury, 2005. **36 Suppl 3**: p. S13-9.
10. Allen, M.R., J.M. Hock, and D.B. Burr, *Periosteum: biology, regulation, and response to osteoporosis therapies.* Bone, 2004. **35**(5): p. 1003-12.
11. Squier, C.A., S. Ghoneim, and C.R. Kremenak, *Ultrastructure of the periosteum from membrane bone.* J Anat, 1990. **171**: p. 233-9.
12. Asaumi, K., et al., *Expression of neurotrophins and their receptors (TRK) during fracture healing.* Bone, 2000. **26**(6): p. 625-33.

13. Ito, Y., et al., *Localization of chondrocyte precursors in periosteum.* Osteoarthritis Cartilage, 2001. **9**(3): p. 215-23.
14. Nakahara, H., et al., *Bone and cartilage formation in diffusion chambers by subcultured cells derived from the periosteum.* Bone, 1990. **11**(3): p. 181-8.
15. Fang, J. and B.K. Hall, *Chondrogenic cell differentiation from membrane bone periostea.* Anat Embryol (Berl), 1997. **196**(5): p. 349-62.
16. Muramatsu, K. and A.T. Bishop, *Cell repopulation in vascularized bone grafts.* J Orthop Res, 2002. **20**(4): p. 772-8.
17. Tran Van, P.T., A. Vignery, and R. Baron, *Cellular kinetics of the bone remodeling sequence in the rat.* Anat Rec, 1982. **202**(4): p. 445-51.
18. Hutmacher, D.W. and M. Sittinger, *Periosteal cells in bone tissue engineering.* Tissue Eng, 2003. **9 Suppl 1**: p. S45-64.
19. Fan, W., R. Crawford, and Y. Xiao, *Structural and cellular differences between metaphyseal and diaphyseal periosteum in different aged rats.* Bone, 2008. **42**(1): p. 81-9.
20. Eyre-Brook, A.L., *The periosteum: its function reassessed.* Clin Orthop Relat Res, 1984(189): p. 300-7.
21. Bliziotes, M., et al., *Periosteal remodeling at the femoral neck in nonhuman primates.* J Bone Miner Res, 2006. **21**(7): p. 1060-7.
22. Chanavaz, M., *[The periosteum: the "umbilical cord" of bone. Quantification of the blood supply of cortical bone of periosteal origin].* Rev Stomatol Chir Maxillofac, 1995. **96**(4): p. 262-7.
23. Simpson, A.H., *The blood supply of the periosteum.* J Anat, 1985. **140 ( Pt 4)**: p. 697-704.
24. Bjurholm, A., et al., *Neuropeptide Y-, tyrosine hydroxylase- and vasoactive intestinal polypeptide-immunoreactive nerves in bone and surrounding tissues.* J Auton Nerv Syst, 1988. **25**(2-3): p. 119-25.
25. Hill, E.L. and R. Elde, *Distribution of CGRP-, VIP-, D beta H-, SP-, and NPY-immunoreactive nerves in the periosteum of the rat.* Cell Tissue Res, 1991. **264**(3): p. 469-80.

26. Hohmann, E.L., et al., *Innervation of periosteum and bone by sympathetic vasoactive intestinal peptide-containing nerve fibers.* Science, 1986. **232**(4752): p. 868-71.

27. de Souza, R.L., et al., *Sympathetic nervous system does not mediate the load-induced cortical new bone formation.* J Bone Miner Res, 2005. **20**(12): p. 2159-68.

28. Cherruau, M., et al., *Chemical sympathectomy impairs bone resorption in rats: a role for the sympathetic system on bone metabolism.* Bone, 1999. **25**(5): p. 545-51.

29. Hill, E.L., R. Turner, and R. Elde, *Effects of neonatal sympathectomy and capsaicin treatment on bone remodeling in rats.* Neuroscience, 1991. **44**(3): p. 747-55.

30. Sherman, B.E. and R.A. Chole, *Sympathectomy, which induces membranous bone remodeling, has no effect on endochondral long bone remodeling in vivo.* J Bone Miner Res, 2000. **15**(7): p. 1354-60.

31. Haug, S.R., et al., *Sympathectomy causes increased root resorption after orthodontic tooth movement in rats: immunohistochemical study.* Cell Tissue Res, 2003. **313**(2): p. 167-75.

32. Cherruau, M., et al., *Chemical sympathectomy-induced changes in TH-, VIP-, and CGRP-immunoreactive fibers in the rat mandible periosteum: influence on bone resorption.* J Cell Physiol, 2003. **194**(3): p. 341-8.

33. O'Driscoll, S.W. and J.S. Fitzsimmons, *The role of periosteum in cartilage repair.* Clin Orthop Relat Res, 2001(391 Suppl): p. S190-207.

34. Rauch, F., R. Travers, and F.H. Glorieux, *Intracortical remodeling during human bone development-A histomorphometric study.* Bone, 2006.

35. Seeman, E., *Periosteal bone formation--a neglected determinant of bone strength.* N Engl J Med, 2003. **349**(4): p. 320-3.

36. O'Driscoll, S.W., *Articular cartilage regeneration using periosteum.* Clin Orthop Relat Res, 1999(367 Suppl): p. S186-203.

37. Emans, P.J., et al., *In vivo generation of cartilage from periosteum.* Tissue Eng,

2005. **11**(3-4): p. 369-77.

38. Estrada, J.I., et al., *Periosteal distraction osteogenesis: Preliminary experimental evaluation in rabbits and dogs.* Br J Oral Maxillofac Surg, 2006.
39. Dimitriou, R., E. Tsiridis, and P.V. Giannoudis, *Current concepts of molecular aspects of bone healing.* Injury, 2005. **36**(12): p. 1392-404.
40. Engdahl, E., V. Ritsila, and L. Uddstromer, *Growth potential of cranial suture bone autograft. II. An experimental microscopic investigation in young rabbits.* Scand J Plast Reconstr Surg, 1978. **12**(2): p. 125-9.
41. O'Driscoll, S.W. and J.S. Fitzsimmons, *The importance of procedure specific training in harvesting periosteum for chondrogenesis.* Clin Orthop Relat Res, 2000(380): p. 269-78.
42. O'Driscoll, S.W. and R.B. Salter, *The repair of major osteochondral defects in joint surfaces by neochondrogenesis with autogenous osteoperiosteal grafts stimulated by continuous passive motion. An experimental investigation in the rabbit.* Clin Orthop Relat Res, 1986(208): p. 131-40.
43. O'Driscoll, S.W., et al., *Method for automated cartilage histomorphometry.* Tissue Eng, 1999. **5**(1): p. 13-23.
44. Wakitani, S. and T. Yamamoto, *Response of the donor and recipient cells in mesenchymal cell transplantation to cartilage defect.* Microsc Res Tech, 2002. **58**(1): p. 14-8.
45. Uddstromer, L., *The osteogenic capacity of tubular and membranous bone periosteum. A qualitative and quantitative experimental study in growing rabbits.* Scand J Plast Reconstr Surg, 1978. **12**(3): p. 195-205.
46. Uddstromer, L. and V. Ritsila, *Healing of membranous and long bone defects. An experimental study in growing rabbits.* Scand J Plast Reconstr Surg, 1979. **13**(2): p. 281-7.
47. Oni, O.O. and P.J. Gregg, *An investigation of the contribution of the extraosseous tissues to the diaphyseal fracture callus using a rabbit tibial fracture model.* J Orthop Trauma, 1991. **5**(4): p. 480-4.
48. Oni, O.O., H. Stafford, and P.J. Gregg, *A study of diaphyseal fracture repair*

*using tissue isolation techniques.* Injury, 1992. **23**(7): p. 467-70.

49. Brighton, C.T. and R.M. Hunt, *Early histologic and ultrastructural changes in microvessels of periosteal callus.* J Orthop Trauma, 1997. **11**(4): p. 244-53.

50. Bruder, S.P., D.J. Fink, and A.I. Caplan, *Mesenchymal stem cells in bone development, bone repair, and skeletal regeneration therapy.* J Cell Biochem, 1994. **56**(3): p. 283-94.

51. O'Driscoll, S.W. and J.S. Fitzsimmons, *The role of periosteum in cartilage repair.* Clinical Orthopedics and Related Research, 2001. **391S**: p. S190-S207.

52. Ueno, T., et al., *Immunohistochemical observations of cellular differentiation and proliferation in endochondral bone formation from grafted periosteum: expression and localization of BMP-2 and -4 in the grafted periosteum.* Journal of Craniomaxillofacial Surgery, 2003. **31**: p. 356-361.

53. Ueno, T., et al., *Regeneration of the mandibular head from grafted periosteum.* Annals of Plastic Surgery, 2003. **51**: p. 77-83.

54. Laurencin, C.T., et al., *Tissue engineering: Orthopedic applications.* Annual Review of Biomedical Engineering, 1999. **1**: p. 19-46.

55. Zhang, X., et al., *A perspective: engineering periosteum for structural bone graft healing.* Clin Orthop Relat Res, 2008. **466**(8): p. 1777-87.

56. Neel, M., *The use of a periosteal replacement membrane for bone graft containment at allograft-host junctions after tumor resection and reconstruction with bulk allograft.* Orthopedics, 2003. **26**(5 Suppl): p. s587-9.

57. Hattori, K., et al., *Bio-artificial periosteum for severe open fracture--an experimental study of osteogenic cell/collagen sponge composite as a bio-artificial periosteum.* Biomed Mater Eng, 2005. **15**(3): p. 127-36.

58. Zhang, K.G., B.F. Zeng, and C.Q. Zhang, *[Periosteum construction in vitro by small intestinal submucosa combined with bone marrow mesenchymal stem cell].* Zhonghua Wai Ke Za Zhi, 2005. **43**(24): p. 1594-7.

59. Augustin, G., A. Antabak, and S. Davila, *The periosteum. Part 1: anatomy, histology and molecular biology.* Injury, 2007. **38**(10): p. 1115-30.

60. Nacamuli, R.P. and M.T. Longaker, *Bone induction in craniofacial defects.*

Orthod Craniofac Res, 2005. **8**(4): p. 259-66.

61. Weiner S, W.H., *The material bone: structure-mechanical function relations.* Annu Rev Mater Sci 1998. **28**: p. 271-298.
62. Mastrogiacomo, M., et al., *Tissue engineering of bone: search for a better scaffold.* Orthod Craniofac Res, 2005. **8**(4): p. 277-84.
63. Henkel, K.O., et al., *Macroscopical, histological, and morphometric studies of porous bone-replacement materials in minipigs 8 months after implantation.* Oral Surg Oral Med Oral Pathol Oral Radiol Endod, 2006. **102**(5): p. 606-13.
64. Quarto, R., et al., *Repair of large bone defects with the use of autologous bone marrow stromal cells.* N Engl J Med, 2001. **344**(5): p. 385-6.
65. Saito, M., et al., *The role of beta-tricalcium phosphate in vascularized periosteum.* J Orthop Sci, 2000. **5**(3): p. 275-82.
66. LD., S., in *Introduction to biomaterials*. 2005, Tsinghua University Press & World scientific: Beijian,China. p. 44-45.
67. Cong, Z., W. Jianxin, and Z. Xingdong, *Osteoinductivity and biomechanics of a porous ceramic with autogenic periosteum.* J Biomed Mater Res, 2000. **52**(2): p. 354-9.
68. JE., D., in *Bone engineering*. 2000, Em squared incorporated Toronto, Canada p. 454-455.
69. Wahl, D.A. and J.T. Czernuszka, *Collagen-hydroxyapatite composites for hard tissue repair.* Eur Cell Mater, 2006. **11**: p. 43-56.
70. Weinand, C., et al., *Hydrogel-beta-TCP scaffolds and stem cells for tissue engineering bone.* Bone, 2006. **38**(4): p. 555-63.
71. Bilgen G, O.G., Tokgõz Z, Guner G, Yalçin S, *Collagen Content and Electrophoretic Analysis of Type I Collagen in Breast Skin of Heterozygous Naked Neck and Normally Feathered Commercial Broilers.* J Veter & Ani Sci, 1999. **23**: p. 483–487.
72. LD., S., in *Introduction to biomaterials*. 2005, Tsinghua University Press & World scientific: Beijian,China. p. 159.
73. Horch, R.E., et al., *Tissue engineering of cultured skin substitutes.* J Cell Mol

Med, 2005. **9**(3): p. 592-608.

74. Amiel, G.E., et al., *Engineering of blood vessels from acellular collagen matrices coated with human endothelial cells.* Tissue Eng, 2006. **12**(8): p. 2355-65.

75. Saadeh, P.B., et al., *Repair of a critical size defect in the rat mandible using allogenic type I collagen.* J Craniofac Surg, 2001. **12**(6): p. 573-9.

76. Vickers, S.M., L.S. Squitieri, and M. Spector, *Effects of cross-linking type II collagen-GAG scaffolds on chondrogenesis in vitro: dynamic pore reduction promotes cartilage formation.* Tissue Eng, 2006. **12**(5): p. 1345-55.

77. Kremer, M., E. Lang, and A. Berger, *Organotypical engineering of differentiated composite-skin equivalents of human keratinocytes in a collagen-GAG matrix (INTEGRA Artificial Skin) in a perfusion culture system.* Langenbecks Arch Surg, 2001. **386**(5): p. 357-63.

78. Gotterbarm, T., et al., *An in vivo study of a growth-factor enhanced, cell free, two-layered collagen-tricalcium phosphate in deep osteochondral defects.* Biomaterials, 2006. **27**(18): p. 3387-95.

79. Kamakura, S., et al., *Octacalcium phosphate combined with collagen orthotopically enhances bone regeneration.* J Biomed Mater Res B Appl Biomater, 2006. **79**(2): p. 210-7.

80. Lynn, A.K., I.V. Yannas, and W. Bonfield, *Antigenicity and immunogenicity of collagen.* J Biomed Mater Res B Appl Biomater, 2004. **71**(2): p. 343-54.

81. Baumann, L.S. and F. Kerdel, *The treatment of bovine collagen allergy with cyclosporin.* Dermatol Surg, 1999. **25**(3): p. 247-9.

82. LD., S., in *Introduction to biomaterials*. 2005, Tsinghua University Press & World scientific: Beijian,China. p. 189-190.

83. Middleton, J.C. and A.J. Tipton, *Synthetic biodegradable polymers as orthopedic devices.* Biomaterials, 2000. **21**(23): p. 2335-2346.

84. Cao, D., et al., *In vitro tendon engineering with avian tenocytes and polyglycolic acids: a preliminary report.* Tissue Eng, 2006. **12**(5): p. 1369-77.

85. Terada, S., et al., *Hydrogel optimization for cultured elastic chondrocytes*

*seeded onto a polyglycolic acid scaffold.* J Biomed Mater Res A, 2005. **75**(4): p. 907-16.

86. Hutmacher, D.W., J.C. Goh, and S.H. Teoh, *An introduction to biodegradable materials for tissue engineering applications.* Ann Acad Med Singapore, 2001. **30**(2): p. 183-91.

87. Stock, U.A. and J.E. Mayer, Jr., *Tissue engineering of cardiac valves on the basis of PGA/PLA Co-polymers.* J Long Term Eff Med Implants, 2001. **11**(3-4): p. 249-60.

88. Barralet, J.E., L.L. Wallace, and A.J. Strain, *Tissue engineering of human biliary epithelial cells on polyglycolic acid/polycaprolactone scaffolds maintains long-term phenotypic stability.* Tissue Eng, 2003. **9**(5): p. 1037-45.

89. Verheyen, C.C., et al., *Evaluation of hydroxylapatite/poly(L-lactide) composites: mechanical behavior.* J Biomed Mater Res, 1992. **26**(10): p. 1277-96.

90. Bergsma, E.J., et al., *Foreign body reactions to resorbable poly(L-lactide) bone plates and screws used for the fixation of unstable zygomatic fractures.* J Oral Maxillofac Surg, 1993. **51**(6): p. 666-70.

91. LD., S., in *Introduction to biomaterials*. 2005, Tsinghua University Press & World scientific: Beijian,China. p. 191.

92. Sedrakyan, S., et al., *Tissue engineering of a small hand phalanx with a porously casted polylactic acid-polyglycolic acid copolymer.* Tissue Eng, 2006. **12**(9): p. 2675-83.

93. Yoshida, M., J. Mata, and J.E. Babensee, *Effect of poly(lactic-co-glycolic acid) contact on maturation of murine bone marrow-derived dendritic cells.* J Biomed Mater Res A, 2007. **80**(1): p. 7-12.

94. Yoon, J.J., et al., *Immobilization of cell adhesive RGD peptide onto the surface of highly porous biodegradable polymer scaffolds fabricated by a gas foaming/salt leaching method.* Biomaterials, 2004. **25**(25): p. 5613-20.

95. Dawes, E. and N. Rushton, *The effects of lactic acid on PGE2 production by macrophages and human synovial fibroblasts: a possible explanation for*

*problems associated with the degradation of poly(lactide) implants?* Clin Mater, 1994. **17**(4): p. 157-63.

96. Wiesmann, H.P., U. Joos, and U. Meyer, *Biological and biophysical principles in extracorporal bone tissue engineering. Part II.* Int J Oral Maxillofac Surg, 2004. **33**(6): p. 523-30.

97. Hennink, W.E. and C.F. van Nostrum, *Novel crosslinking methods to design hydrogels.* Adv Drug Deliv Rev, 2002. **54**(1): p. 13-36.

98. Athanasiou, K.A., G.G. Niederauer, and C.M. Agrawal, *Sterilization, toxicity, biocompatibility and clinical applications of polylactic acid/polyglycolic acid copolymers.* Biomaterials, 1996. **17**(2): p. 93-102.

99. Sittinger, M., D.W. Hutmacher, and M.V. Risbud, *Current strategies for cell delivery in cartilage and bone regeneration.* Curr Opin Biotechnol, 2004. **15**(5): p. 411-8.

100. Cavalcanti-Adam, E.A., et al., *RGD peptides immobilized on a mechanically deformable surface promote osteoblast differentiation.* J Bone Miner Res, 2002. **17**(12): p. 2130-40.

101. Awad, H.A., et al., *Chondrogenic differentiation of adipose-derived adult stem cells in agarose, alginate, and gelatin scaffolds.* Biomaterials, 2004. **25**(16): p. 3211-22.

102. Nuttelman, C.R., M.C. Tripodi, and K.S. Anseth, *In vitro osteogenic differentiation of human mesenchymal stem cells photoencapsulated in PEG hydrogels.* J Biomed Mater Res A, 2004. **68**(4): p. 773-82.

103. He, S., et al., *Injectable biodegradable polymer composites based on poly(propylene fumarate) crosslinked with poly(ethylene glycol)-dimethacrylate.* Biomaterials, 2000. **21**(23): p. 2389-94.

104. Behravesh, E., et al., *Synthesis of in situ cross-linkable macroporous biodegradable poly(propylene fumarate-co-ethylene glycol) hydrogels.* Biomacromolecules, 2002. **3**(2): p. 374-81.

105. Chenite, A., et al., *Novel injectable neutral solutions of chitosan form biodegradable gels in situ.* Biomaterials, 2000. **21**(21): p. 2155-61.

106. Bensaid, W., et al., *A biodegradable fibrin scaffold for mesenchymal stem cell transplantation.* Biomaterials, 2003. **24**(14): p. 2497-502.

107. Hegewald, A.A., et al., *Hyaluronic acid and autologous synovial fluid induce chondrogenic differentiation of equine mesenchymal stem cells: a preliminary study.* Tissue Cell, 2004. **36**(6): p. 431-8.

108. Spitzer, R.S., et al., *Matrix engineering for osteogenic differentiation of rabbit periosteal cells using alpha-tricalcium phosphate particles in a three-dimensional fibrin culture.* J Biomed Mater Res, 2002. **59**(4): p. 690-6.

109. McGlohorn, J.B., et al., *Characterization of cellular carriers for use in injectable tissue-engineering composites.* J Biomed Mater Res A, 2003. **66**(3): p. 441-9.

110. Bianco, P., et al., *Bone marrow stromal stem cells: nature, biology, and potential applications.* Stem Cells, 2001. **19**(3): p. 180-92.

111. Bianco, P., et al., *Postnatal skeletal stem cells.* Methods Enzymol, 2006. **419**: p. 117-48.

112. Loomans, C.J., et al., *Angiogenic murine endothelial progenitor cells are derived from a myeloid bone marrow fraction and can be identified by endothelial NO synthase expression.* Arterioscler Thromb Vasc Biol, 2006. **26**(8): p. 1760-7.

113. Schatteman, G.C., M. Dunnwald, and C. Jiao, *Biology of Bone Marrow-Derived Endothelial Cell Precursors.* Am J Physiol Heart Circ Physiol, 2006.

114. Reyes, M., et al., *Purification and ex vivo expansion of postnatal human marrow mesodermal progenitor cells.* Blood, 2001. **98**(9): p. 2615-25.

115. Derubeis, A.R. and R. Cancedda, *Bone marrow stromal cells (BMSCs) in bone engineering: limitations and recent advances.* Ann Biomed Eng, 2004. **32**(1): p. 160-5.

116. Joyner, C.J., A. Bennett, and J.T. Triffitt, *Identification and enrichment of human osteoprogenitor cells by using differentiation stage-specific monoclonal antibodies.* Bone, 1997. **21**(1): p. 1-6.

117. Herbertson, A. and J.E. Aubin, *Cell sorting enriches osteogenic populations in rat bone marrow stromal cell cultures.* Bone, 1997. **21**(6): p. 491-500.

118. Haynesworth, S.E., M.A. Baber, and A.I. Caplan, *Cell surface antigens on human marrow-derived mesenchymal cells are detected by monoclonal antibodies.* Bone, 1992. **13**(1): p. 69-80.

119. Koch, S., et al., *Enhancing angiogenesis in collagen matrices by covalent incorporation of VEGF.* J Mater Sci Mater Med, 2006. **17**(8): p. 735-41.

120. Sarkar, S., et al., *Development and characterization of a porous micro-patterned scaffold for vascular tissue engineering applications.* Biomaterials, 2006. **27**(27): p. 4775-82.

121. Shepherd, B.R., et al., *Vascularization and engraftment of a human skin substitute using circulating progenitor cell-derived endothelial cells.* Faseb J, 2006. **20**(10): p. 1739-41.

122. Zisch, A.H., *Tissue engineering of angiogenesis with autologous endothelial progenitor cells.* Curr Opin Biotechnol, 2004. **15**(5): p. 424-9.

123. Levenberg, S., *Engineering blood vessels from stem cells: recent advances and applications.* Curr Opin Biotechnol, 2005. **16**(5): p. 516-23.

124. Urbich, C. and S. Dimmeler, *Endothelial progenitor cells: characterization and role in vascular biology.* Circ Res, 2004. **95**(4): p. 343-53.

125. Reyes, M., et al., *Origin of endothelial progenitors in human postnatal bone marrow.* J Clin Invest, 2002. **109**(3): p. 337-46.

126. Kaushal, S., et al., *Functional small-diameter neovessels created using endothelial progenitor cells expanded ex vivo.* Nat Med, 2001. **7**(9): p. 1035-40.

127. Muraglia, A., R. Cancedda, and R. Quarto, *Clonal mesenchymal progenitors from human bone marrow differentiate in vitro according to a hierarchical model.* J Cell Sci, 2000. **113 ( Pt 7)**: p. 1161-6.

128. Lucarelli, E., et al., *Bone reconstruction of large defects using bone marrow derived autologous stem cells.* Transfus Apher Sci, 2004. **30**(2): p. 169-74.

129. Mastrogiacomo, M., et al., *Engineering of bone using bone marrow stromal*

*cells and a silicon-stabilized tricalcium phosphate bioceramic: Evidence for a coupling between bone formation and scaffold resorption.* Biomaterials, 2006.

130. Fuchs, B., S.P. Steinmann, and A.T. Bishop, *Free vascularized corticoperiosteal bone graft for the treatment of persistent nonunion of the clavicle.* J Shoulder Elbow Surg, 2005. **14**(3): p. 264-8.
131. Vogelin, E., et al., *Healing of a critical-sized defect in the rat femur with use of a vascularized periosteal flap, a biodegradable matrix, and bone morphogenetic protein.* J Bone Joint Surg Am, 2005. **87**(6): p. 1323-31.
132. Akiyama, M., et al., *Periosteal cell pellet culture system: a new technique for bone engineering.* Cell Transplant, 2006. **15**(6): p. 521-32.
133. Perka, C., et al., *Segmental bone repair by tissue-engineered periosteal cell transplants with bioresorbable fleece and fibrin scaffolds in rabbits.* Biomaterials, 2000. **21**(11): p. 1145-53.
134. Zhang, X., et al., *Periosteal progenitor cell fate in segmental cortical bone graft transplantations: implications for functional tissue engineering.* J Bone Miner Res, 2005. **20**(12): p. 2124-37.
135. Agata, H., et al., *Effective bone engineering with periosteum-derived cells.* J Dent Res, 2007. **86**(1): p. 79-83.
136. Tonna, E.A., *Electron microscopic study of bone surface changes during aging. The loss of cellular control and biofeedback.* J Gerontol, 1978. **33**(2): p. 163-77.
137. O'Driscoll, S.W., et al., *The chondrogenic potential of periosteum decreases with age.* J Orthop Res, 2001. **19**(1): p. 95-103.
138. De Bari, C., F. Dell'Accio, and F.P. Luyten, *Human periosteum-derived cells maintain phenotypic stability and chondrogenic potential throughout expansion regardless of donor age.* Arthritis Rheum, 2001. **44**(1): p. 85-95.
139. Tonna, E.A., *Periosteal osteoclasts, skeletal development and ageing.* Nature, 1960. **185**: p. 405-7.
140. Koga, Y., et al., *Recovery course of full-thickness skin defects with exposed bone: an evaluation by a quantitative examination of new blood vessels.* J

Surg Res, 2007. **137**(1): p. 30-7.

141. Ellender, G., S.A. Feik, and S.M. Ramm-Anderson, *Periosteal changes in mechanically stressed rat caudal vertebrae.* J Anat, 1989. **163**: p. 83-96.

142. Ahlborg, H.G., et al., *Bone loss and bone size after menopause.* N Engl J Med, 2003. **349**(4): p. 327-34.

143. Pead, M.J., T.M. Skerry, and L.E. Lanyon, *Direct transformation from quiescence to bone formation in the adult periosteum following a single brief period of bone loading.* J Bone Miner Res, 1988. **3**(6): p. 647-56.

144. Gronthos, S., et al., *The STRO-1+ fraction of adult human bone marrow contains the osteogenic precursors.* Blood, 1994. **84**(12): p. 4164-73.

145. Dennis, J.E., et al., *The STRO-1+ marrow cell population is multipotential.* Cells Tissues Organs, 2002. **170**(2-3): p. 73-82.

146. Massey, H.M. and A.M. Flanagan, *Human osteoclasts derive from CD14-positive monocytes.* Br J Haematol, 1999. **106**(1): p. 167-70.

147. Hayase, Y., Y. Muguruma, and M.Y. Lee, *Osteoclast development from hematopoietic stem cells: apparent divergence of the osteoclast lineage prior to macrophage commitment.* Exp Hematol, 1997. **25**(1): p. 19-25.

148. Rifas, L., et al., *Macrophage-derived growth factor for osteoblast-like cells and chondrocytes.* Proc Natl Acad Sci U S A, 1984. **81**(14): p. 4558-62.

149. Takeshita, S., K. Kaji, and A. Kudo, *Identification and characterization of the new osteoclast progenitor with macrophage phenotypes being able to differentiate into mature osteoclasts.* J Bone Miner Res, 2000. **15**(8): p. 1477-88.

150. Li, M. and N. Amizuka, *[Histopathological observations on osteolytic bone metastasis].* Clin Calcium, 2006. **16**(4): p. 591- 97.

151. Asou, Y., et al., *Osteopontin facilitates angiogenesis, accumulation of osteoclasts, and resorption in ectopic bone.* Endocrinology, 2001. **142**(3): p. 1325-32.

152. Nakagawa, M., et al., *Vascular endothelial growth factor (VEGF) directly enhances osteoclastic bone resorption and survival of mature osteoclasts.*

FEBS Lett, 2000. **473**(2): p. 161-4.

153. Seeman, E., *Reduced bone formation and increased bone resorption: rational targets for the treatment of osteoporosis.* Osteoporos Int, 2003. **14 Suppl 3**: p. S2-8.

154. Rauch, F., R. Travers, and F.H. Glorieux, *Intracortical remodeling during human bone development--a histomorphometric study.* Bone, 2007. **40**(2): p. 274-80.

155. Pogoda, P., et al., *Bone remodeling: new aspects of a key process that controls skeletal maintenance and repair.* Osteoporos Int, 2005. **16 Suppl 2**: p. S18-24.

156. Seeman, E., *Invited Review: Pathogenesis of osteoporosis.* J Appl Physiol, 2003. **95**(5): p. 2142-51.

157. Xiao, Y., et al., *Gene expression profiling of bone marrow stromal cells from juvenile, adult, aged and osteoporotic rats: with an emphasis on osteoporosis.* Bone, 2007. **40**(3): p. 700-15.

158. Ferretti, J.L., et al., *Perspectives on osteoporosis research: its focus and some insights from a new paradigm.* Calcif Tissue Int, 1995. **57**(6): p. 399-404.

159. Parfitt, A.M., *Size of bone in the aged endocortical resorption.* J Bone Miner Res, 2002. **17**(7): p. 1306; author reply 1307-8.

160. Furst, A., et al., *Effect of age on bone mineral density and micro architecture in the radius and tibia of horses: an Xtreme computed tomographic study.* BMC Vet Res, 2008. **4**: p. 3.

161. Blahos, J., *Treatment and prevention of osteoporosis.* Wien Med Wochenschr, 2007. **157**(23-24): p. 589-92.

162. Kameda, T., et al., *Estrogen inhibits bone resorption by directly inducing apoptosis of the bone-resorbing osteoclasts.* J Exp Med, 1997. **186**(4): p. 489-95.

163. Cho, S.W., et al., *Small-diameter blood vessels engineered with bone marrow-derived cells.* Ann Surg, 2005. **241**(3): p. 506-15.

164. Peng, H., et al., *VEGF improves, whereas sFlt1 inhibits, BMP2-induced bone formation and bone healing through modulation of angiogenesis.* J Bone

Miner Res, 2005. **20**(11): p. 2017-27.

165. Imai, S. and Y. Matsusue, *Neuronal regulation of bone metabolism and anabolism: calcitonin gene-related peptide-, substance P-, and tyrosine hydroxylase-containing nerves and the bone.* Microsc Res Tech, 2002. **58**(2): p. 61-9.

166. Farhadi, J., et al., *Differentiation-dependent up-regulation of BMP-2, TGF-beta1, and VEGF expression by FGF-2 in human bone marrow stromal cells.* Plast Reconstr Surg, 2005. **116**(5): p. 1379-86.

167. Ohno-Matsui, K., et al., *Vascular endothelial growth factor upregulates pigment epithelium-derived factor expression via VEGFR-1 in human retinal pigment epithelial cells.* Biochem Biophys Res Commun, 2003. **303**(3): p. 962-7.

168. Zhang, S.X., et al., *Pigment epithelium-derived factor downregulates vascular endothelial growth factor (VEGF) expression and inhibits VEGF-VEGF receptor 2 binding in diabetic retinopathy.* J Mol Endocrinol, 2006. **37**(1): p. 1-12.

169. Chen, J., et al., *Intravenous administration of human bone marrow stromal cells induces angiogenesis in the ischemic boundary zone after stroke in rats.* Circ Res, 2003. **92**(6): p. 692-9.

170. Oswald, J., et al., *Mesenchymal stem cells can be differentiated into endothelial cells in vitro.* Stem Cells, 2004. **22**(3): p. 377-84.

171. Zhang, S.J., et al., *Is it possible to obtain "true endothelial progenitor cells" by in vitro culture of bone marrow mononuclear cells?* Stem Cells Dev, 2007. **16**(4): p. 683-90.

172. Jiang, Y., et al., *Pluripotency of mesenchymal stem cells derived from adult marrow.* Nature, 2002. **418**(6893): p. 41-9.

173. Xia, Z., R.M. Locklin, and J.T. Triffitt, *Fates and osteogenic differentiation potential of human mesenchymal stem cells in immunocompromised mice.* Eur J Cell Biol, 2008. **87**(6): p. 353-64.

174. Connelly, J.T., A.J. Garcia, and M.E. Levenston, *Interactions between integrin*

*ligand density and cytoskeletal integrity regulate BMSC chondrogenesis.* J Cell Physiol, 2008. **217**(1): p. 145-54.

175. Lamagna, C. and G. Bergers, *The bone marrow constitutes a reservoir of pericyte progenitors.* J Leukoc Biol, 2006. **80**(4): p. 677-81.

176. Bexell, D., et al., *Bone marrow multipotent mesenchymal stroma cells act as pericyte-like migratory vehicles in experimental gliomas.* Mol Ther, 2009. **17**(1): p. 183-90.

177. Ozerdem, U., et al., *Contribution of bone marrow-derived pericyte precursor cells to corneal vasculogenesis.* Invest Ophthalmol Vis Sci, 2005. **46**(10): p. 3502-6.

178. Shibuya, M., *Vascular endothelial growth factor-dependent and -independent regulation of angiogenesis.* BMB Rep, 2008. **41**(4): p. 278-86.

179. Otrock, Z.K., J.A. Makarem, and A.I. Shamseddine, *Vascular endothelial growth factor family of ligands and receptors: review.* Blood Cells Mol Dis, 2007. **38**(3): p. 258-68.

180. Yamazaki, Y. and T. Morita, *Molecular and functional diversity of vascular endothelial growth factors.* Mol Divers, 2006. **10**(4): p. 515-27.

181. Harlozinska, A., et al., *Vascular endothelial growth factor (VEGF) concentration in sera and tumor effusions from patients with ovarian carcinoma.* Anticancer Res, 2004. **24**(2C): p. 1149-57.

182. Notari, L., et al., *Identification of a lipase-linked cell membrane receptor for pigment epithelium-derived factor.* J Biol Chem, 2006. **281**(49): p. 38022-37.

183. Sena, K., D.R. Sumner, and A.S. Virdi, *Modulation of VEGF expression in rat bone marrow stromal cells by GDF-5.* Connect Tissue Res, 2007. **48**(6): p. 324-31.

184. Wrobel, T., et al., *Increased expression of vascular endothelial growth factor (VEGF) in bone marrow of patients with myeloproliferative disorders (MPD).* Pathol Oncol Res, 2003. **9**(3): p. 170-3.

185. Cai, S., et al., *Expression of human VEGF(121) cDNA in mouse bone marrow stromal cells.* Chin Med J (Engl), 2002. **115**(6): p. 914-8.

186. Lee, H., et al., *Cobalt chloride, a hypoxia-mimicking agent, targets sterol synthesis in the pathogenic fungus Cryptococcus neoformans.* Mol Microbiol, 2007. **65**(4): p. 1018-33.

187. Ohnishi, S., et al., *Effect of hypoxia on gene expression of bone marrow-derived mesenchymal stem cells and mononuclear cells.* Stem Cells, 2007. **25**(5): p. 1166-77.

188. Knothe Tate, M.L., et al., *Testing of a new one-stage bone-transport surgical procedure exploiting the periosteum for the repair of long-bone defects.* J Bone Joint Surg Am, 2007. **89**(2): p. 307-16.

189. Fujii, T., et al., *Comparison of bone formation ingrafted periosteum harvested from tibia and calvaria.* Microsc Res Tech, 2006. **69**(7): p. 580-4.

190. Jensen, S.S., et al., *Comparative study of biphasic calcium phosphates with different HA/TCP ratios in mandibular bone defects. A long-term histomorphometric study in minipigs.* J Biomed Mater Res B Appl Biomater, 2009. **90**(1): p. 171-81.

191. Hu, X., et al., *Transplantation of hypoxia-preconditioned mesenchymal stem cells improves infarcted heart function via enhanced survival of implanted cells and angiogenesis.* J Thorac Cardiovasc Surg, 2008. **135**(4): p. 799-808.

192. Li, T.S., et al., *Improved angiogenic potency by implantation of ex vivo hypoxia prestimulated bone marrow cells in rats.* Am J Physiol Heart Circ Physiol, 2002. **283**(2): p. H468-73.

193. Loboda, A., et al., *Heme oxygenase-1-dependent and -independent regulation of angiogenic genes expression: effect of cobalt protoporphyrin and cobalt chloride on VEGF and IL-8 synthesis in human microvascular endothelial cells.* Cell Mol Biol (Noisy-le-grand), 2005. **51**(4): p. 347-55.

194. Shapiro, F., *Bone development and its relation to fracture repair. The role of mesenchymal osteoblasts and surface osteoblasts.* Eur Cell Mater, 2008. **15**: p. 53-76.

195. Hedberg, E.L., et al., *Methods: a comparative analysis of radiography, microcomputed tomography, and histology for bone tissue engineering.* Tissue

Eng, 2005. **11**(9-10): p. 1356-67.